STUDY OF METHANE REFORMING IN

WARM NON-EQUILIBRIUM PLASMA DISCHARGES

A Thesis

by

SREEKAR PARIMI

Submitted to the Office of Graduate Studies of
Texas A&M University
in partial fulfillment of the requirements for the degree of

MASTER OF SCIENCE

December 2010

Major Subject: Mechanical Engineering

STUDY OF METHANE REFORMING IN

WARM NON-EQUILIBRIUM PLASMA DISCHARGES

A Thesis

by

SREEKAR PARIMI

Submitted to the Office of Graduate Studies of
Texas A&M University
in partial fulfillment of the requirements for the degree of

MASTER OF SCIENCE

Approved by:

Chair of Committee,	David Staack
Committee Members,	Kalyan Annamalai
	Mehrdad Ehsani
Head of Department,	Dennis O'Neal

December 2010

Major Subject: Mechanical Engineering

ABSTRACT

Study of Methane Reforming in Warm Non-Equilibrium Plasma Discharges.

(December 2010)

Sreekar Parimi, B.Tech., J.B. Institute of Engineering and Technology

Chair of Advisory Committee: Dr. David Staack

Utilization of natural gas in remote locations necessitates on-site conversion of methane into liquid fuels or high value products. The first step in forming high value products is the production of ethylene and acetylene. Non-thermal plasmas, due to their unique non-equilibrium characteristics, offer advantages over traditional methods of methane reforming.

Different kinds of non-thermal plasmas are being investigated for methane reforming. Parameters of these processes like flow rate, discharge size, temperature and other variables determine efficiency of conversion. An efficient process is identified by a high yield and low specific energy of production for the desired product. A study of previous work reveals that higher energy density systems are more efficient for methane conversion to higher hydrocarbons as compared to low energy density systems. Some of the best results were found to be in the regime of warm discharges. Thermal equilibrium studies indicate that higher yields of ethylene are possible with an optimal control of reaction kinetics and fast quenching. With this idea, two different glow discharge reactor systems are designed and constructed for investigation of methane reforming. A counter

flow micro plasma discharge system was used to investigate the trends of methane reforming products and the control parameters were optimized to get best possible ethylene yields while minimizing its specific energy. Later a magnetic glow discharge system is used and better results are obtained. Energy costs lower than thermal equilibrium calculations were achieved with magnetic glow discharge systems for both ethylene and acetylene. Yields are obtained from measurements of product concentrations using gas chromatography and power measurements are done using oscilloscope. Energy balance and mass balances are performed for product measurement accuracy and carbon deposition calculations. Carbon deposition is minimized through control of the temperature and residence time conditions in magnetic glow discharges. Ethylene production is observed to have lower specific energies at higher powers and lower flow rates in both reactors. An ethylene selectivity of 40% is achieved at an energy cost of 458MJ/Kg and an input energy cost of 5 MJ/Kg of methane.

DEDICATION

To my loving and ever supporting parents, P. Prabhakar Sastry , P. Lalitha

And to my dearest friends Satyanarayana , Manasa , Harika.

ACKNOWLEDGEMENTS

I would like to express my sincere gratitude to Dr. David Staack for all the guidance and support he has provided me in the past couple of years. I would not have made so much progress in my research and academics at A&M without his guidance and advice. I would like to thank Aditya Chitre and Robert Geiger for sharing their knowledge and helping me in my experimental work. I would like to thank my committee members, Dr. Kalyan Annamalai and Dr. Mehrdad Ehsani, for their valuable input.

Finally, I want to thank my parents, Mr. Prabhakar Sastry parimi and Mrs. Lalitha parimi, for their continuous support and encouragement throughout my life. They went through all the hardships to support my higher education. My parents, sister, and friends have always believed in my capabilities and have supported me in every walk of my life.

TABLE OF CONTENTS

Page

Page

Page

Page

LIST OF FIGURES

Page

Page

LIST OF TABLES

1. INTRODUCTION

1.1 Background and motivation

1.1.1 Methane Reforming and Uses

Natural gas is an important and abundant source of energy. It is also a clean source and releases lower levels of harmful by products as compared to fossil fuels. Used for cooking, electricity and heating in most parts of U.S, natural gas is second only to petroleum products for energy supply. It is mainly composed of hydrocarbons, primarily methane. Although its composition could vary, typically natural gas has 70-90% of methane, 5-15% of ethane propane and butane and traces of around 1% in oxygen, nitrogen, hydrogen. Combustion of natural gas releases water vapor, CO_2 and small amounts of sulfur dioxide, nitrogen oxide [1].

Natural gas while mostly found underneath earth as a separate reservoir it is often an additional product found along with oil deposits [2]. More and more reservoirs are found in remote locations where no pipeline facilities exist. Because of its low density natural gas is difficult to transport through pipelines across oceans. Due to this reason methane produced from oil deposits is often released into atmosphere, flared or fed back to the underground storage resulting in excess cost [1]. To lower the cost and environmental impact, an onsite conversion of methane into transportable fuels is necessary.

This thesis follows the style of *Plasma Source and Technology*.

These fuels could be either liquids or else high value products such as ethylene or acetylene. These higher hydrocarbons are also safer for transport. In addition to being transportable fuels, these fuels are huge raw materials for polymer industry and petrochemical industry. These applications and requirements form the driving force to develop technology for converting natural gas into liquid fuels and chemicals such as C_2H_2, C_2H_4.

1.1.2 Current Methane Reforming Methods and Disadvantages

Methods of methane utilization can be broadly classified as direct and indirect methods. Generation of desired end product directly from methane, not involving any intermediate steps, characterizes direct methods. Indirect methods mostly involve syn gas intermediate step. An outline of all current methods of methane reforming is shown in Figure 1.1.

1.1.2.1 Indirect methods: Steam reforming, carbon dioxide reforming and partial oxidation are the major indirect methods. Partial oxidation and combustion are highly exothermic, whereas carbon dioxide, steam reforming are endothermic and requires heat or electrical energy input . Methods with intermediate syn gas step, like Fischer-Tropsch process, involve expensive heat transfer equipment and the ones with catalysts have coke deposition as a major problem [3]. Commercial scale processes like MTG (methane to gasoline) process and MTO (methane to olefin) process are both catalyst based processes. While MTG is expensive when compared to existing methods of gasoline production, MTO is not suitable for remote locations [4].

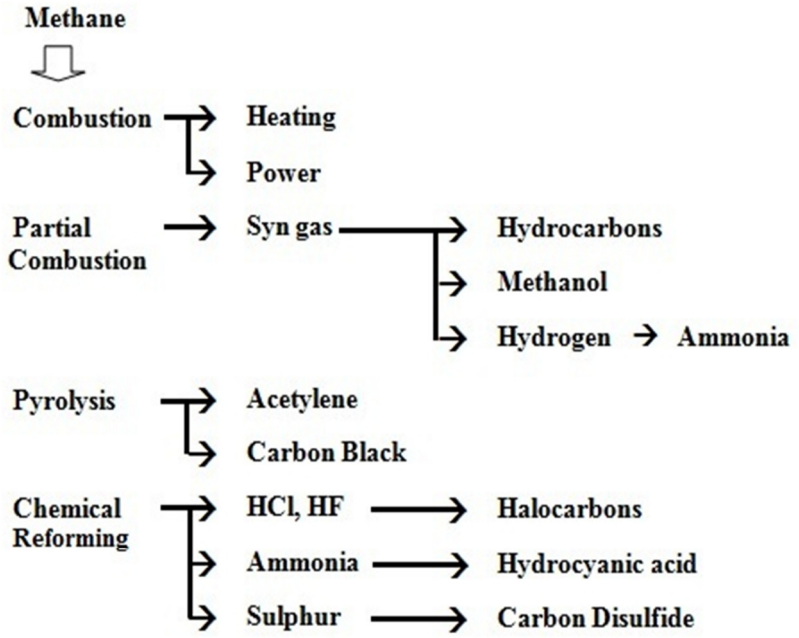

Figure 1.1 Methane reforming methods [*Anders Holeman, ref: 5*]

1.1.2.2 Direct methods: A large number of research groups are investigating direct methods of methane conversion [4-10]. Some of the direct method approaches are:

1. Thermal processing (With/Without catalysts)

Thermally methane can be formed only at high temperatures (>1300K). Hence, energy is supplied in different ways and methane is cracked by exposing it to high temperatures [7]. In oxidative coupling methane reacts with oxygen over catalysts. Although initial major products are ethane and ethylene, they tend to combust into CO_2 thereby the yields of C_2 hydrocarbons are limited to less than 26% [4]. Regenerative techniques & recycling were employed to improve ethylene yields but the entire process still remains un-economical [8]. Partial oxidation to methanol, with and without catalysts, is found to

a potential direct route for methane conversion. But methods without catalyst are thermal and are troubled by heat management issues, while catalytic approaches have not been successful so far. Conversion rates and yields achieved are very low (< 0.1%) and research is still in process [9, 10].

2. Plasma processing

i. *Thermal* - Thermal plasmas have been used to perform pyrolysis of methane for decades. Except for the Huels and Dupont none of those methods have been demonstrated on industrial scale [11]. The Huels process uses electrical energy to generate a thermal arc in which methane and hydrogen mixtures are reformed followed by water spray quenching to cool the product stream. Operated at power levels of 8 MW, this process has natural gas as input feed and achieved acetylene yields of 50% with a conversion efficiency of 70% [12]. Dupont process operated on the same lines of Huels with a magnetically rotated discharge and achieved better yields of higher hydrocarbons (65% - 70%) [13]. Westinghouse used a hydrogen plasma reactor to produce acetylene from natural gas by the use of thermal arc generated by H_2 gas and later quenched with liquid propane [14]. Carbon deposit on the electrodes calls for periodic shut down of the conversion process and cleaning of the electrodes in these thermal arc processes. All these methods have product separation, coke deposition and high temperature operation as unsolved problems [11].

ii. *Non-thermal* - Non thermal plasmas are gaining a lot of attention for fuel reforming due to their ability to offer selectivity and maintain bulk temperature close to

room temperature. Their role in overcoming the limitations posed by other methods will be discussed in next section.

On the whole, several approaches to efficient methane reforming are tried, each of them with their own limitations. Most of these methods are limited by heat management issues while others have low yields. Economic feasibility is crucial to all of these methods.

1.2 Thesis statement

Warm non-equilibrium discharges are employed for methane conversion into acetylene and ethylene as they offer fast quenching and lower residence times. A parametric study of methane reforming under different glow discharge conditions is made. Ethylene is produced from methane, while minimizing the energy cost and carbon deposition.

1.2.1 Plasma Reforming

Plasmas are ionized gases which are effective in activating gas molecules at lower temperatures [15]. Methane can only be activated at higher temperatures and products like ethylene and acetylene are stable only above 1300K. These reactions are highly endothermic and require high energy inputs to make C_2 hydrocarbons. Plasma technology is used to reform methane by activating methane molecules by highly energized electrons or ions [7]. Plasmas are mainly classified as thermal and non thermal plasmas. While thermal plasmas are high temperature ionized gases with uniform temperature (T ~ 10,000K), non thermal plasmas possess a lower translational

temperature (300K – 2000K) while possessing electrons of high energy (>1 eV or 11,000 K) [16]. In methane reforming as the input feed flows through electrically generated plasma discharge, the methane interacts with energetic plasma components and forms other hydrocarbons [17].

1.2.2 Advantages

1.2.2.1 Fast quenching: Methane activation into ethylene or acetylene could be initiated either by thermal processes or highly energetic electrons. Products formed at this temperature are near their thermal equilibrium, but as the gas moves out of reactor and the gas temperature is brought down to room temperature, most of these products may react to form carbon and hydrogen [17]. To prevent this, the temperature change has to be as quick as possible. This is called as quenching. The faster the quenching, the better are the possibilities of retaining the product composition as and when it is formed. In an ideal case, called ideal quenching, it is assumed products formed at those temperatures are retained in exactly the same proportions after quenching [7].

Plasmas offer the advantage of fast quenching. In the discharge zone the temperature is raised to more than 1500K and products are formed [17]. As they move out of plasma, the small size of discharge allows the product mixture to rapidly reach slightly above room temperatures with a quenching rate on the order of 10^6 K/s [18].

1.2.2.2 Lower residence time: Residence time is the amount of time a gas is reacting in a plasma discharge. The product distribution from methane reforming depends on

temperature and residence time of methane and its products along with quenching. Methane forms ethylene and acetylene through coupling of methyl radicals and stepwise dehydrogenation eventually leading to carbon formation (soot) [19]. For better ethylene yields, it is necessary to control this reaction kinetics and limit it to formation of ethylene. Lower residence times are necessary to prevent the intermediate products to decompose to unwanted end products like hydrogen and carbon [20, 21]. Plasma discharges discussed in this work offer lower residence times (on the order of 0.1 ms) and so are useful in controlling reaction kinetics towards desired end products.

Typically, lower residence times and high temperatures along with rapid quenching favor ethylene and acetylene as products with minimal sooting. Hence discharge conditions favoring better ethylene yields and minimal carbon in the products are expected.

1.3 Research objectives

- Experimentally investigate the effects of residence time and input specific energy on the ethylene selectivity in glow discharges.
- Evaluate the trends of conversion rate and product specific energy under different discharge conditions.
- This work will attempt to lower the cost of ethylene production while maximizing the selectivity of it in the products using different reactor systems.
- Focus on minimizing carbon generation and deposition while producing ethylene through plasma reforming of methane.

- Results from methane reforming using various discharge systems from literature will be reviewed. A comparison of past and current work including this thesis to thermal equilibrium results will be made in terms of achieved product specific energies.

1.4 Thesis overview

This document starts with an initial introduction and motivation for this research. Plasma basics and a thermodynamic review of methane reforming and results from literature are presented in second section. Third and fourth sections cover the system design and diagnostic techniques used for this work. Then we proceed to fifth section that details the experimental outline, output measurement methods and uncertainty analysis. Finally we present the results from this work in sixth section and conclude the thesis along with recommendations for future work in seventh section. Thereafter, appendices and references follow towards the end of the document.

2. LITERATURE REVIEW OF PLASMA METHANE REFORMING

2.1 Plasma

Plasma is an ionized gas. It essentially consists of a free moving electrons and ions. It is also called as distinct fourth state of matter. These free charges make plasma electrically conductive, internally interactive, and strongly responsive to electromagnetic fields [16]. Plasma offers three major features :

1. Temperatures of at least some plasma components and energy density can significantly exceed those in conventional chemical technologies [17].
2. Plasmas produce very high concentrations of energetic and chemically active species [17].
3. They can be far from thermodynamic equilibrium providing active species and at the same time keeping the bulk temperature low [17].

2.1.1 Plasma Applications

Because plasmas are conductive and respond to electric and magnetic fields and can be efficient sources of radiation, they are usable in numerous applications where such control is needed or when special sources of energy or radiation are required [22]. Applications of plasma are found in numerous fields today, such as:

i. Plasma light radiation – High efficiency lighting, fluorescent bulbs, flat panel displays

ii. Plasma physics – Thrusters, Fusion, Sputtering

iii. Plasma chemistry

a) Low pressure – Semiconductor manufacturing, surface cleaning, plastic processing.

b) High pressure – Thermal spray coatings, gas treatment, surface sterilization, waste destruction, tissue engineering.

2.1.2 Types of Plasmas

For fuel reforming we are considering atmospheric pressure processing, because low pressure vacuum processing is too expensive. There are two distinct categories of atmospheric-pressure plasmas, thermal and non-thermal.

2.1.2.1 Thermal plasmas: Thermal plasmas are also called as hot plasmas. The electron and bulk gas temperatures along with energy content for thermal plasmas are very high. These plasmas partially ionized but sufficiently conductive [17]. There exists a local thermodynamic equilibrium, described by a saha equation as given below

$$\frac{n_i}{n_n} = 2.4 \times 10^{21} \left(\frac{T^{\frac{3}{2}}}{n_i}\right) e^{-\frac{U_i}{KT}} \qquad \text{.....(2.1)}$$

where T [^{0}K] is Temperature, n_i [m^{-3}] is Density of ionized atoms, n_n [m^{-3}] is Density of neutral atoms, K [eV/K] is Boltzmann's constant and U_i [eV] is Ionization energy. The temperature of all the plasma components are close and hence entire plasma

is will be at single temperature (T) at all points of its space. The plasma gas temperature ranges from 5000 to 20,000 Kelvin [17].

2.1.2.2 Non-thermal plasmas: Plasmas can also exist far from thermodynamic equilibrium and different plasma particles and different degrees of freedom can have different temperatures. In such cases electron temperature significantly exceeds the temperature of ions. These are non thermal plasmas and they are also called non-equilibrium plasmas [16]. Ionization and chemical processes in these plasmas are directly determined by electron temperature and are not so sensitive to thermal processes and temperature of gas. Typically the order of temperature in collision weakly ionized plasmas is $T_e > T_v > T_r \sim T_i \sim T_0$. Electron temperature ($T_e$) is highest followed by temperature of vibrational (T_v) excitation of molecules. The lowest is shared by heavy neutrals (T_n), ions (T_i) and rotational (T_r) degrees of freedom of molecules .Typically $T_e \sim 10{,}000$ Kelvin and T_0 is from room temperature 300 – 2000 Kelvin [17].

2.1.3 Characteristics

Plasmas are chemically reactive. Its components include large concentrations of active species like ions, electrons, excited molecules (vibrational and electron excitation), atoms, radicals and photons. All these components affect the reaction kinetics in their own way. Electrons distribute energy from electric field among remaining plasma components. While heavy particles often contribute by lowering activation energies of chemical reactions, vibrationally excited molecules often make the most significant

contribution because plasma electrons transfer most of their energy in gases into vibrational excitation. The contribution of radicals and atoms becomes a part of overall reaction kinetics [17].

Non thermal plasmas are usually generated at low pressures or low powers or in pulsed discharge systems, while thermal plasmas need high powers or high pressures. Thermal plasmas include those produced in high intensity arcs, plasma torches, or in high intensity high frequency discharges [23]. The characteristic difference between these two types of plasmas is that, thermal plasmas are more powerful or high energy density plasmas whereas non thermal plasmas are more selective. This feature of selectivity allows control of plasma chemistry to be directed through an optimal mechanism [17].

2.1.4 Different Plasmas and Glow Discharge

Plasmas are gas discharges generated from electrical energy. Hence different discharges are differentiated by the discharge conditions, V-I characteristics where V is voltage and I is current. Some of the commonly used plasmas are direct current glow discharge, pulsed glow discharge, Capacitive coupled /inductively coupled RF discharges, Corona discharge, magnetron discharge, Dielectric barrier discharge, Microwave discharge and Gliding arc discharge [17].

Figure 2.1 shows a V-I characteristic of discharge generated between two electrodes for a wide range of currents. Different regimes are shown in the plot for different

discharges. Initially, when breakdown happens a self sustaining glow discharge is generated between electrodes. The resulting discharge is limited in its current by the resistance of the circuit. The current limitations determine the kind of discharge that exists in system. Depending on current very low power, non-thermal – dark discharge, moderate power, non thermal –glow, high power thermal arc [18].

Glow discharge – When a high electrical potential is applied to the electrodes, a small fraction of ions and electrons are generated through breakdown process. These ions driven towards cathode and electrons are driven towards anode while ionizing the neutrals that they collide with. Ions bombarding the cathode produce significant number of electrons (called secondary electron emission) that sustains a high electron density in the discharge. A simple glow discharge with its regions across the length of its discharge is shown in Figure 2.2. These regions are defined by the light emission patterns of plasma components in those locations. At atmospheric pressure due to small length scales of the near electrode sheaths only PC, FS and NG are visible.

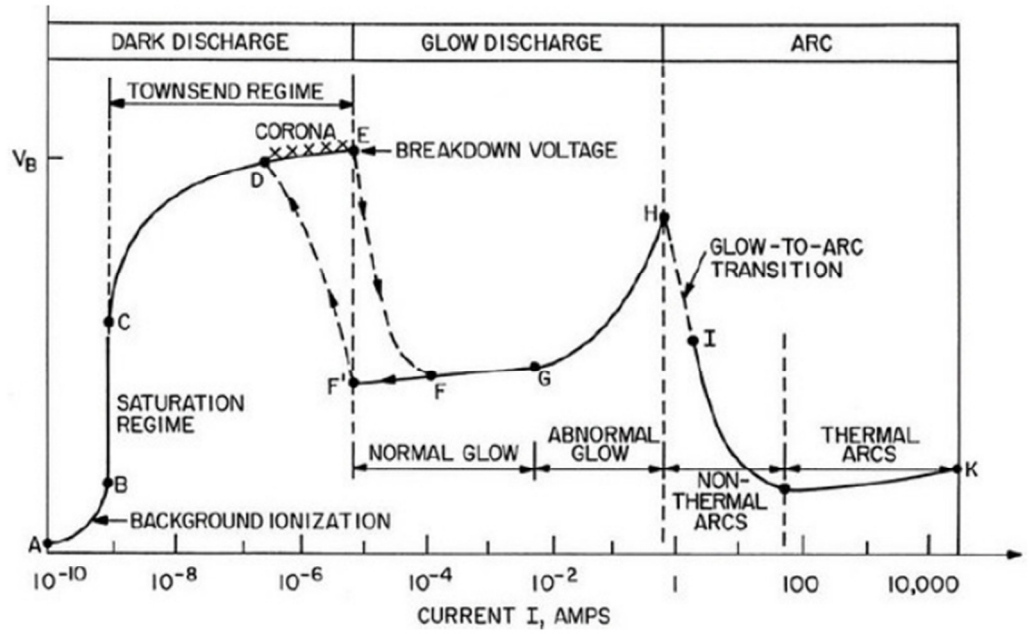

Figure 2.1 V-I characteristic plot showing various discharge regimes [24]

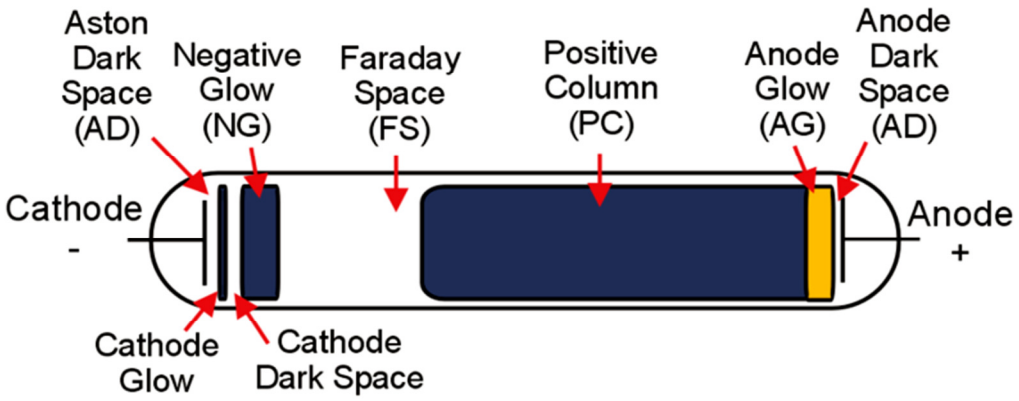

Figure 2.2 Glow discharge regions [25]

2.2 Methane reforming using different plasmas – A literature review

Various atmospheric discharge techniques, such as pulsed corona and spark discharges [26-40], dielectric barrier discharges (DBDs) [41-46], microwave discharges [47- 49] have been employed for oxygen-free conversion of methane. Table 2.1 presents a summary of the results obtained utilizing various discharge types for non-oxidative conversion of methane to higher hydrocarbons. Data presented in the references was converted to common units for comparison. The parameters being compared are methane flow rate, discharge power, methane conversion rate, acetylene selectivity, specific energy input. An efficient methane conversion is reflected by high selectivity for acetylene and low energy cost for production of acetylene. Generally sufficient data was available to thoroughly evaluate the different methods. An exception is Babaritskyi [48] which has been cited several times to various accuracy in the literature. Babaritskyi's results though partial are also included for completeness. In general it has been found that higher energy density systems including high frequency pulsed corona, pulsed microwave and gliding arc discharges were rather more efficient for methane conversion to hydrogen and acetylene than DBDs and lower frequency pulsed and lower power density discharges.

Focusing on the three main types of discharges: 1) Pulsed Corona and Spark Discharges (PD), 2) Dielectric Barrier Discharges (DBD) and 3) Microwave discharges (MW). In several PD studies the the selectivity of acetylene is consistently higher than that reported for dielectric barrier discharges. Generally the highest efficiencies for such

discharges are reported when the specific energy input is maximized [26] and hydrogen and acetylene are the dominating products [27]. The correspondence of high conversion efficiency with specific energy input has been shown by increasing power, voltage, and

Table 2.1 Summary of recent research in the non-oxidative conversion of-

- methane to higher hydrocarbons

Discharge type	Flow Rate (L/min)	Power (W)	Methane Conversion (%)	Acetylene Selectivity (%)	Acetylene specfic energy (eV/Molecule)	Specific energy input (eV/ CH4 Molecule)
High Frequency Pulsed Plasma [37]	0.3	32	39	83.2	9.16	1.48
Pulsed Microwave [46]	0.19	81	93	71.1	20.2	5.95
Enhanced Microwave Pulsed [47]	0.3	120	59.2	88	21.42	5.58
RF Discharge [50]	0.372	100	46.4	56.9	Ethane -28.46	3.75
Stable kHz Spark Discharge [30]	0.076	32.5	81.5	52.6	27.6	5.965
Pulsed Spark Discharge [31]	0.01	12	69	78.2	62	16.74
Abnormal Glow Discharge [51]	0.3*	400	91.6	90.2	225	93
Pulsed Corona Discharge 1 [27]	0.025	33.37	44.5	15.4	123	18.62
Pulsed Corona Discharge 2 [28]	0.02	58	67	73.7	192.6	40.45
Pulsed Corona Discharge 3 [26]	1.68	154	8	80	39.8	1.27
Moderate Pressure Microwave Discharge [48]	NA	NA	80	80	6	2.6
Huels [52]	2.9***	1**	82.4	80	8.3	3.9
*Total Feed flux = 0.3 L/min (Methane 20% + Hydrogen 80%), ** MW, *** Tonnes						

repetition rate or by lower flow rate with fixed power [28]. Selectivity towards acetylene as high as 95% are reported though at the cost of high energy inputcost (300 eV/molecule) [29]. Xiao-Song Li et al.'s [30] Stable kilohertz spark discharges is one more new discharge with a unique waveform of discharge current for high-efficiency conversion of methane to hydrogen and acetylene at atmospheric pressure an energy cost of 27.6 eV per C_2H_2 molecule is reported. Xiao-Song Li et al [31] also compared four

different electric discharge techniques, pulsed streamer discharges, pulsed spark discharges and pulsed DC DBD, AC DBD. Former two have acetylene as the dominant product with highest acetylene yield obtained, using a needle-to-plate reactor by pulsed spark discharges the DBD systems have ethane as the dominant product with pulsed DC DBD process provides the highest ethane yield. So far the most efficient conversion of methane to acetylene using PD attained has an energy cost of 27.6 eV/molecule with a methane conversion of 81.5% and selectivity of 52.6%. Catalysts addition and electrode construction can improve product distributions [32-35] Some of the best results are observed in high frequency pulsed plasma (~$8x10^3$ pulse/sec) the observed conversion efficiency is still lower than that using arc plasma such as the huels process, but higher than those of microwave , with the exception of Baritskii's work [36-40].

The DBD are characterized by lower power densities and ethane was found to be the most abundant reaction product, followed by propane and butane. [41]. Using an atmospheric pressure coaxial DBD the methane conversion was about 25%. Yield of ethane about 17% and ethane selectivity of 60% are reached [42,45]. Variations with operating parameters are unclear some showing improved methane conversion but less selectivity with increased electric field [43] while others18 show voltage independence, gas residence time effects, electrode geometry effects and synergistic effects with Helium addition are also reported [44,45].

The MW can have a higher energy density and a higher ratio of electron temperature to ion temperature than pulsed corona discharges. Here the product distribution is shifted

with increasing input power density from ethane to ethylene and finally to acetylene, the main reaction product at higher powers [46]. Conversion of 81% methane and high selectivity 71.1% is achieved by M. Heintze et al [46]. Hydrogen addition improves selectivity and efficiency though only significantly at the lower energy inputs. The best results are achieved for pulsed microwave discharges of moderate (~0.1 us) duration. Too long pulses lead to the saturation of the methane conversion degree with acetylene as major product and much too long pulses lead to eventual sooting [46]. Too short pulses (.30ms) results in insufficient dehydrogenation. High increase methane conversion rate and thereby lower energy cost, was obtained by simultaneously increasing the power delivered to the discharge and the methane flow rate [46]. Pressure [46,47] and electrode geometry [47] effects were also observed in MW systems. The highest efficiency using microwave radiation so far is by Babaritskyi (See Table 2.1), achieved using non-thermal moderate pressure (10-80 Torr) microwave discharges [48].

The effects of reaction temperature, electron density and mean residence time were studied in Radio Frequency (RF) discharges[49,50] though ethane was the major product. Some novel discharge configurations such as abnormal glow discharges [51] with its higher electron density and higher temperature, or a higher energy density in reaction space abnormal glow discharge is said to induce higher conversion and higher selectivity.

Summarizing the above, various non-thermal atmospheric discharges have been studied but still few are better than the thermal Huels process. Lower power density DBD and

corona discharges favors ethane formation while higher power density pulsed corona discharges, glow discharges, and microwave discharges favors acetylene as major products. It would seem that still higher energy and pulse frequency are needed to achieve the most efficient C_2 yield. The best results (matching or beating that of thermal plasmas, i.e. Huels [52] for acetylene production are obtained with "warm" non-equilibrium discharges ($T_{vib}>T_{trans}$ but still quite high T_{trans} ~1000K.) The precise nature of the relation between T_{vib}, T_o, and E_a though has not been investigated. An additional poorly understood factor is gas residence time and processing pressure. With specific energy input constant it would appear that higher flow rates and shorter pulses are preferred over long ones and this means short residence time may also be a crucial parameter.

Review of results for Ethylene - Very few results are reported for production of the ethylene through non thermal plasma methods [53-56]. A summary of best literature results are shown in Table 2.2 Few processes like MTO (Methane to Olefins) and oxidative coupling with different reactors have demonstrated to produce ethylene at high selectivity's but are not economically feasible [57]. For non thermal plasmas ethylene is always the least selective product and high selectivity's were possible only through use of catalysts or recycling methods [7,54,55].

Table 2.2: Summary of recent research in the non-oxidative conversion of methane to ethylene

Discharge	Flow rate [L/min]	Power [W]	Methane Conv. [%]	C2H4 Selectivity [%]	Energy Cost C2H4 [eV/mol]	Energy Cost in CH4 [MJ/Kg]
Glow Discharge [53]	0.03	12.3	11.2	26	394.50	34.40
Gliding [54]	0.005	6	50.0	80	656.55	100.69
Pd catalyst [56]	5	270	18.0	NA	37.67	11.33
PSD - Pd caltayst PFC reactor [56]	0.025	11.2	70.0	78	68.69	112.78
DC corona [55]	NA	4.5	10.0	65	22.39	NA

It has been mentioned that alumina in conjunction with pt and pd metal has been effective in reducing soot deposition. Since plasma generates CH_2 and C_2 radicals, it is attributed that catalysts accelerate reactions of carbon radicals with hydrogen thereby increasing C_2 yields and reducing soot. Although not experimentally proved, heterogeneous dissociation of CH_4 molecules and acetylene hydrogenation is said to be enhanced by use of Pt and Pd catalysts [56]. It must be noted though, that the results from catalysts have also systems in which residence times are smaller or could be optimized enough for production of ethylene and ethane. Other than catalysts, pseudo glow discharge and gliding discharge have been applied with specific energies of ethylene higher than 1000 MJ/kg [53]. Discharge preferences for ethylene are similar to

acetylene. While DBD s are energy expensive, corona and pseudo glow discharges investigated so far proved to be less selective for ethylene [54,55].

2.3 Thermodynamics of methane reforming

2.3.1 Thermal Reforming

Thermal mechanism of methane disassociation deals with the thermodynamics of methane reforming and its pathways into end products. The reaction mechanisms and its kinetics must be understood for creating favorable conditions necessary for efficient performance of any methane reforming.

Methane disassociation into higher hydrocarbons is an endothermic reaction. Figure 2.3 shows heat of formation for methane and other higher hydrocarbons. As we can see in the plot, heat of formation for ethylene and acetylene is positive and for methane it's negative. Hence lot of energy is necessary to thermally convert methane into ethylene/acetylene.

In thermal reforming, these endothermic reactions are initiated by raising the temperature of reactant feed to more than 1300K. Methane is unstable at temperatures more than 1000K as seen from the Figure 2.4. The relative stability of different hydrocarbons with respect to temperature is shown on in the same figure.

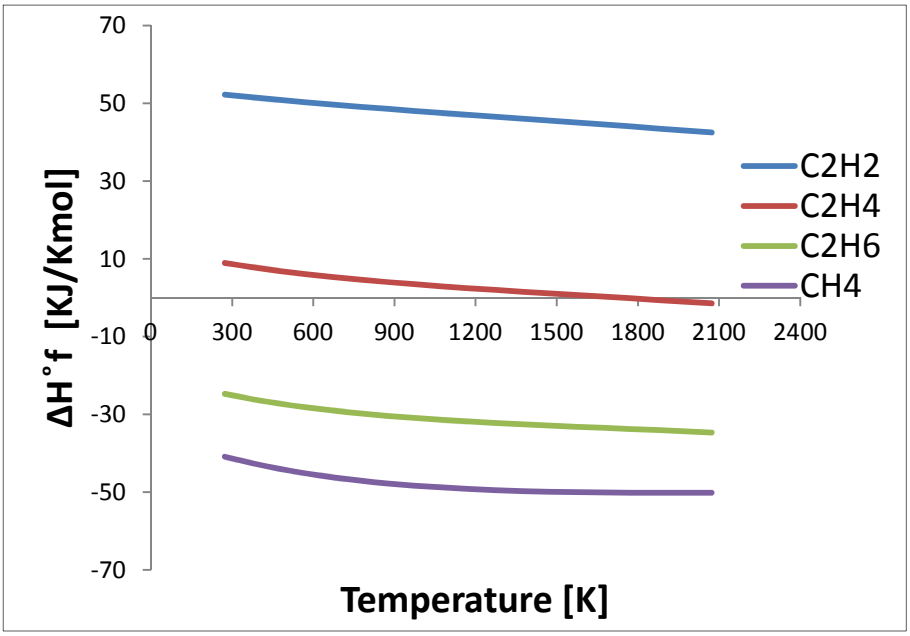

Figure 2.3 Heat of formation as a function of temperature

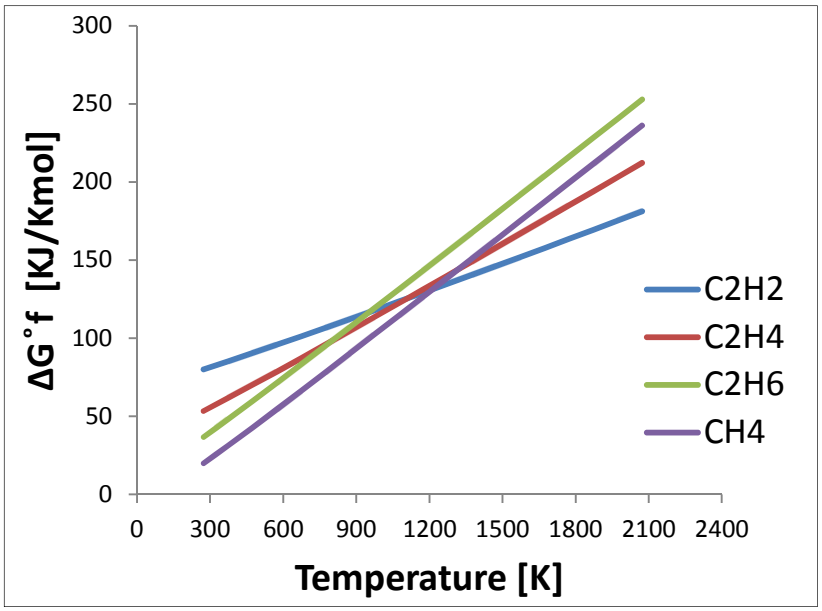

Figure 2.4 Standard free energy of formation as a function of temperature

Ethylene and acetylene are stable than methane only at high temperatures requiring the reforming reactor to operate at temperatures greater than 1500K. Note than carbon and hydrogen, being in their natural state, will still be stable than acetylene. Hence with enough time all intermediate products tend to dissociate into hydrogen and carbon.

2.3.1.1 Thermal mechanism: Using Cantera [58] and GRI -3 mechanism [59] variation of reactant and product concentrations with respect to temperature are plotted in matlab. The equilibrium yields of product species along with methane at different temperatures is shown in Figure 2.5. This plot is made at constant pressure of 1atm under assumptions of no sooting and ideal quenching. By no sooting, we are not considering carbon to be product of methane reforming and ideal quenching means products are any temperature are retained in exactly same amounts as the system is brought down to room temperature.

Equilibrium plot shows that at high temperature products can be ethane, ethylene, acetylene or benzene. Methane dissociation begins at temperature above 800K. As the temperature reaches 1800K there is very little methane left with most of it converted to acetylene with a maximum theoretical yield of 98% at 2175K. While yields of acetylene are low below 1670K., yields of ethylene are low at all temperatures, with the maximum being 0.5% in the range of 1400-1600 K. Hence ethylene yield is thermodynamically limited.

2.3.1.2 Necessity of quenching: Since hydrocarbons form only at elevated temperatures it is necessary to raise the reactants to a temperature where the desired hydrocarbon

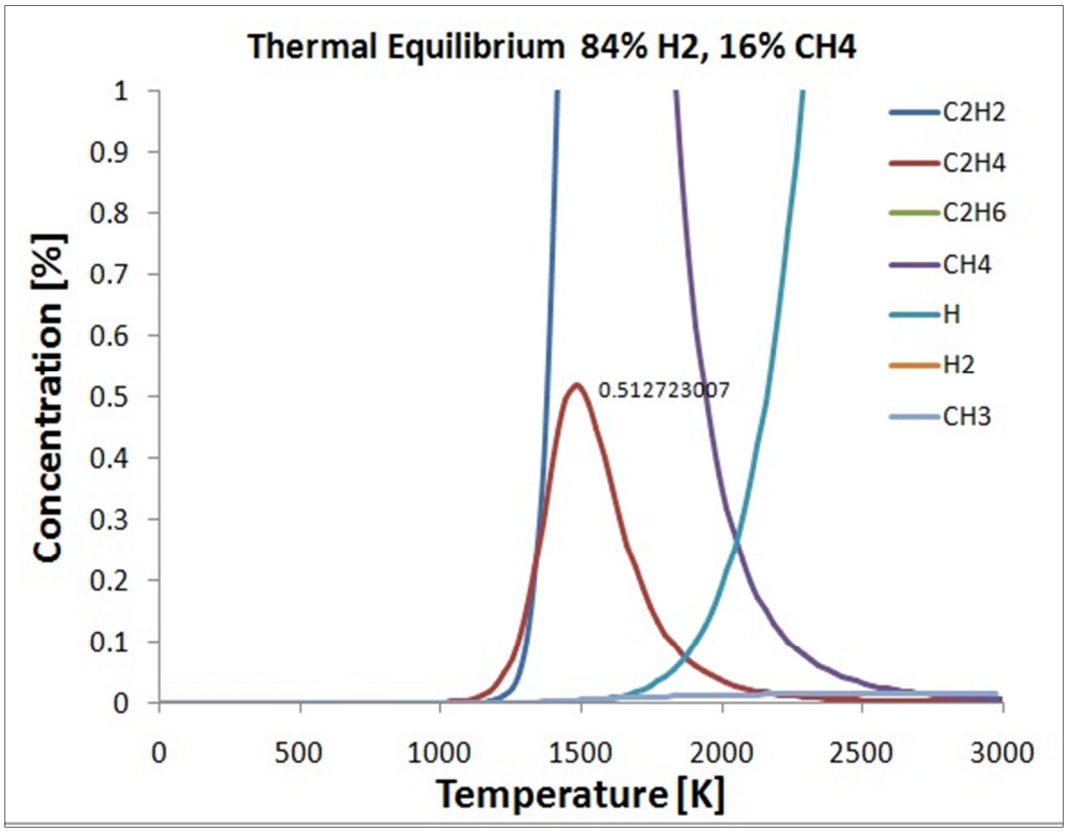

Figure 2.5 Molar concentrations of products from methane dissociation at different temperatures under equilibrium conditions at atmospheric pressure

product is stable. These products decompose into carbon and soot, if the system is brought down to room temperature slowly. To preserve the products this reduction in temperature must be as fast as possible. This is called quenching.

2.3.1.3 Reaction mechanism: Thermal coupling of methane is explained by following stepwise dehydrogenation mechanism [19].

Overall reaction of this dehydrogenation goes as:

$$CH_4 \rightarrow C_2H_{6\ (+H_2)} \rightarrow C_2H_{4\ (+H_2)} \rightarrow C_2H_{2\ (+H_2)} \rightarrow C_{(+H_2)} \quad \ldots\ldots\ldots\ldots\ (1)$$

The chain is initiated by generation of methyl free radicals from methane .

$$CH_4 \rightarrow C\dot{H}_3 + \dot{H} \quad \ldots\ldots\ldots\ldots\ (2)$$

This initiation sequence is the primary source of methyl radicals and most important step of entire reaction mechanism. In the next step formation of ethane occurs through coupling of methyl radicals.

$$C\dot{H}_3 + C\dot{H}_3 \rightarrow C_2H_6 \quad \ldots\ldots\ldots\ldots\ (3)$$

Subsequent dehydrogenation by methyl free radicals leads to formation of ethylene and ethylene in turn dehydrogenates into acetylene. This formation of acetylene from ethylene follows a similar free radical mechanism.

$$C_2H_6 + \dot{H} \rightarrow C_2\dot{H}_5 + H_2 \quad \ldots\ldots\ldots\ldots\ (4)$$

$$C_2H_6 + C\dot{H}_3 \rightarrow C_2\dot{H}_5 + CH_4 \quad \ldots\ldots\ldots\ldots\ (5)$$

$$C_2\dot{H}_5 \rightarrow C_2H_4 + \dot{H} \quad \ldots\ldots\ldots\ldots\ (6)$$

$$C_2H_4 + \dot{H} \rightarrow C_2\dot{H}_3 + H_2 \quad \ldots\ldots\ldots\ldots\ (7)$$

$$C_2H_4 + C\dot{H}_3 \rightarrow C_2\dot{H}_3 + CH_4 \quad \ldots\ldots\ldots\ldots\ (8)$$

$$C_2\dot{H}_3 \rightarrow C_2H_2 + \dot{H} \quad \ldots\ldots\ldots\ldots\ (9)$$

Formation of other hydrocarbons and aromatics is shown in the reaction network diagram in Figure 2.6. This network was made from a set of reactions involving species. Carbon formation is not considered in this model.

Exact route of carbon formation is still unexplained but the route through formation of polycyclic aromatic hydrocarbons (PAHs) is considered as a major nucleation mechanism for soot [60,61,62]. Primary soot particles are formed from PAHs and these particles continue to grow with decomposition of acetylene on their surfaces. Hence acetylene decomposition finally leads to carbon and hydrogen [63]. Of the reaction sequence the rate of formation of unsaturated hydrocarbons is much faster than the complete decomposition reaction and the subsequent formation of solid carbon soot [64]. Hence decomposition of them into carbon and hydrogen can be prevented with the control of reaction time. Also, valuable intermediate products can be obtained by limiting the reaction time.

2.3.2 Plasma Reforming

In non thermal plasma electrons initiate the methyl radical generation subsequently leading c2 products in the same way as in thermal mechanism. Depending on discharge conditions there could be certain exceptions. Although several reaction mechanisms are proposed, none of them experimentally verified. In non-equilibrium plasma systems, the formation of free radicals and ion-radicals is accepted as important step for subsequent products.

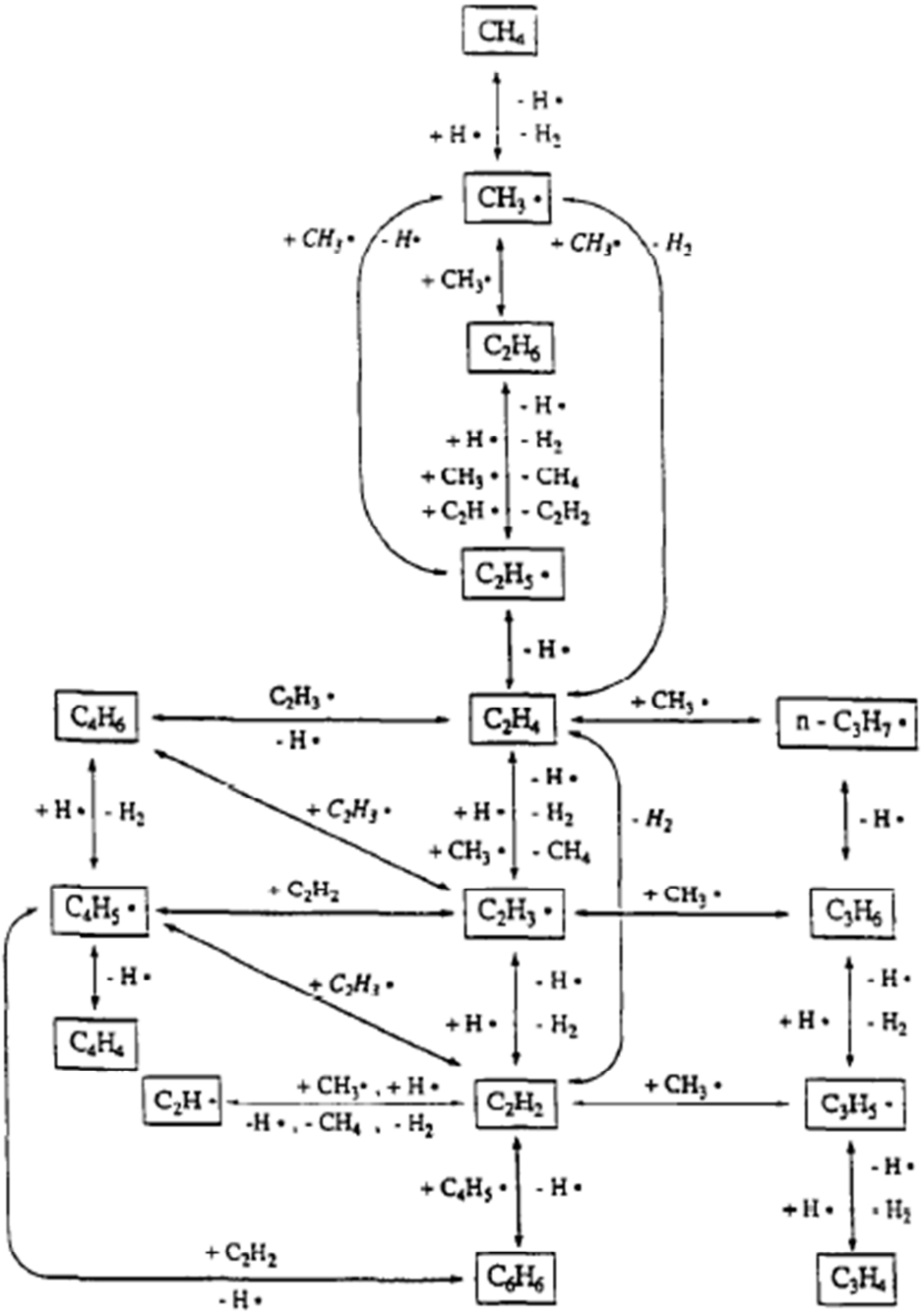

Figure 2.6 Reaction network diagram for stepwise dehydrogenation [65]

The overall reaction rate is controlled by the concentration of energized electrons with only a weak effect of temperature and reactant concentrations [23]. Since vibrational energy excitation (energy transfer into vibrational motion of molecules) can be higher in molecules, it is proposed that vibrational excitation by electrons of even moderate energies can be more effective than electronic excitation (electrons moving to higher energy levels) by electrons of higher energies.

The following reaction mechanism model from *Farouk et. al.* [71] summarizes the gas-phase hydrocarbon reactions that would happen in methane-hydrogen plasma.

Table 2.3 Methane reforming reaction mechanism in non-equilibrium plasma

Electron – Neutral reactions	Neutral - Neutral
$v \rightarrow \ Vibrational\ exciation$	$\mathbf{C\dot{H}_3 + C\dot{H}_3 \rightarrow C_2H_6}$
$CH_4 + 3e \rightarrow CH_4(v = 1,2,3) + 3e$	$\mathbf{C\dot{H}_3 + \dot{H} \rightarrow CH_4}$
$C_2H_2 + 3e \rightarrow C_2H_2\ (v = 1,2,3) + 3e$	$C_2\dot{H}_5 + \dot{H} \rightarrow 2C\dot{H}_3$
$C_2H_4 + 3e \rightarrow C_2H_4\ (v = 1,2,3) + 3e$	$C\dot{H} + CH_4 \rightarrow C_2H_5$
$C_2H_6 + 3e \rightarrow C_2H_6\ (v = 1,2,3) + 3e$	$C\dot{H}_2 + CH_4 \rightarrow 2\ C\dot{H}_3$
$CH_4 + e \rightarrow C\dot{H}_3 + \dot{H} + e$	$C\dot{H}_2 + CH_4 \rightarrow\ C_2H_4 + H_2$
$CH_4 + e \rightarrow C\dot{H}_2 + 2\dot{H} + e$	$C\dot{H} + CH_4 \rightarrow C_2H_4 + \dot{H}$
$CH_4 + e \rightarrow CH_4^+ + 2e$	$C_2\dot{H}_5 + \dot{H} \rightarrow C_2H_4 + H_2$
$CH_4 + e \rightarrow CH_3^+ + \dot{H} + 2e$	$CH_4 + \dot{H} \rightarrow C\dot{H}_3 + H_2$

Table 2.3 continued

$C_2H_6 + e \rightarrow C_2\dot{H}_5 + \dot{H} + e$ $\mathbf{C_2H_4 + e \rightarrow C_2H_2 + 2\dot{H} + e}$ $C_2H_6 + e \rightarrow {C_2H_4}^+ + 2e + H_2$ $C_2H_4 + e \rightarrow {C_2H_4}^+ + 2e$ $C_2H_2 + e \rightarrow {C_2H_2}^+ + 2e$	$C\dot{H}_3 + \dot{H} \rightarrow C\dot{H}_2 + H_2$ $C_2H_6 + \dot{H} \rightarrow C_2\dot{H}_5 + \dot{H}$ $C\dot{H} + C\dot{H}_3 \rightarrow C_2\dot{H}_3 + \dot{H}$ $C_2H_6 + C\dot{H}_3 \rightarrow C_2\dot{H}_5 + CH_4$ $C\dot{H} + C\dot{H}_2 \rightarrow C_2H_2 + \dot{H}$ $C_2H_4 + \dot{H} \rightarrow C_2\dot{H}_3 + H_2$ $C_2\dot{H}_3 + \dot{H} \rightarrow C_2H_2 + H_2$ $C_2\dot{H}_3 + C\dot{H}_2 \rightarrow C_2H_2 + C\dot{H}_3$ $C\dot{H}_2 + C\dot{H}_2 \rightarrow C_2H_2 + H_2$ $C_2\dot{H}_3 + C\dot{H} \rightarrow C_2H_2 + C\dot{H}_2$ $C_2H_2 \rightarrow 2C_s + H_2$ $\mathbf{C_2\dot{H}_5 + H_2 \rightarrow C_2H_6 + \dot{H}}$
Ion - Neutral	Electron – Ion
$CH_4^+ + CH_4 \rightarrow CH_5^+ + C\dot{H}_3$ $CH_3^+ + CH_4 \rightarrow {C_2H_5}^+ + H_2$ $CH_5^+ + C_2H_6 \rightarrow {C_2H_5}^+ + CH_4 + H_2$ $H_3^+ + CH_4 \rightarrow CH_5^+ + H_2$ $H_3^+ + C_2H_6 \rightarrow {C_2H_5}^+ + 2H_2$ $H_3^+ + C_2H_4 \rightarrow {C_2H_5}^+ + H_2$	$CH_4^+ + 2e \rightarrow CH_4 + e$

Hence glow discharge or gliding arc discharge are expected to perform better than corona or DBD. The highlighted reactions of methane in neutral-neutral reactions are recognized as the most efficient by certain modeling studies [56] in which free radicals are consumed similar to thermal mechanism to produce ethane. Ethylene production is attributed to electron impact ionization of ethane and C_3 products and consecutive ion recombination. The highlighted transformation from ethylene to acetylene in electron-neutral reactions is considered to be the cause of low ethylene yields.

2.3.3 Effects of Kinetics and Dilution

Product yields of methane reforming are highly dependent on reaction conditions. Product distribution and conversion rate is dependent on temperature and residence time. Figure 2.7 shows variation in the conversion rate of methane for different temperatures with respect to residence times. Higher the temperature more the rapid is the change in conversion rate. In general C_2 products are favored at high temperatures and short residence times. High yields of acetylene or ethylene are only possible at low hydrocarbon partial pressures [7]. An increase of the partial pressure of acetylene above a certain limit will result in a dramatic increase in carbon formation.

2.3.3.1 Hydrogen addition: With hydrogen dilution, the reactions involving hydrogen radicals become more important than the reactions involving methyl radicals. Dilution of the methane feed with hydrogen was found to be effective in suppressing carbon formation. It inhibits reactions leading to carbon, aromatic hydrocarbons; hence it decreases the selectivity for benzene and increases the selectivity's for C_2 compounds

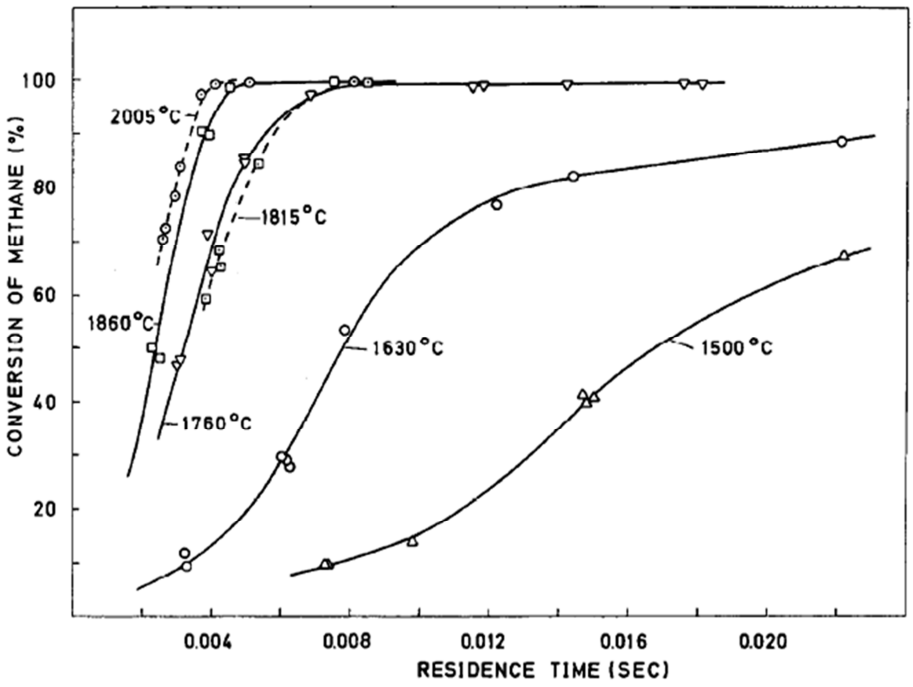

Figure 2.7 Conversion rate of methane with change in residence time [70]

[19, 66-69]. This also comes with a disadvantage of increasing the reverse reaction rate methane to methyl radicals, thereby decreasing the conversion rate of methane.

3. PLASMA REACTOR SETUP

It is seen from our literature review that low energy DBDs and corona discharges favor ethane as end product, whereas high energy density systems favor acetylene as product. As we move from highly non-thermal plasmas to more of thermal plasmas, the product selectivity moves from ethane, lower yields to acetylene along with carbon, higher yields. Our aim is to design a system that can maintain the discharge conditions close to non-thermal operation but with slightly higher temperatures, hence a glow discharge with "warm" conditions will be used to perform reforming.

3.1 System design

The basic idea of the system is to generate a glow discharge between two electrodes of small diameter facing each other and aligned axially. This discharge will be setup in a glass chamber through which the feed mixture flows at constant rate. Products from reaction of glow discharge with feed gas will then flow towards exit.

Requirements of our system:

1. Glow discharge of currents in the range of 5-50mA.
2. Operate the system at atmospheric pressure.
3. Minimize heat loss and at the same time try to keep the discharge ambience at lower temperatures.

4. Effective flow conditions - Since the discharge size will be on the order of few microns, it is necessary to make a system where most of input feed will pass through discharge.

5. Visibility of discharge is important to study the changes under different operating conditions.

6. The chamber used should sustain high temperatures and be leak proof.

7. Material used for electrodes should be of high melting temperatures and non-reactive to plasma.

8. Along with at least one input and output port for flow of gas, there should be a entry port for high voltage cable connection to anode and another for cable connecting cathode to ground.

9. Rigid construction and placement of electrodes for discharge stability.

10. Construct a simple system with easily available parts at minimum cost.

Preliminary experiments are conducted with a basic setup of two electrodes serving as anode and cathode as seen in Figure 3.1. The electrodes were stainless steel rods of 1.5 mm diameter and the tube is a 8mm transparent quartz tube. Heavy sooting at flow rates less than 1 slpm, high reactor temperatures and hot spots on both electrodes were observed. Currents in this system were limited to 18 mA.

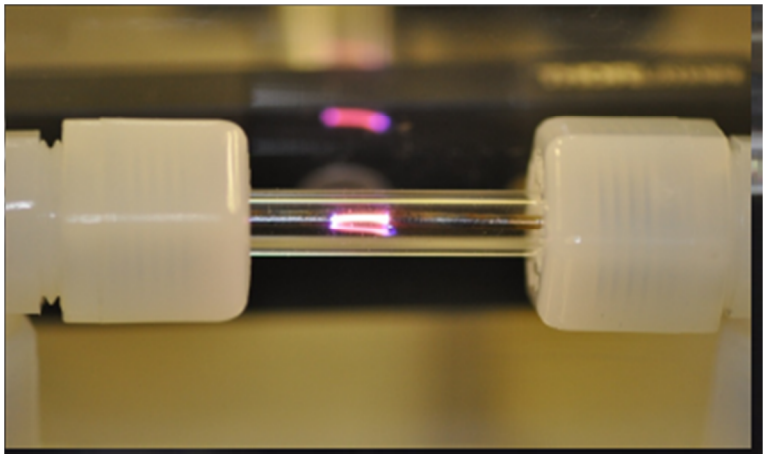

Figure 3.1 Initial plasma reactor setup for test runs

To enhance heat transfer, so as to keep the reactor ambient gas temperature close to room temperature, most of heat loss has to occur through conduction and not convection. Hence the idea of using small diameter (< 2 mm) capillary tubes as electrodes in a glass chamber was initially conceived. This system is our first setup to experiment for methane reforming and is called as counter flow micro plasma. Later a second system

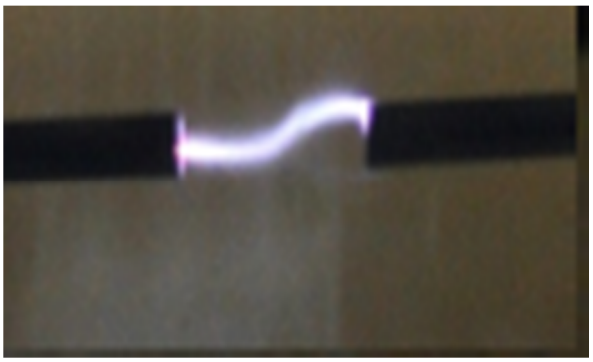

Figure 3.2 Counter flow micro plasma

Figure 3.3 Magnetic glow discharge

with a rotating glow discharge fulfilling same requirements is designed. A DC glow discharge generated between a grounded tube and a axial high voltage electrode. This discharge is subjected to magnetic field by use of a strong magnet around the grounded tube. Under influence of magnetic field the discharge rotates. Gas fed into this system flows perpendicular to discharge and through it. This system is termed as magnetic glow discharge system for remaining part of this writing. Figure 3.2 shows a counter flow micro plasma and Figure 3.3 shows a magnetic glow discharge as it appears to eye.

3.2 Experimental setup

3.2.1 Reactor Setup

3.2.1.1 Counter flow micro plasma: Stainless steel dispensing needles of 0.75mm inner diameter are chosen to serve the purpose of electrodes. These hollow electrodes will conduct the heat away from plasma more efficiently than solid electrodes. Sanitary fittings from st.patricks have been used for the chamber assembly. For the purpose of visibility and holding discharge in the ambience of methane gas, a sight glass s of 25 mm ID and 5 mm thick with stainless steel tri clamp ends has been used. A couple of BSPP thread to triclamp adapters are joined to the reactor chamber setup. Capillary electrodes are held in the center of chamber through these triclamp adapters through a series of compression fittings. This allows to precisely place the openings of electrodes in line and facing each other. Outside ends of triclamp adapters are connected to 1/4th inch high pressure gas carrier tubes. A 1.5" triclamp union with a 1/4" MPT is added to reactor

chamber on the side of ground electrode. The MPT opening can be used as an exit choice, if not it could be sealed with a cap. This was installed to check the effects of flow configurations on the discharge conditions. The chamber is sealed with heavy duty clamp pins on either sides. This system is rated for pressures below 150 Psi. High voltage wire from power supply is clamped to the triclamp adapter on anode side using a steel ring. Since our cathode is directly connected, entire cathode portion of reactor

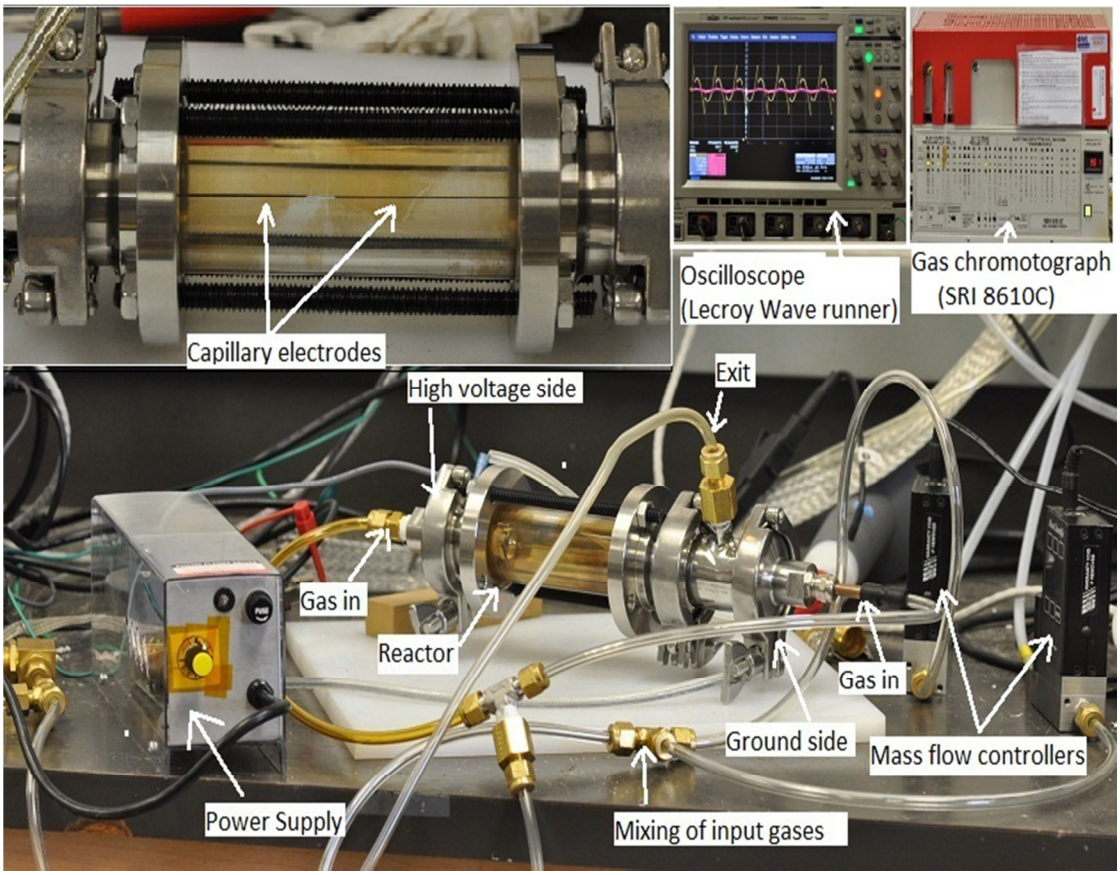

Figure 3.4 Counter flow micro plasma reactor setup

will be at high voltage when powered. In addition, it helps in conducting heat away from electrodes. Figure 3.4 shows this reactor setup with its parts.

3.2.1.2 Magnetic glow discharge system: A 3/4" ID and 1/2" OD copper tube is used as ground electrode. A copper rod of 1mm diameter placed concentrically in the tube serves as high voltage electrode. 3/4" Tee-compression fittings are joined on both sides of copper tube. While the T sections on both sides serve as gas input and exit ports, the axial section brings the high voltage copper rod out of system on one side and on other

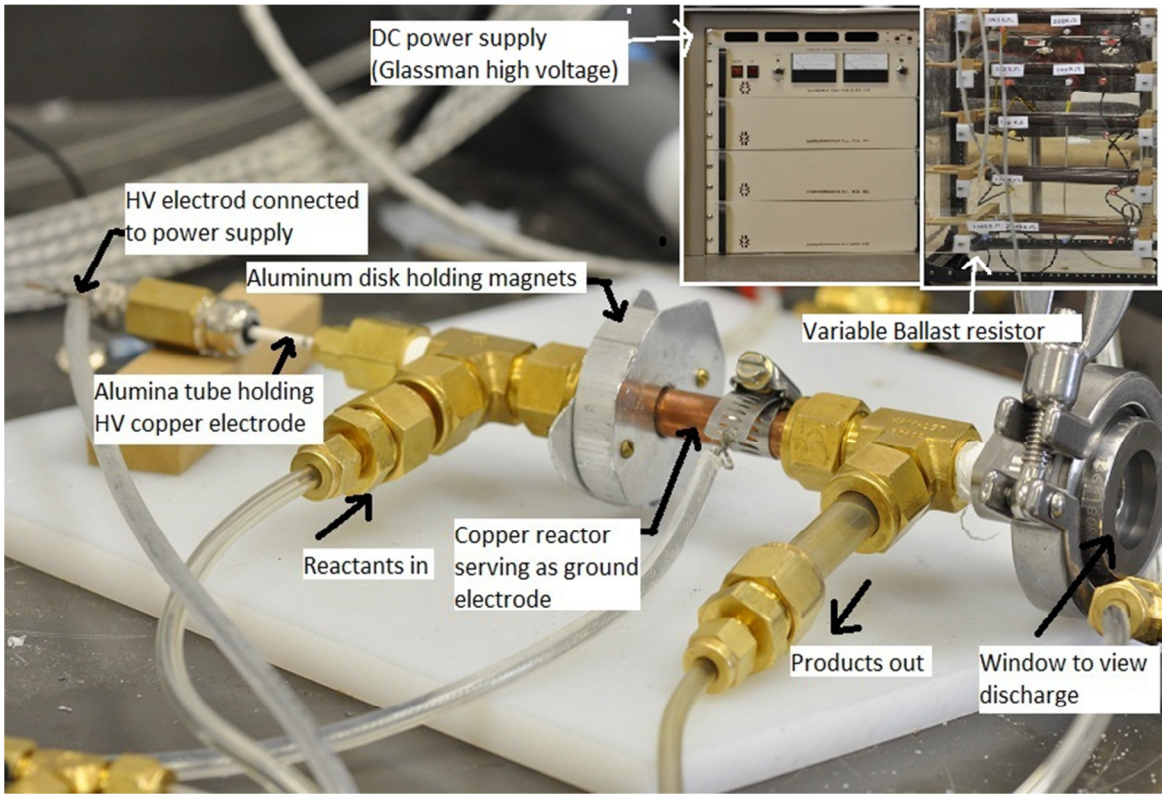

Figure 3.5 Magnetic glow discharge reactor system

side it ends with a triclamp adapter. To contain the discharge to single location of 2mm, an alumina tube is placed over copper rod over covering entire rod except at desired location of discharge. Alumina is chosen in particular owing to its high thermal resistance and low thermal, electrical conductivity.

The input side of system is joined to 1/2" to 1/8" compression fittings, with alumina covered copper rod exiting out of it. Copper rod in alumina is sealed with temperature resistant adhesive. Whereas the outside with triclamp adapter is sealed with a glass window using heavy duty clamp pin. This window serves the purpose of discharge visibility. Six powerful cylindrical magnets are are used to setup magnetic field around copper tube at this location. An aluminum disk is hung at the discharge position around the copper tube to hold the six magnets in position. A small aluminum cylinder is machined to hold the alumina tube inside the copper tube. This disk helps in precise positioning of electrode concentrically with copper tube. Six small holes are drilled around the central hole of this disk allowing the gas to flow to exit. This also helps in maintaining the visibility of rotating discharge. Figure 3.5 shows reactor setup with its parts.

3.2.2 Flow Lines

Input gases used for experiments are industrial grade (99.8% purity) methane and hydrogen purchased from AOC welding supplies. Two lines of 1/4" high pressure PVC gas carrier tubes bring these gases to reactor system. Flow of gases and proportion is controlled with two Alicat scientific mass flow controllers. Lines passing through mass

flow controllers are merged using a Tee-compression fitting for mixing input gases. On the exhaust line, a Tee-compression fitting is inserted followed by a ball valve for the purpose of collecting samples for gas chromatography studies. A 30mm plastic syringe is used for taking product sample to gas chromatograph.

3.2.2.1 Counter flow micro plasma: For micro plasma reactor the gaseous mixture is divided into two lines using another Tee - compression. These lines are connected to either sides of reactor to feed the gas into reactor through both the hollow electrodes. The MPT opening of triclamp union on ground side serves as flow exit to exhaust line. To facilitate discharge gap variation, ground electrode connections are slightly modified. It is removed from triclamp and a copper tube is joined to it. This copper tube joins input feed gas connection through a brass cable gland. Discharge gap is varied by loosening the cable gland and changing it whenever needed.

3.2.2.2 Micro glow discharge system: For magnetic glow system, gaseous mixture is fed into the system to its input t section through mass flow controllers and exits through the window side t section to exhaust line.

3.2.3 Power Lines

A commercial power meter 'watts up pro' is used to measure line power. Another lab made power meter is lined up in series with watts up pro to ensure accurate readings, in case failure with watts up pro. Electric circuit and performance comparison is given in appendix A.

3.2.3.1 Counter flow micro plasma: This reactor system is powered using a PVM 400X Plasma driver. Output of this power supply is a AC 1-15 KV of 27 KHz frequency with rms currents varying from 13-25 mA. High voltage wires join reactor to power supply and ground. Voltage and current are measured on a Lecroy Waverunner 204Mxi oscilloscope using a PMK-14KV AC voltage probe and Bergoz CT-B0.5 Current transformer respectively. Digital processing of waveforms from this oscilloscope is discussed in section 5.1.

3.2.3.2 Magnetic glow discharge system: A high voltage DC power supply is used to power magnetic glow system using high voltage wires. Its output varies in the range of 1-9.9 KV with maximum possible currents up to 250 mA. A variable ballast resistor setup (30 - 400 KΩ) is added to limit the currents in the discharge. Copper tube is grounded. Although voltage and currents can be measured on the power supply, oscilloscope was also used for accurate measurements . A small resistor (10Ω) is added to circuit on the ground side for current measurement on oscilloscope. The circuit and details are explained in power measurements section (5.1).

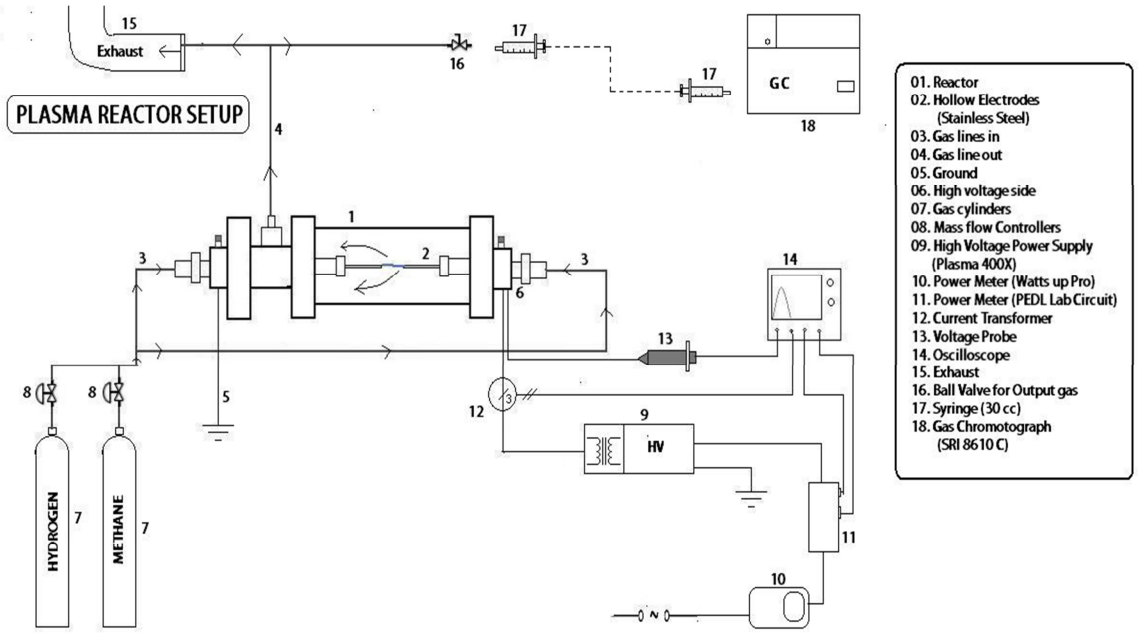

Figure 3.6 Counter flow micro plasma experimental setup block diagram (view 1)

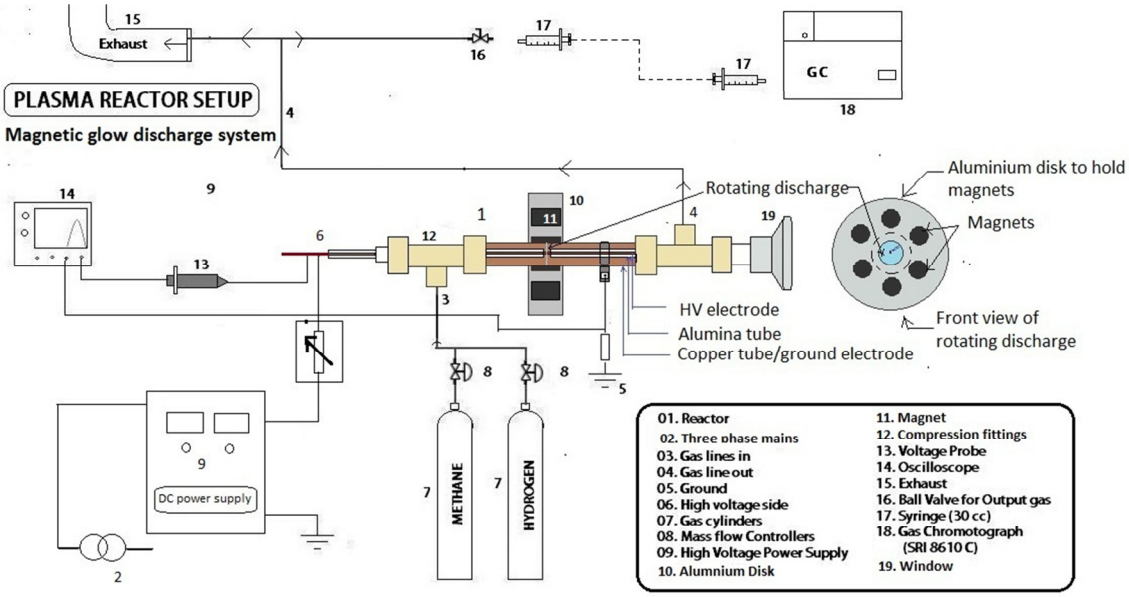

Figure 3.7 Counter flow micro plasma experimental setup block diagram (view 2)

3.2.4 Gas Chromatograph

Output composition of gas is determined using SRI 8610 C multiple gas analyzer # 3 gas chromatograph. This system is equipped with a carbon Molecular Sieve 13X and Hayesep D columns in series. Hayesep D is replaced with silica gel column for better separation of C_2 products. Gases are detected using a Thermal conductivity detector and a helium ionization detector with detection limits of 1% and 50 ppm respectively. More details on specifications of all the instruments are provided in appendix A.

The basic outline of experimental setup along with flow lines, electrical connections and accessories is shown in the Figure 3.6 for micro plasma reactor and in Figure 3.7 for magnetic glow discharge reactor.

3.3 Reactor configuration

3.3.1 Counter Flow Micro Plasma

Micro plasma is generated between the stainless steel hollow electrodes in different flow configurations. Flow entering from anode, exiting through cathode and vice versa. This is axial flow configuration. This kind of flow seems to produce hot spots on either of electrodes with large temperature rise on cathode or anode and operation at higher powers is not feasible. Hence flow entering the reactor from both electrodes and exiting through a third opening is chosen. This offered two advantages. It allows higher powers without hot spots on either of electrodes and also this flow conditions result in a stagnation point, thereby allowing better interaction of input gaseous mixture with

discharge and better mixing. Methane and hydrogen molecules enter through the electrodes react with plasma components. Temperature of the mixture is raised to above

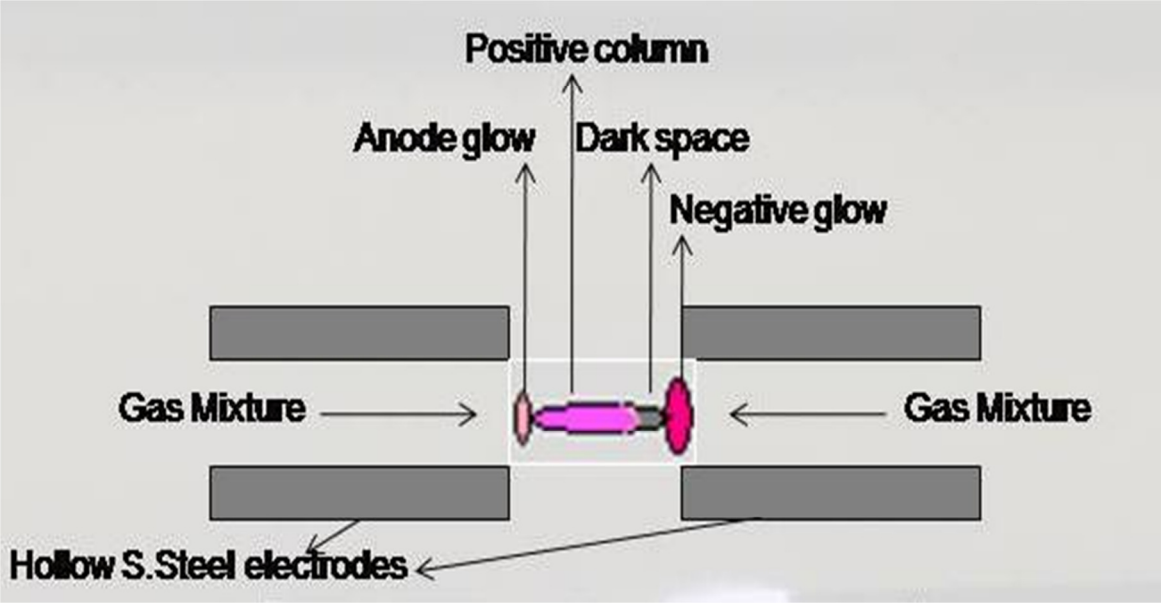

Figure 3.8 Reactor configuration showing glow discharge and its components for micro plasma

1500K, reactants form products during the time it spends in discharge gap and then flows outward along with products. This stream is now mixed immediately with previously cooled gas stream and un-reacted methane gas reducing its temperature to above room temperatures. Figure 3.8 shows the counter flow micro glow discharge with glow discharge components.

3.3.2 Magnetic glow discharge system

High voltage electrode is covered with alumina tube on either sides of location of discharge, leaving a 2mm gap at the point. Alumina prevents the discharge from happening at any other place . When the central high voltage electrode is raised to high voltage it breaks into a glow discharge. In the absence of magnetic field, the discharge looks like a single filament between electrodes. It just stay s there. When a magnetic field is applied ,as shown in the Figure 3.9, this electrons and ions in the discharge move in the direction perpendicular to their motion and magnetic field , i.e. radial direction to the cross section. This results in rotation of entire discharge. The frequency of this discharge depends on input power and in this system it varies between 200-400 Hz. We can still see the filaments in the discharge. Input feed gas flows into this discharge, forms products and along with un-reacted gas moves down-stream to exit.

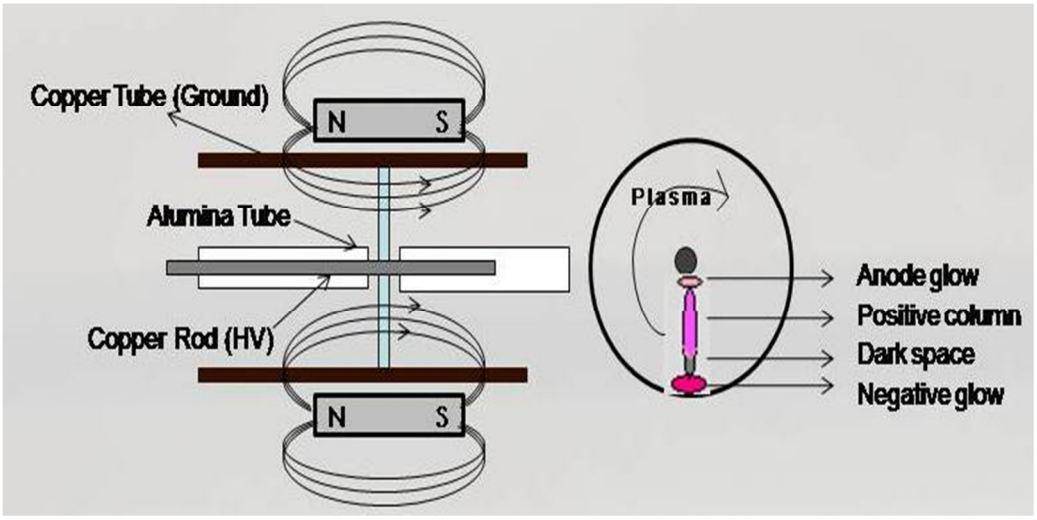

Figure 3.9 Reactor configuration showing glow discharge and its components for magnetic glow system

Table 3.1 A comparison of both the discharge systems

Characteristics	**Counter flow micro plasma system**	**Magnetic glow discharge system**
Type of power	AC	DC
Residence time	0.04-0.3 ms	0.3 – 2.9 ms
Flow alignment with discharge	Aligned until half way and then moves outward	Perpendicular to discharge
Flow in reactor	Counter flow	Axial in one direction
Specific characteristic	Stagnation point	Rotating discharge
Power limits (for FL >= 1 slpm)	Up to 45W	Up to 120 W
Electrode type	Hollow stainless steel tubes	Solid copper rod
External field	NO	Magnetic field
Discharge gap	6.01 mm	3.04 mm
Stable run time	Short ~ 40mins @ 0.5 slpm	Longer; >80 mins @ 0.5 slpm

This plasma appears like disc when directly viewed, but its variations can be seen in the figure at different shutter speed. At constant flow rate, the amount of gas exposed to plasma depends on frequency of discharge. For instance, referring to 200 Hz frequency, image taken at a shutter speed of $1/400^{th}$ of second, residence time of gas at 1 ms, only 20% of plasma is the section interacting with the gas molecules. The remaining gas just passes without anything.

Table 3.1 highlights the differences between counter flow micro plasma system and magnetic glow discharge system.

4. DIAGNOSTIC TECHNIQUES AND ANALYSIS METHODS

Power and product composition are measured using oscilloscope and gas chromatograph respectively. The measurement methods are designed to ensure maximum possible accuracy. The following section discusses the procedure of calculating values and performing mass and energy balances using them.

4.1 Voltage and current

Methane reforming in any experimental system utilizes certain amount of power and for feasible economics we wish to minimize the energy spent. Hence, accurate measurements of power should be made for measuring the productivity of the experimental system. Here we define two powers that will be measured with appropriate instrumentation and these numbers determine the productivity of system.

4.1.1 Plasma Power

Plasma power, also called discharge power, is defined the energy expended by the reactor system in converting methane and mixture into their corresponding products, while losing some energy into heating the gases and reactor. Plasma power in other words is power measured at high voltage input electrode outside the reactor for both the reactor systems. This measured power value will be considered as the energy spent in converting a kg of methane or for producing a kg of product and it will be a measure of economical efficiency of this process.

4.1.1.1 Method of measurement: During the experiment a voltage probe and current transformer are used to generate voltage and current waveforms respectively on oscilloscope. These waveforms are then saved as matlab files. This digital information is loaded into matlab for post processing. Figures 4.2 & 4.3 shows a oscilloscope generated voltage and current waveforms for a sample run in matlab. A matlab code is written to generate a power waveform and integrate it for average power. This matlab code for is provided in appendix B.

$$P = \frac{1}{T} \int_0^T I(t).V(t)\, dt \qquad \text{.....(4.1)}$$

In addition rms voltage, rms current is also calculated. To ensure minimum uncertainty in

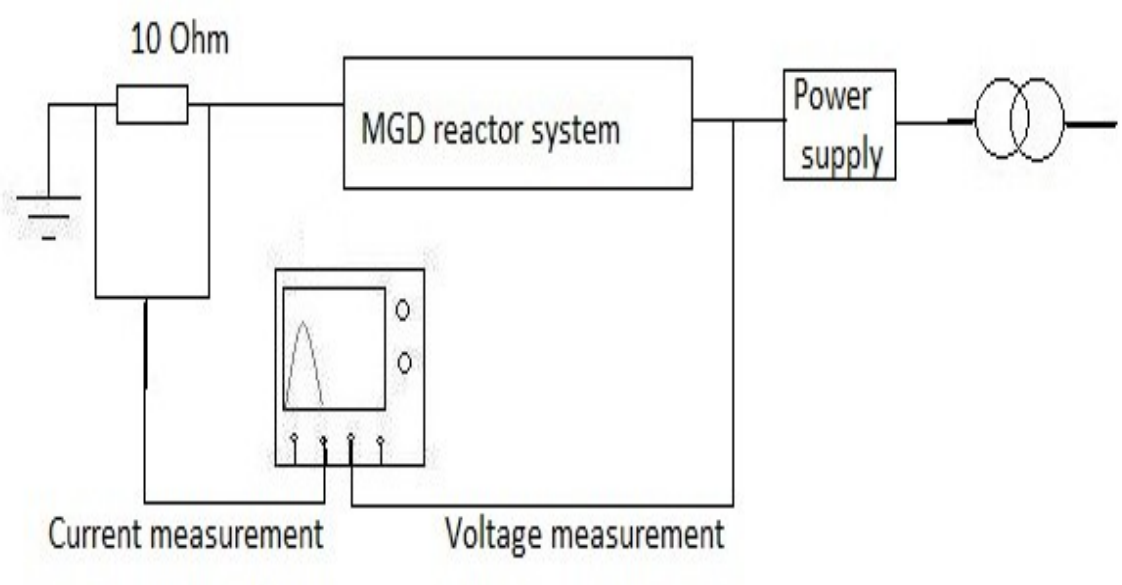

Figure 4.1 Voltage and current measurement in micro discharge system

this calculation, the waveform data is ensured to have more than 12 cycles if the power is AC. In the case of magnetic glow system, current is measured across an end resistor added to the grounded end of plasma circuit. This is shown in Figure 4.1. Voltage drop across this small resistor (10Ω) it is measured on oscilloscope. The resulting signal is attenuated with a factor of 10 to generate results for current. Mean values of current, voltage and power waveforms are then calculated.

We can see an increase in current and voltage, and when break down happens there is a constant voltage indicating glow discharge mode and due to pulsing input a decrease in current and voltage happens. In the case of magnetic glow discharge it's a constant DC voltage around 1KV with currents ranging between 12-50mA for our experiments. A general comparison of the discharge in their electrical parameters is shown in Table 4.1.

4.1.2 Line Power

Line power is defined as the total power input into the methane reforming system. There is energy lost to power supply system, heating of the ballast resistors, connecting wires and then energy spent for reactor and the process inside it. This is necessary for determining the economics of the process. Most of the power supplies are 30-50% efficient and loss of heat in ballast resistors is considerably high in case of high power systems. Figure 4.5 illustrates the difference in plasma power and line power. Line power is measured with watts up Pro commercial power meter. But these meters fail if a pulsed discharge is generated in reactors which produce electro-magnetic due to the

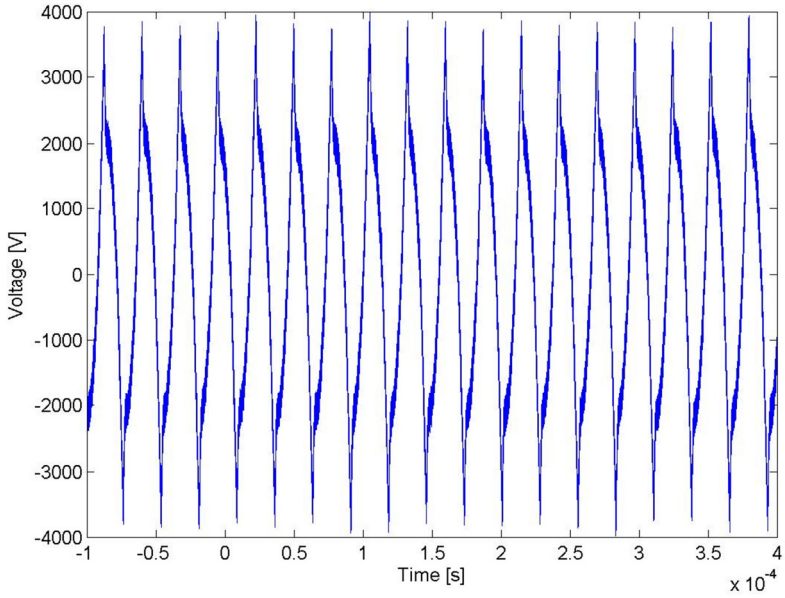

Figure 4.2 Voltage vs time for micro plasma. At 1 slpm; 26 W;

16% methane + 84% Hydrogen; Gap = 6 mm

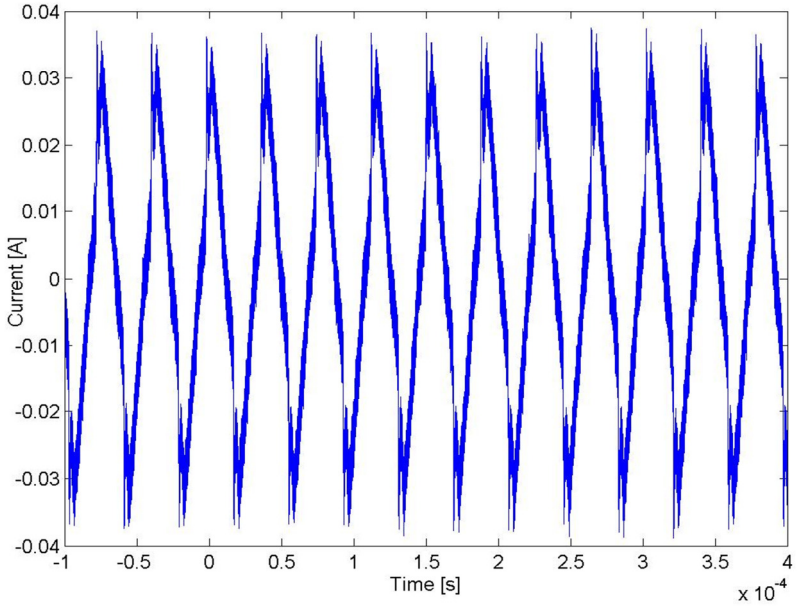

Figure 4.3 Current vs time for micro plasma. At 1 slpm; 26 W;

16% methane + 84% Hydrogen; Gap = 6 mm

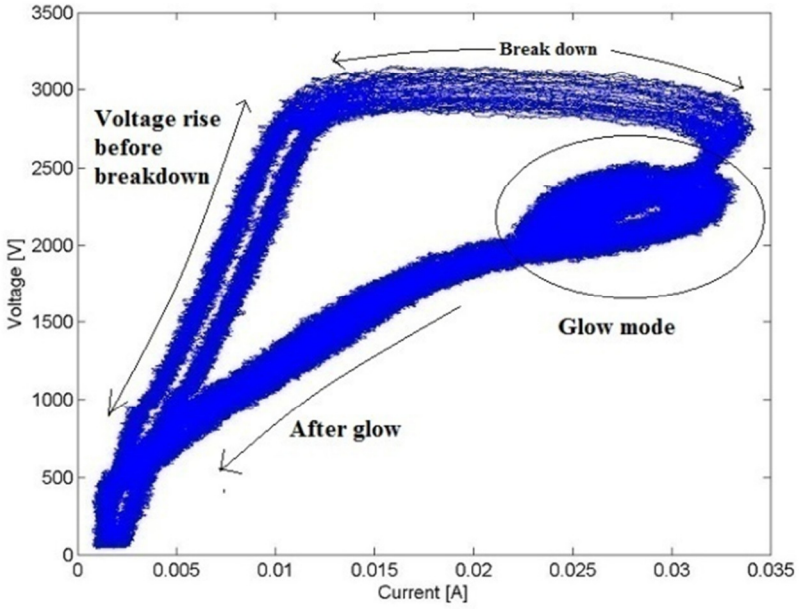

Figure 4.4 VI plot of micro plasma

Table 4.1 Power characteristics of micro plasma and magnetic glow systems

Parameter	**Counter flow micro plasma with PVMx**	**Magnetic glow discharge system with DC Power supply**
Voltage range	0.8-2.5Kv	1-9.9 Kv
Currents	12-25mA	12-250mA
Power	13-45W	3 – 300 W
Frequency	AC : 27.1 KHz	Rotating DC : 200Hz

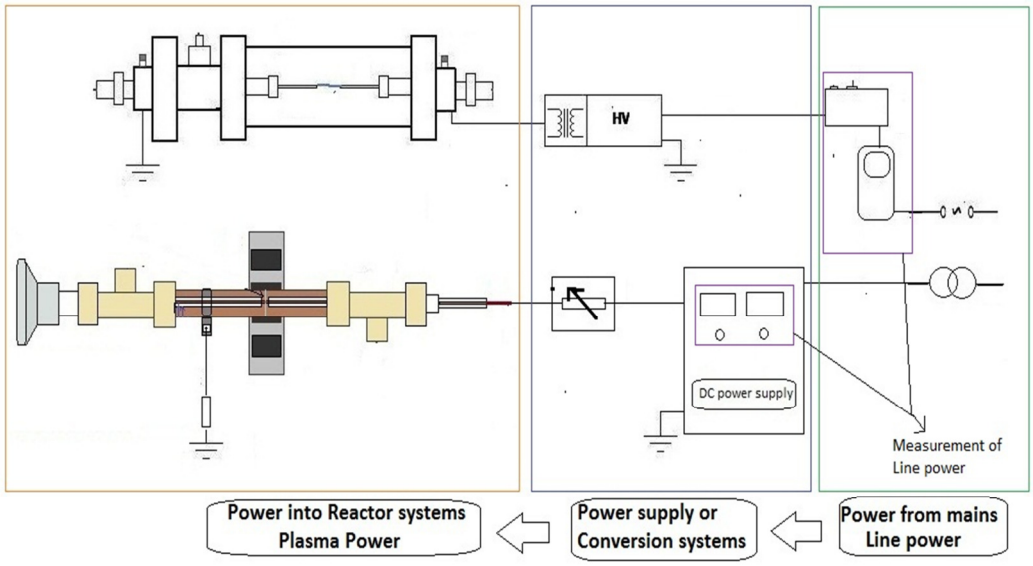

Figure 4.5 Line power and plasma power measurements for both reactors

possible effect of back EMI through cables. Hence a simple circuit for measuring line power is designed to measure line voltage and line current on oscilloscope. The basic idea is to make and setup a circuit between load and mains. Then connect it to Oscilloscope and measure waveform, Current, Power being drawn by load.

A simple circuit with a large resistance connected across the load and one small resistor in series with load. Voltage drop across small resistor and large resistor will be a measurement of current and voltage respectively. Voltage measurement across this resistor gives us data for line voltage. Two isolation amplifiers (ISO 122P) powered by DC power supplies (TEL 3-1213) are connected across these resistances aid in measuring the voltage drop. The output of these amplifiers can be generated as

waveforms on oscilloscope through BNC connectors and cables. The finished circuit is shown in Figure 4.6.

Specifications of the electronics and detailed working of the circuit, circuit diagram along with block diagram are provided in Appendix A.

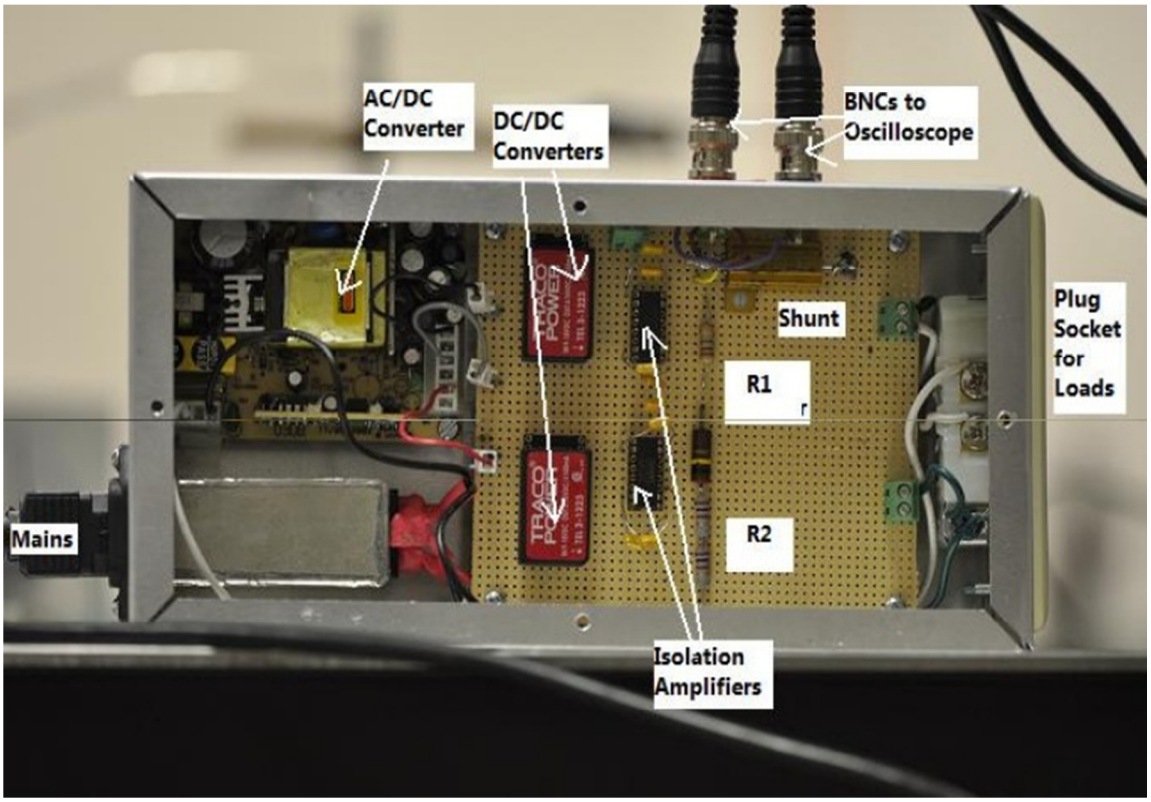

Figure 4.6 Lab made electronic device for measuring line power on oscilloscope

Voltage and current waveforms generated on oscilloscope are used to calculate power by post processing them in mat lab in the same fashion as described for plasma power. The calculated power will be the total power utilized the entire experimental system. In addition to this value, this setup itself utilizes some power for working and it is

measured to be 6.5W with watts up pro meter. Hence the total line power expended for this system will be

Linepower [W] = Power measured [W] + 6.5W. ……..(4.2)

4.1.3 Power Efficiency

Efficiency of a power supply is calculated to be a ratio of plasma power to line power.

η = Plasma power / Line power. ……..(4.3)

This efficiency is of the power supply used for discharges and in general for most loads its close to 50%. If there are external resistors added in between the circuit, like ballast resistors then the heat loss mode from ballast resistors will be considerably high and hence it lowers the efficiency. Note that in such a case heat lost form resistors has to be subtracted from line power for efficiency. Although line power is important in for the economics of methane conversion in industry, efficiencies can be considerably improved with better power supplies and hence our economical analysis in this research will be concerned with plasma power rather than line power.

4.2 Gas chromatography

4.2.1 Description

Product stream gas composition and their individual concentrations are determined using a SRI made gas chromatograph system. A gas chromatograph essentially separates

Table 4.2 Efficiencies of power supplies used for two discharge systems

Micro plasma			Magnetic glow discharge		
Line power [W]	**Plasma power [W]**	**Efficiency [%]**	**Line power [W]**	**Plasma power [W]**	**Efficiency [%]**
35	**18**	**51**	**50**	**24**	**48**
59.5	**28**	**47**	**72.8**	**28.6**	**39.2**
105	**40**	**38**	**108.9**	**36.3**	**33.3**

components of sample gas with pre-installed columns . These separated products as they flow out system go through TCD and HID detectors in series. These detectors generate signals in proportion to the amount of gas flowing through them. Signals generated are plotted against run time on software. The plot of signal response to time is called as chromatogram, which holds all the information about product and its concentration in the injected sample. Chromatogram shows different peaks at different times. These peaks represent each component in the gas and their concentration will be in direct proportion to area under the peak. The proportionality constant for each components of gas is different and it varies with the gas component, detector, carrier gas, operation temperature of detector and flow rate of carrier gas. This proportionality constant is called as calibration constant. At constant conditions of flow rate and temperature and

carrier gas, higher the concentration, higher the area of peak. Two sets of signals are generated, one for TCD detector and one for HID detector. A TCD detector is used to detect high concentrations varying from 1-99%, whereas a HID detector is used to detect concentrations under 1% or 100000 ppm until 50ppm. The carrier gas used for our GC is Helium of ultra high purity (99.999%) purchased from AOC welding supplies.

Figure 4.7 shows a sample chromatogram with all the gases we deal in our experiments. The time at which these products come out or being detected is called retention time which again depends on the weight of the individual components. In our GC, the following gases can be detected (mentioned in the order of their retention times) - Hydrogen, oxygen, nitrogen, argon, methane, carbon monoxide, ethane, carbon dioxide, ethylene, acetylene and higher hydrocarbons. While gases from Hydrogen to CO are separated by molecular sieve 13x, the remaining high molecular weight compounds are separated on a silica gel column. Gas chromatogram specifications are provided in appendix A.

4.2.2 Calibration

Any measurement is validated by the accurate calibration of the instrument used. GC is no exception and calibration in gas chromatography is most essential part of measuring product concentrations. Calibration is a comparison between measurements - one of known magnitude or correctness made or set with one device and another measurement made in as similar a way as possible with a second device. The device with the known or assigned correctness is called the standard. In case of gas chromatography, the retention

times, product concentrations depend on lot of factors like columns used, column temperature, carrier gas type, carrier gas flow rate, detectors installed, detector temperature and more. Hence, GC has to be calibrated at regular intervals of time (one week to a month, depending on the change in signal response), especially before a new set of experiments to ensure best results.

4.2.1.1 Procedure of calibration: A calibration mixture composed of ethylene, ethane, acetylene each in 5% and another with methane, CO, CO2, hydrogen, oxygen each in 4% are purchased from Air liquide. Multiple runs are performed on GC with samples from these standards to ensure accuracy and precision. A standard temperature profile and event table for GC is made for all the experiments to avoid errors between multiple runs. This gives us a single calibration constant for a set of experiments done in a span of two days. A calibration constant is the ratio of signal a set generated to the known input concentration for a single data point. For better accuracy we find the area of peaks at different known levels of concentration and generate a graph of area Vs concentration. This is called calibration graph.

A good calibration is identified by linearity of the graph over the entire range of detection limits of a particular detector. For that, we need at least three data points to identify the pattern of calibration graph. If it is not possible to obtain linearity over entire range, then we can identify the linear part or parts of curve for calculating calibration constants for those ranges. Calibration curves for hydrocarbons are shown in appendix A for reference.

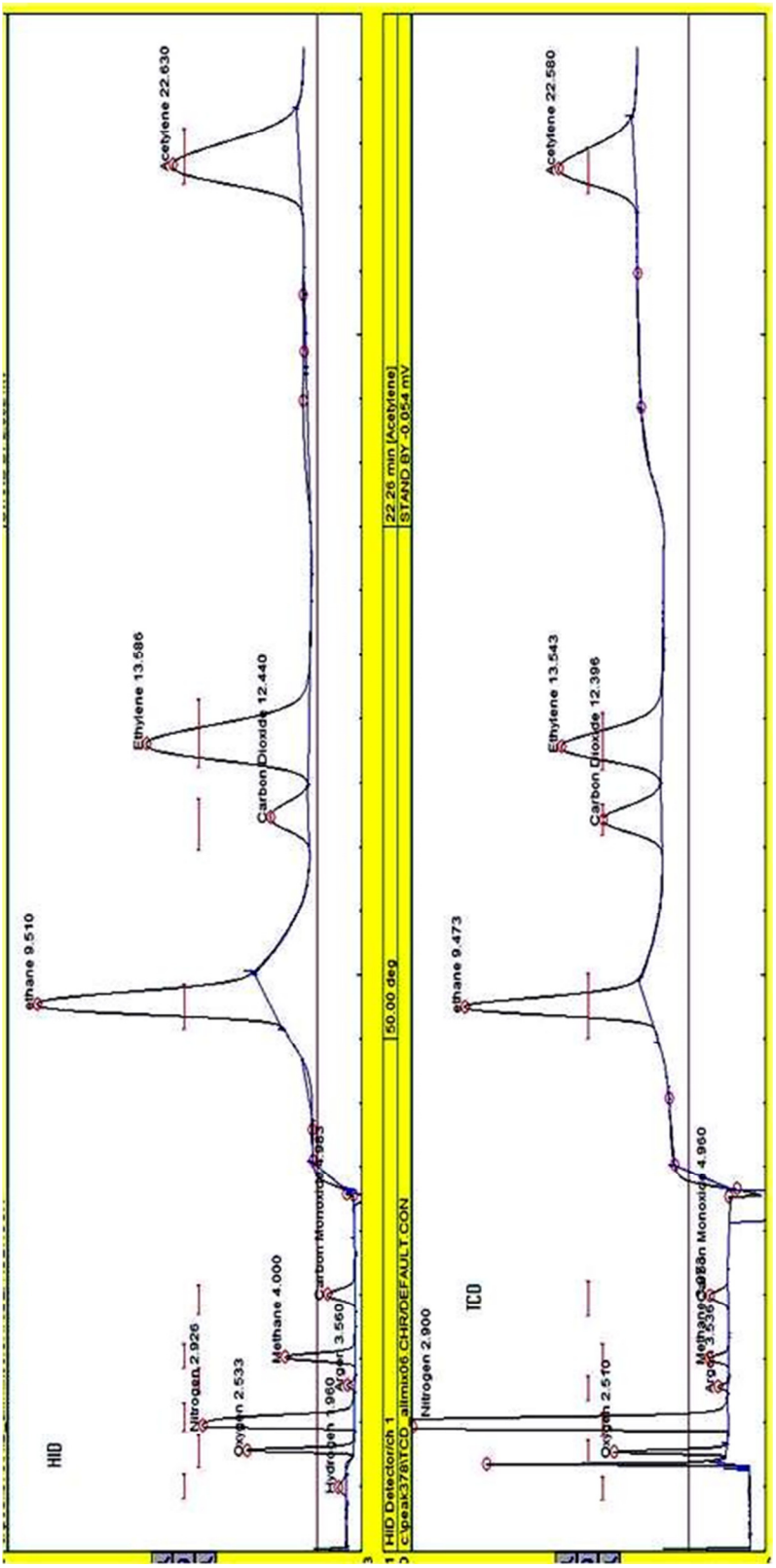

Figure 4.7 A sample run in SRI 8610C gas chromatogram showing all the gases that can be detected

4.3 Discharge gap

Variation in discharge gap will result in an increase the breakdown voltage and larger current, there by changing the discharge power. In addition to that, increase in discharge gap means an increase in residence time.

Figure 4.8 Calculation of discharge gap using matlab imtool

Discharge gap is not included as a parameter to study in this research. Hence it is maintained at constant gap. But as the experiments are being performed, a need to dissemble the reactor may arise. Upon re-assembly of the system, it's essential to ensure that the discharge gap is maintained at same constant value or same for at least a set of experiments. In the case of micro plasma discharge system, discharge gap is measured with imaging techniques. An image of discharge is taken using a digital camera. Calibration of pixels is done with a known electrode length and then the discharge gap is

calculated from it. Figure 4.8 shows a 1200/1600 resolution reactor length L1 and discharge gap length L2. Using image tool in matlab, calibration is identified and L2 Is calculated as follows.

a = 3943.17; b = 88mm (L1); d = 284.89;

Discharge gap (L2) = d*(b/a); For the case shown in picture it is 6.3 mm.

4.4 Mass balance

A mass balance is a way to check for consistency and accuracy in the results of product concentrations from gas chromatography. Essentially mass balance is an application of law of conservation to the analysis of reactor systems.

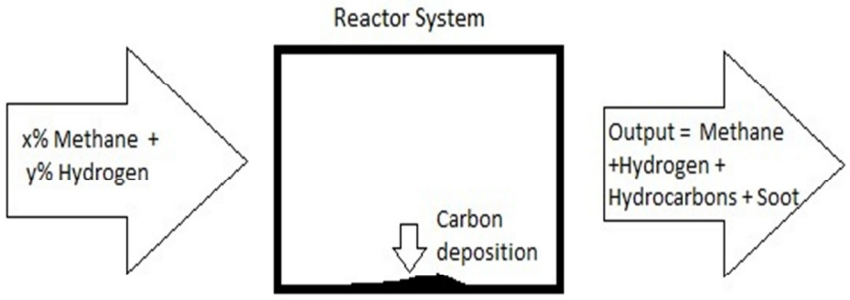

Figure 4.9 Mass balance

By accounting for material entering and leaving a system, mass flows can be identified which might have been unknown, or difficult to measure without this technique. This unknown mass in our case is carbon and any other undetected hydrocarbons. Reactor

systems in this research are continuous steady state systems, hence a differential mass balance is applied at any instant of time. For any steady state reactor system, the mass of reactants must equal to that of products.

i.e. ∑ Masses entering via input feed streams = ∑ Masses exiting via product streams

We can perform a total balance for masses entering and exiting the reactor or else for selected individual components. Since we aim to determine the unidentified components, carbon generated and volume flow rate exiting the reactor, we choose to perform a component balance for our reactor systems. Carbon and hydrogen are the only two components of input feed gas. We do a carbon balance that could give us the carbon generated. A hydrogen balance is not useful, as hydrogen participates in chemical reactions. Therefore, the mass balance will be

$$\sum \text{Mass of carbon}_{in} = \sum \text{Mass of carbon}_{out} + \text{Mass of carbon deposited in reactor}$$

$$\sum \text{Mass of carbon}_{in} = \text{Mass of carbon from methane}$$

$$\sum \text{Mass of carbon}_{out} = \text{Mass of carbon from methane} + \text{Mass of carbon in Hydrocarbons} + \text{Mass of carbon in soot}$$

Few test runs have been conducted to approximately quantify the carbon in gas phase. Low flow rates and high power conditions result in high carbon generation. Hence, lowest flow rate tested in this work 0.5slpm and highest power possible for steady state conditions of reactor (35W) are chosen for test runs. Glass wool is heated to make it free of water vapor and its weight is measured on a precision mass measuring instrument.

This wool is placed in pathway of output flow and methane reforming is performed at above mentioning conditions for 30mins. Carbon particles in gas phase, typically of 100μ size get collected in the glass wool. At end of test run this glass wool with carbon particles is carefully removed and measured again for weight. The difference in weight is the amount of carbon generated in 30mins. Since the runs are at steady state conditions, a value for maximum mass flow rate of carbon in these reactors is calculated, which is 5.88E-06 Kg/s. This accounts for 0.006% of converted methane which is insignificant. Hence most of the carbon generated is considered to be deposited inside reactor, either on walls or electrodes. Therefore,

$\sum$ Mass of carbon $_{out}$ = Mass of carbon from methane + Mass of carbon in Hydrocarbons

Therefore, mass of carbon deposited in reactor = $\sum$ Mass of carbon $_{in}$ - $\sum$ Mass of carbon $_{out}$

Table 4.3 shows calculated mass of carbon using mass balance for a variety of conditions. The results lie below 0.001% of converted CH_4 and some of the results turned out to be negative. The mass balance essentially involves product concentrations from GC which have an uncertainty of 5%. The conversion rates achieved in our reactor systems are small, because of which the uncertainty in carbon mass calculations and the carbon mass results are on the same order. Due to this reason, carbon balance cannot be used in our case to identify the carbon generated.

Table 4.3 Carbon calculation using mass balance

Flow Rate [slpm]	CH4 in [%]	CH4 out [%]	C2H6 [%]	C2H4 [%]	C2H2 [%]	carbon [Kg/min]	Carbon in conv methane [%]
0.5	16	15.05164	0.154	0.2926	0.3056	1.70E-06	0.00023
1	16	15.85733	0.0646	0.0133	0.0017	-1.36E-07	-0.00017
1	10	9.095834	0.0959	0.1991	0.6091	5.12E-06	0.00057
3	16	14.85292	0.0133	0.1251	1.0087	2.087E-05	0.00182

We can add an inert gas to input feed and a mass balance of it should ideally give volume flow rate of output. But since the uncertainty would still be 5% for the GC, the change in volume flow rates would also be of the same order, thereby making the calculation useless. Therefore, we assume volume flow entering reactor is equal to volume flow rate exiting the reactor, which could be of a 2% error.

4.5 Energy balance

An energy balance is based on the first law of thermodynamics, that energy cannot be created or destroyed. A thermodynamic energy balance would one reactor system is shown in Figure 4.10.

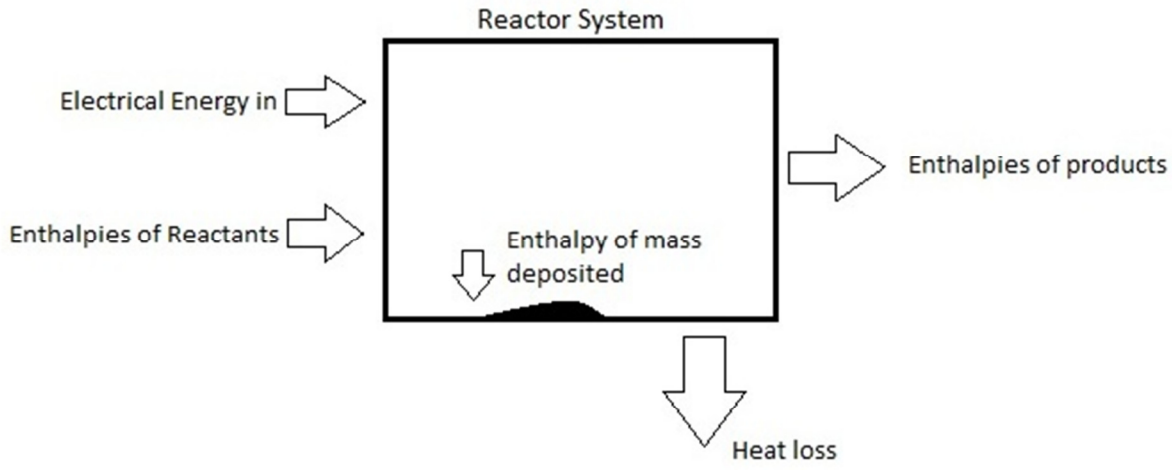

Figure 4.10 Energy balance

$\sum$ Energy $_{in}$ = $\sum$ Energy $_{out}$

where , $\sum$ Energy $_{in}$ = $\sum$ Enthalpies of input gases (1) + Power supplied (2)

$\sum$ Energy $_{out}$ = $\sum$ Enthalpies of output feed (3) + Heat loss (4)

(1) ……...$\sum$ Enthalpies of input feed = $\sum h_{i,in}$; i → number of products; H_2 , CH_4

(2) ……Power supplied = Discharge power {P}

(3) ……$\sum$ Enthalpies of output feed = $\sum h_{i,out}$; i → number of products; H_2 , $C_1 - C_n$

(4) ……Heat loss = $\dot{Q}$

Through an energy balance, we can find out the heat expended by the reactor system. This helps in identifying ways to utilize the waste heat to improve the efficiency of the system. A spreadsheet is setup for thermodynamic analysis of the reactor system.

5. EXPERIMENTAL OUTLINE AND MEASUREMENT METHODS

5.1 Experiment outline

The following describes the steps in which the experiment was carried out. All the runs are carried out in same methodology to minimize human errors and to note the possible bias errors:

1. Input feed gases, Methane and hydrogen are mixed in required proportion and flow rate using Mass flow controllers.
2. Ensure there are no leaks into or out of system by running a pressure test. Close the exit valves and check the flow rates in mass flow controllers. If there is no leak, within short time controllers should show zero reading for mass flow.
3. Check for irregular electrical connections before powering up the reactor.
4. Potential is applied between electrodes for breakdown. In magnetic glow discharge system, check for complete rotation of discharge.
5. System is allowed to run for at least 7 minutes before sampling to ensure it reached steady state conditions.
6. Using the secondary exit valve in the exhaust line, sample is collected in syringe. At the same time, voltage and current waveforms are saved in matlab format.
7. Collected sample is immediately loaded into GC for generation of chromatogram.

8. GC is setup to finish product determination in 17 minutes. Before collecting another sample after 17 minutes check for any changes in voltage and current waveforms, discharge appearance and flow conditions.

9. One parameter is chosen to be varied while holding others constant. Log the changes in power measurements, input variables, their effects on the discharge conditions and any observations.

10. Stay away from the high voltage side of reactor system for safety reasons. Once the experiment is finished, turn off the input power and ground the system before handling it.

11. Clean the reactor system by running discharge in air to burn off carbon deposits before starting a new experiment or making a change to input parameter.

12. Repeat the same steps for remaining experiments.

5.2 Power measurements

Voltage and current waveforms are processed in matlab and integrated to calculate the discharge power. Three separate runs are made for every condition to statistical analysis of results. Voltage and current waveforms generated for each of those runs is saved and post processed for power measurement. This gives 3 separate power measurements for single set of system conditions. A statistical analysis is performed on these measurements to give mean power and its uncertainty.

5.3 Measurement of output composition

For a set of conditions 3 separate samples are collected. These 3 samples are output of methane reforming under exactly same conditions with no change in any input parameter whatsoever. Product composition from each of these samples is determined using GC. All the output chromatograms generated are saved for future reference. Areas for all the products for each run are studiously recorded.

Product concentration [%] = calibration constant × area ……..(5.1)

Using respective calibration constants, product concentrations are determined. A summation of the product concentrations should be very close to 100%. All the concentrations are normalized before the data is used for further calculations of derived parameters.

5.4 Uncertainty analysis

Like most experiments, all measured data are subject to experimental errors. Even though steps are taken to minimize the errors as much as possible, there will be a certain degree of uncertainty in results which must be quantified. basic statistical equations like mean, standard deviation like standard deviation can represent the uncertainty only if the number of samples are large (>20).

The true value of the standard deviation can then be estimated using the following equation

Standard deviation, $s = \sqrt{\frac{\sum_{i=1}^{n}(x_i-\bar{x})^2}{n-1}}$ .....(5.2)

where, $\bar{x} = \frac{\sum_{i=1}^{n} x_i}{n}$ and x_i is sample data point

Percent error for these is then estimated as % error = $2 \cdot \left[\frac{s}{\bar{x}} \cdot \frac{1}{100}\right]$ .....(5.3)

If the measurements follow a normal distribution, 68.26 percent of the measured values will fall within one standard deviation of x, 95.44 percent will fall within two standard deviations of x , and 99.74 percent will fall within 3 standard deviations of x. Therefore, if the set of measurements of the length of the table follows a Gaussian distribution, 68.26 percent of the measured values will fall within one standard deviation of x, 95.44 percent will fall within two standard deviations of x, and 99.74 percent will fall within 3 standard deviations of x . For our measured data we are 95.44 percent confident that any value of x, It means including the true value, will lie within ± 2σ of x . These uncertainties are only valid for measured data.

5.4.1 Uncertainty in Specific Energy Calculations

The equations for calculating specific energy for formation of specific i^{th} product, e_i, are given by equation below. In this equation P is the discharge power calculated by integration over some time, τ, of the measured voltage, V, and current, I, of the discharge. $\dot{m_{out}}$, the mass flow rate out of the reactor of a specific product and is calculated from the measured peak area for that species, A_i, from the gas chromatograph (GC), the calibration constant, k_i, relating measured areas on the GC to species mole

fractions, x_i, the total volumetric flow rate out of the reactor $\dot{V_{out}}$, and the density of that species, ρ_i.

$$P = \frac{1}{T}\int_0^T I(t).V(t)\,dt \qquad \text{……(5.4)}$$

$$e_i = \frac{\frac{1}{T}\int_0^T I(t).V(t)\,dt}{\rho_i A k \dot{V}_{out}} = \frac{P}{\dot{m}_{out,i}} \qquad \text{……(5.5)}$$

$$\dot{m}_{out,i} = \rho_i x_i \dot{V}_i \qquad \text{……(5.6)}$$

$$x_i = A_i k_i \qquad \text{……(5.7)}$$

An uncertainty is associated with the experimentally measured parameters in equation 1 (all parameters but ρ_i and unit conversion factors are experimentally measured) due to mainly to slight variations in the operational parameters of the discharge and inherent uncertainties in the diagnostic methods and analytical equipment used. The uncertainties in measured quantities are uncorrelated and propagate into the determination of the uncertainty of *e* as shown in equation 2 (I's are left off for convenience) below where U_n is the uncertainty of parameter *n*.

$$U_e = \sqrt{\left(\frac{\partial e}{\partial P}U_P\right)^2 + \left(\frac{\partial e}{\partial x}U_x\right)^2 + \left(\frac{\partial e}{\partial \dot{V}}U_{\dot{V}}\right)^2} \qquad \text{……..(5.8)}$$

$$U_P = \sqrt{\left(\frac{\partial P}{\partial V}U_V\right)^2 + \left(\frac{\partial P}{\partial I}U_I\right)^2 + \left(\frac{\partial P}{\partial T}U_T\right)^2} \qquad \text{……..(5.9)}$$

$$U_x = \sqrt{\left(\frac{\partial x}{\partial A}U_A\right)^2 + \left(\frac{\partial x}{\partial k}U_k\right)^2} \qquad \text{……..(5.10)}$$

Uncertainties, U_p/P, U_A/A, U_k/k, and $\dot{U}_{\dot{V}_i}/\dot{V}_i$, are approximately w%, x%, y%, and z%. These are determined by statistically or knowledge of the operation of the instrument. Up ,UA and Uk are determined from estimation of percent errors through basic statistical equations as given below. These estimations are based on 3 samples. Technically $\dot{V}_{out}$ should be measured directly or determined by a species balance, $\dot{V}_{out} = f(\dot{V}_i, x_1, x_2, x_3 \ldots\ldots x_n)$; however, te approximation of $\dot{V}_{out}$ significantly simplifies the uncertainty calculation, and does not lead to significantly larger $\dot{U}_{\dot{V}_i}$ since the equations are doesn't involve higher order terms or any other special functions. We therefore assume $\dot{V}_{out} = \dot{V}_{in}$. This approximation is only reasonable for conversion percentages less than 2%.

Rewriting the uncertainty for, e_i, in terms of percent uncertainties in the specific variable, $U\%_n$, and evaluating the partial derivatives this simplifies to equation 3 below. This relatively simple form occurs because terms are all first order in equation 1. $U\%_P$, and $U\%_V$ vary for each experimental condition. $U\%_A$, varies for each experimental condition and each species. $\underline{U\%_k}$,is a constant for a specific species varying only slightly from day to day due to dirt on the GC.

$$U\%_{e_i} = \sqrt{(U\%_P)^2 + (U\%_{A_i})^2 + (U\%_{k_i})^2 + (U\%_{\dot{V}_{out,i}})^2} \qquad \ldots\ldots\ldots\ldots (5.11)$$

Table 5.1 gives the calculation of these uncertainties and the propagation of uncertainty for the counter-flow micro plasma (CFM), and the micro-magnetic-gliding-glow (MMGG) discharge reactors each operating at 3 SLPM input flow rate of 84% H_2, 16%

CH_4. From these calculations we can see that the uncertainty in specific energy can be as much as xx% and that major sources of error are product concentrations and power.

Table 5.1 Example uncertainty calculations for two reactors

Reactor	P (W)	Species	x_i (%)	e_i (MJ/kg)	$U\%_P$	$U\%_V$	$U\%_k$	$U\%_A$	$U\%_e$
CFM	41.64	C_2H_2	0.021	20999	5.4	5.2	1.13	9.9	12.4
	41.64	C_2H_4	0.052	8029	5.4	5.9	1.28	1.34	8.2
	41.64	C_2H_6	0.09	4349	5.4	5.5	1.20	3.3	8.4
MMGG	26.6	C_2H_2	0.01	6041	2	5	1.13	7.2	9.06
	26.6	C_2H_4	0.02	2562	2	5.3	1.28	2.05	6.15
	26.6	C_2H_6	0.03	1662	2	5.5	1.20	1.31	6.11

5.4.2 Recommendations to minimize errors

1. Ensure the discharge is highly steady and stable during the run time.
2. Carbon deposition, wavering electrodes, stray capacitance are few sources for instability.

3. Since we have a gap of 30 minutes between collections of each sample, ensure all the input variables are absolutely undisturbed, especially power which could reaction system.
4. Collect the first sample only after allowing the system to run for at least 7 minutes.
5. Gas chromatograph is maintained at exactly same conditions of temperature, pressure along with its event tables and temperature program.

5.5 Precautions

1. Gas flowing through a mass flow controller has to be selected to ensure accurate readings of mass/volume flow through them.
2. Make sure the pressure in the system is atmospheric i.e. 14.78 psi by checking for pressure readings in mass flow controllers.
3. Cables connecting power supply to reactor to ground should be free of any dielectric discharges.
4. Voltage probe, reactor system, oscilloscope should be properly grounded before running the experiment.
5. The voltage probe attenuation factor should be 1000 and current transformer attenuation should be 2. Sometimes due to EMI, the attenuation factor for voltage

probe is not read properly by oscilloscope. Check for such instances and note the factor used by oscilloscope in displaying the waveforms.

6. Allow the system to reach steady state conditions before collecting sample. A run time of at least 7 minutes before sampling should be enough for steady state conditions.

7. While saving voltage and current waveforms ensure that there are no peaks off the limits and there the data is saved with proper notations and names so that the conditions to which these data are applicable will not end in a mismatch.

8. Minimize air leaks into sample collection syringe by properly following a method. In our case we made a ball valve + syringe system, where product stream from exhaust line is allowed to flow out through this valve and syringe, by pulling the plunger out of the syringe. Then plunger is pushed back into syringe. This ensures that space from exhaust line to plunger head is only filled with product stream. Now plunger is pushed forth and pulled back for 3 times slowly to ensure the stream is mixed properly. After loading gas into syringe for third time, ball valve is immediately closed. Now this syringe plus ball valve combination is taken to GC. Before opening valve, a slight pressure is applied with plunger, so that as valve is opened gas will immediately start flowing into sampler, not allowing any air to enter the system.

9. When working with low flow rates and high powers, make sure the electrodes are not developing any hot spots.

6. RESULTS AND DISCUSSION

6.1 Measurement methods for involving variables

The primary input variables of the reactor system are power, flow rate, gas mixture composition and discharge gap. Operating conditions of the system can be changed by them. These variables are measured directly using well calibrated instruments, which was discussed in section 5.3. To determine the productivity of experiments and to comprehend the effects of input variables on the discharge conditions, the output measurements are expressed in different variables. These derived variables describe the parameters that are investigated in this research. Trends of variation in these parameters with respect to changes in input variables help us in to predict the reaction changes in the system and deduce appropriate conclusions. These parameters are defined below:

1. CH4 converted [%] - It is the amount of methane that is being converted to reaction products.

   Converted methane can be calculated in two ways :

   a) Methane in output stream is measured on GC with TCD detector and subtracted from input methane feed.

$$CH_{4,Conv}\,[\%] = CH_{4,in}[\%] - CH_{4,out}[\%] \qquad \text{.....(6.1)}$$

   b) Summation of all the carbon products other than methane in product stream.

   In the first method the difference is obtained from TCD measured values which have an uncertainty of 2% in them. For conversion rates less than 2% this difference is in the same order of errors with TCD measurements. Hence second method is chosen

over the first for calculating converted methane. This excludes methane converted to carbon, but considering carbon deposition is less than 0.006% of the output methane stream, this approximation is justified.

$$CH_{4,Conv} = \sum_{x=1}^{n} C_i \qquad \ldots\ldots\ldots\ldots (6.2)$$

$CH_{4,Conv}$ [%] → Amount of converted methane

C_i [%] → Amount of products; $C_2 - C_6$ hydrocarbons

2. Specific energy [MJ/Kg], [eV/molecule] - It is amount of energy spent per kg of reactant or product gas. Product specific energy is amount of energy that is used in generating a Kg of product and input specific energy is energy spent per Kg of input methane. We intend to minimize these parameters while trying to maximize the concentrations of desired product.

   It is given as

$$E_i = \frac{60}{\rho_i} \times \frac{P}{V_i} \qquad \ldots (6.3)$$

where, $V_i = V_t$ [sccm] $\times \frac{C_i\ [\%]}{100}$; $i \rightarrow CH_{4,conv}, C_2 - C_6$

$E_i \left[\frac{MJ}{Kg}\right]$ → Specific energy input i^{th} reactant or product

V_t [sccm] → Total input or output flow rate

P [W] → Power input at discharge

Converting [MJ/Kg] to [eV/molecule],

$$E_i \left[\frac{ev}{molecule}\right] = \left[\frac{1000 \times M_i}{e \times N_a}\right] \times E_i \left[\frac{MJ}{Kg}\right] \qquad \ldots (6.4)$$

where $e \rightarrow Conversion\ factor\ for\ eV\ to\ joules$

$$1\text{eV} = 1.602176469 \times 10^{-19}\ \text{joules}$$

$$N_a = 6.02214 \times 10^{-26}\ [\text{Kmol}^{-1}]$$

$\text{M}_\text{i}\left[\frac{\text{Kg}}{\text{Kmol}}\right] \rightarrow$ Molecular weight of i^{th} reactant or product

3. Normalized yield [%] - Methane reforming results in a number of hydrocarbon products. The ratio of amount of particular product to the total converted methane gives us the normalized yield of that particular product. Normalized yield also called as selectivity. This is calculated as

$$\text{S}_\text{i} = \frac{\text{C}_\text{i}}{\text{CH}_{4,\text{Conv}}} \times 100 \qquad \ldots\ldots\ldots\ldots (6.5)$$

$\text{S}_\text{i}[\%] \rightarrow$ Selectivity of products ; C_i & $\text{CH}_{4,\text{Conv}}$ in %

Selectivity of a product gives us information to predict about the possible state and direction of reaction system in the discharge.

4. Flow Residence Time [ms] – Flow Residence time is a measure of the time a reactant molecules spends in the discharge or the time for which reactant mixture is exposed to plasma discharge. Unless or otherwise mentioned, residence time in this work refers to flow residence time. It is in this time the high energetic electrons of plasma interact with methane molecules in the mixture and generate methyl radicals initiating the reaction chemistry which subsequently leads to end products. This is calculated as

$$\text{T} = 47.1238 \times \left[\frac{\text{d}^2 \times \text{L}}{\text{V}}\right] \qquad \ldots\ldots\ldots\ldots (6.6)$$

τ [ms] → Residence time ; D [mm] → Diameter of capillary tube

L [mm] → Discharge gap ; V [sccm] → Volumetric flow rate

5. Efficiency [%] - Efficiency of a system is determined by the energy ratio of product enthalpy to total energy used for reforming. Ideally, the energy spent in converting methane entirely into acetylene or ethylene is their reaction specific enthalpy and they are

   For ethylene ...

   $2CH_4 \rightarrow C_2H_4 + 2H_2$; $\Delta h = 7.184 \left[\frac{MJ}{Kg}\right]_{ethylene}$ or $2.09 \left[\frac{eV}{molecule}\right]_{ethylene}$

   For acetylene

   $2CH_4 \rightarrow C_2H_2 + 3H_2$; $\Delta h = 14.1 \left[\frac{MJ}{Kg}\right]_{acetylene}$ or $3.1 \left[\frac{eV}{molecule}\right]_{acetylene}$

   Hence the efficiency for a reactor system is given as

$$\eta = 100 \times \left[\frac{E_o}{E_i + W}\right] \quad \text{.....(6.7)}$$

   η [%] → Efficiency of system ; E_i → Input specific enthapies i^{th} reactant

   W → Electrical energy in ; E_o → Product specific enthalpies for i^{th} product

Efficiency is a measure of how closer our plasma reactor system is to the ideal case or how good it is in converting methane to products using any given input energy. A 100% efficient system for a product means that it is utilizing all the given input energy to convert entire methane to that particular product without any modes of energy loss.

Our results will be presented through these parameters and the variation in them enables us to understand different discharge systems in better way and make necessary changes to achieve the desired end results.

6.2 Tests with varying proportions of methane and hydrogen

Holding power, flow rate and discharge gap at constant values (30W, 1slpm and 6.04 mm respectively), a test run with varying proportions of methane and hydrogen is conducted. Methane input in the mixture is increased from a minimum of 5% to a maximum of 30%.

Amorphous carbon is the unwanted byproduct in methane reforming. A portion of carbon generated from reactions deposits on the walls of reactor, electrodes and the rest , in gas phase, flows out of the reactor along as a part of product stream. Carbon formation, thereby deposition increases with increase in proportion of methane in the input feed. Over an input methane feed of 22%, carbon deposition starts to affect the discharge conditions. Deposition on electrode not only results in unsteady voltage and current measurements but also affects the reaction system of methane in the discharge. At input methane feed more than 25%, there is a rapid growth of carbon filaments observed on both the electrodes that finally bridges the electrode gap resulting in disruption of the discharge process. Under these conditions it is not possible to run the system for more than 5 minutes. This necessitates a shut down and an entire clean up of reactor chamber ,by running discharge in air, before starting the reforming process again. At all the varying methane proportions, products in output stream are just C2

hydrocarbons and carbon. No other higher hydrocarbons are detected. With the detection limits being 50 ppm for HID detector on GC, all other possible products from methane reforming are considered to be less than 50 ppm and therefore negligible. Steady discharge conditions and output flow over a long time (>60 minutes) is necessary to take more than two samples of product stream for determining composition. The product concentrations in these samples determine the trends in the output parameters with respect to changing input variables.

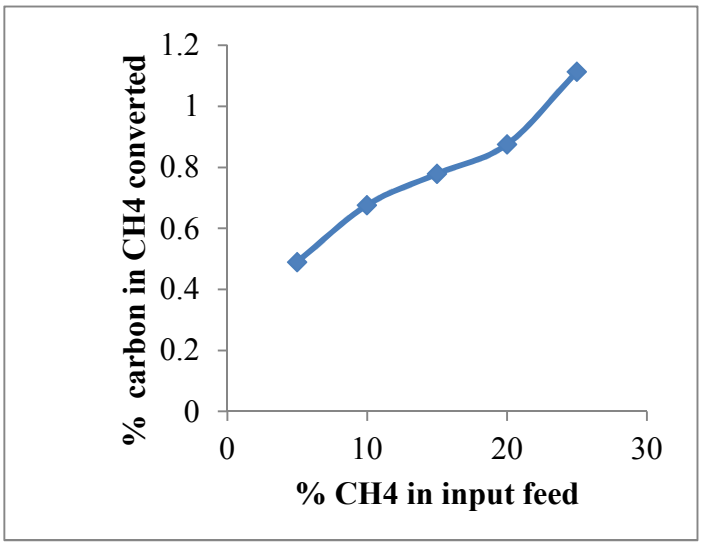

Figure 6.1 Carbon deposition rate Vs % CH4 in

Hence, any kind of sources causing discharge instabilities or changes to input or output parameters over the run time have to be eliminated. It is observed that carbon deposition is lower at methane input less than 20% and the maximum input methane at which we can maintain constant discharge conditions for more than 180 minutes at lowest flow

rate being tested (0.5 slpm) is 16%. Thus, 16% methane and 84% hydrogen is chosen to be the input feed mixture for performing the rest of experiments.

Our criterion for carbon formation is much more stringent than it would be in industrial process. In Huels process carbon production is up-to 7% of the output flow rate, whereas in our systems carbon deposition was always less than 0.05% of output flow rate. Also note that methane to hydrogen proportion was limited by carbon deposition on electrodes but not due to carbon in gas phase.

6.2.1 Effect of Hydrogen Dilution

Dilution with hydrogen in methane has shown a reduction in carbon deposition. This is in agreement with the prediction of thermal equilibrium results. As reasoned there, this reduction is attributed to hydrogen radicals preventing the reactions proceeding to form carbon. The disadvantage is that some energy from discharge is expended in heating hydrogen gas and the hydrogen radicals generated react with methyl radicals to produce methane back, thereby decreasing the conversion rate.

6.3 Effect of input variables on output parameters

Results concerning the effect of varying flow rate and power on output parameters are presented here. A change in flow rate causes the residence time to change. The residence time change with respect to varying flow rate is shown in the Figure 6.1. Owing to the higher gas velocities at higher flow rates, residence time decreases with increasing flow rate if the area of cross section is constant. The residence times for different flow rates in

both reactor systems is given in Table 6.1. When power is varied, energy density of discharge is changed. Higher the power, higher the input energy into methane and so more number of energetic electrons interacting with the feed gas *i.e.* more number of methane molecules in plasma can get activated.

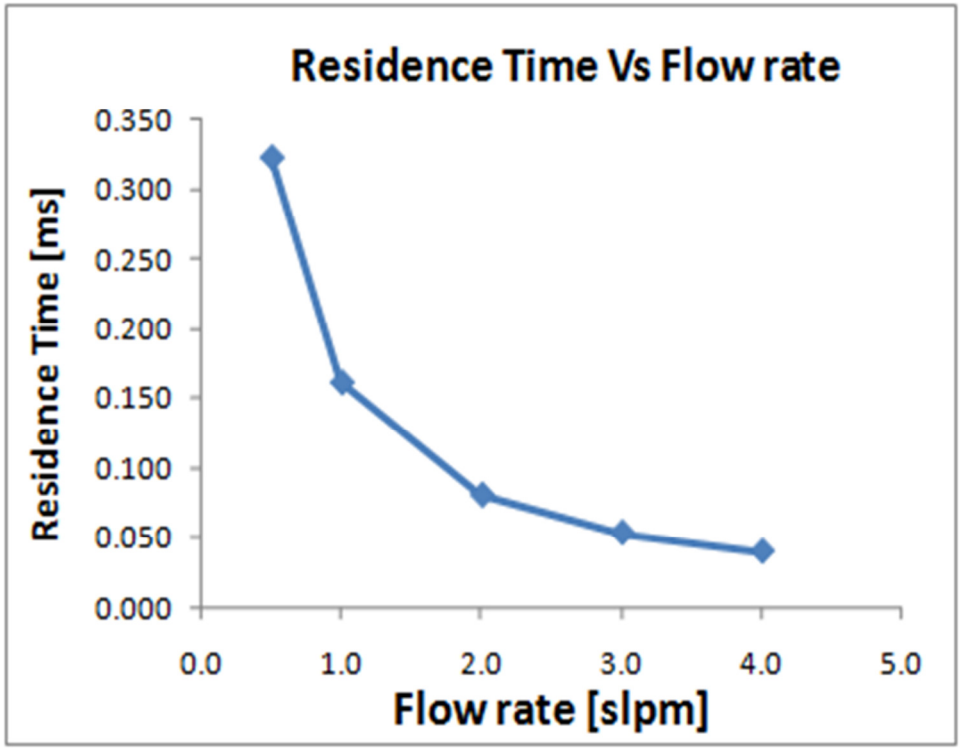

Figure 6.2 Variation of residence time with flow rate

Table 6.1 Residence times at different flow rates

	Residence time [ms]	
Flow Rate [slpm]	Counter flow micro plasma	Magnetic glow discharge
0.5	0.323	2.903
1	0.162	1.452
2	0.081	0.726
3	0.054	0.484
4	0.04	0.363

Two sets of experiments are conducted. In set 1, flow rate is varied while holding all the remaining input parameters constant. In set 2, power is varied while holding the remaining parameters constant. These experiments are conducted in both counter flow micro plasma system and magnetic glow discharge system. Tables 6.2 & 6.3 gives an overview of the experimental parameters.

Measurements of output flow concentrations are made for these experiments and variation in specific energy cost, concentration and normalized yield of products are calculated and plotted.

Table 6.2 Experimental parameters in different reactor systems for varying flow rate

Set 1: Varying flow rate

Input parameter	Counter flow micro plasma	Magnetic glow discharge
Flow rate [slpm] (Variable)	*0.5 , 1, 2, 3 , 4*	*0.5 , 1, 2, 3*
Power [W]	33	27
Discharge gap [mm]	6.01	3.04
Mixture Proportion	16% methane + 84% Hydrogen	16% methane + 84% Hydrogen

Table 6.3 Experimental parameters in different reactor systems for varying discharge power

Set 2: Varying discharge power

Input parameter	Counter flow micro plasma	Magnetic glow discharge
Flow rate [slpm]	3	3
Power [W] (Variable)	*27, 34 , 38, 41, 44*	*26.6, 37.4, 51.4, 70*
Discharge gap [mm]	6.01	3.04
Mixture Proportion	16% methane + 84% Hydrogen	16% methane + 84% Hydrogen

6.3.1 Effect on Normalized Yields

6.3.1.1 Flow rate variation: Flow rate variation in both reactors systems is conducted and its effect on normalized yields is discussed below.

i. Counter flow micro plasma - Variation of normalized yields in this system with changing flow rate is shown in Figure 6.3. Ethylene and acetylene show a normalized yield of 40% at 0.5 slpm. At the flow rates above 0.5slpm selectivity of ethylene and acetylene drops from 40% to 25% and 20% respectively, while ethane becomes more and more selective among the products. At 0.5 slpm we can see that acetylene begins to dominate the product composition and ethylene curve approaches saturation. Hence at flow rates lower than 0.5slpm higher normalized yield of acetylene and a drop in ethylene normalized yield are expected.

The effect of residence time is clearly indicated by normalized yield versus residence time plot (Figure 6.5). At higher flow rates, due to the lower residence times the reaction kinetics limits the products to ethane and hence ethane dominates the products whereas at lower flow rates ,due to increased residence times reactions proceed to yield ethylene and acetylene. At flow rates less than 0.5 slpm, with residence times longer than 0.3 ms, the conditions of plasma discharge offer enough time for most of the converted methane to end up as acetylene and soot.

ii. Magnetic glow discharge - Variation of normalized yields in this system with changing flow rate and residence time are shown in fig 6.4 and 6.6. Normalized yields are relatively constant over all the flow rates tested. Considering the residence time

change is not small, from 0.2 ms to 2.9 ms, it can be concluded that residence time in magnetic glow discharge has negligible effect on normalized yields. Also, note that discharge rotates at constant rate due to non-varying power. Since the discharge is perpendicular to flow of gas, the actual time a gas molecule spends in the discharge is more dependent on diffusion rather than residence time. As a result of the diffusion, which is same for all the flow rates, the residence time effects are minimal for the flow rate changes made in this experiment. The same reason cannot be applied if the flow rate changes are large, as can be seen from the changing normalized yields at 4slpm and more. The normalized yield trends also explain the reduction in carbon deposition as compared to micro plasma which that has much lower residence times but higher carbon particle generation than magnetic glow discharge.

6.3.1.2 Variation of discharge power: Discharge power is varied in both reactors systems is conducted and its effect on normalized yields is discussed below.

i. Counter flow micro plasma - Variation in product normalized yields with respect to changing power in micro plasma is shown in fig 6.7. Higher powers show better selectivity towards ethylene and acetylene while lowering the selectivity of ethane. This is the effect of increase in electron density leading to generation of more methyl radicals, thereby producing more ethane and converting ethane to ethylene and acetylene. Ethylene normalized yield rises from 17% at 27W to 29% at 34W and thereafter seems to approach saturation. An ethylene selectivity of 38% is achieved at 44W and 3 slpm. A higher current also means higher temperature of the gas, therefore more acetylene in

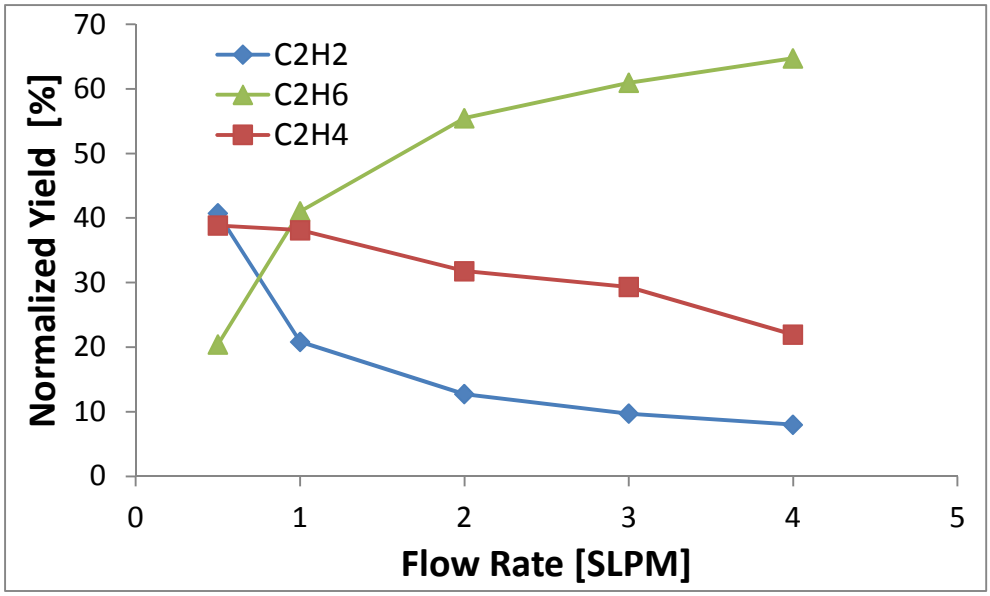

Figure 6.3 Variation of normalized yields with flow rate

in counter flow micro plasma system

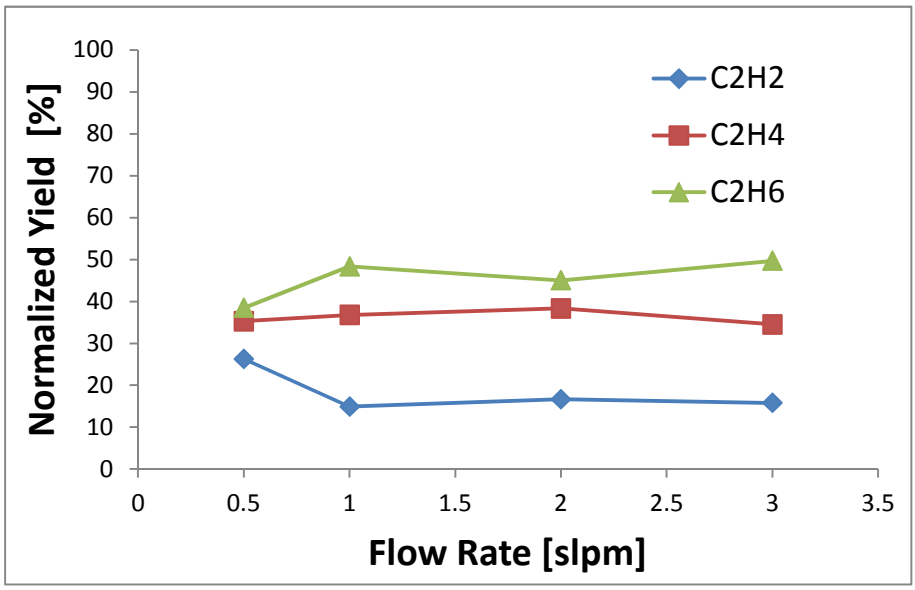

Figure 6.4 Variation of normalized yields with flow rate

in magnetic glow discharge system

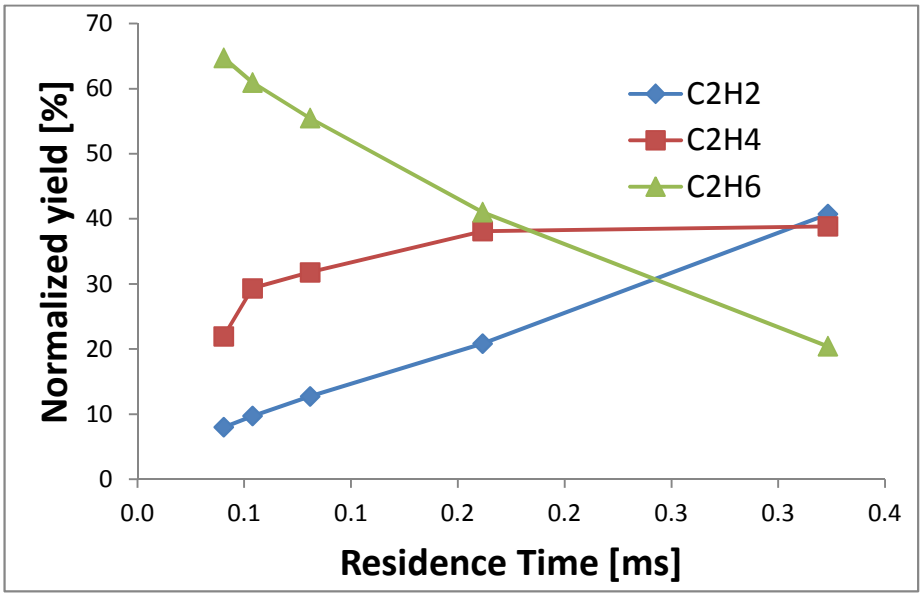

Figure 6.5 Variation of normalized yields with residence time in counter flow micro plasma system

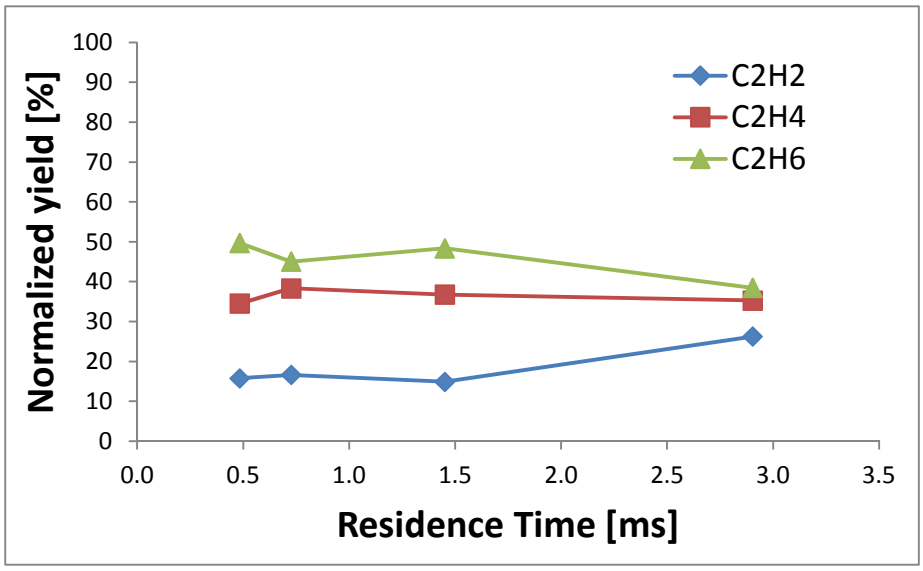

Figure 6.6 Variation of normalized yields with residence time in magnetic glow discharge system

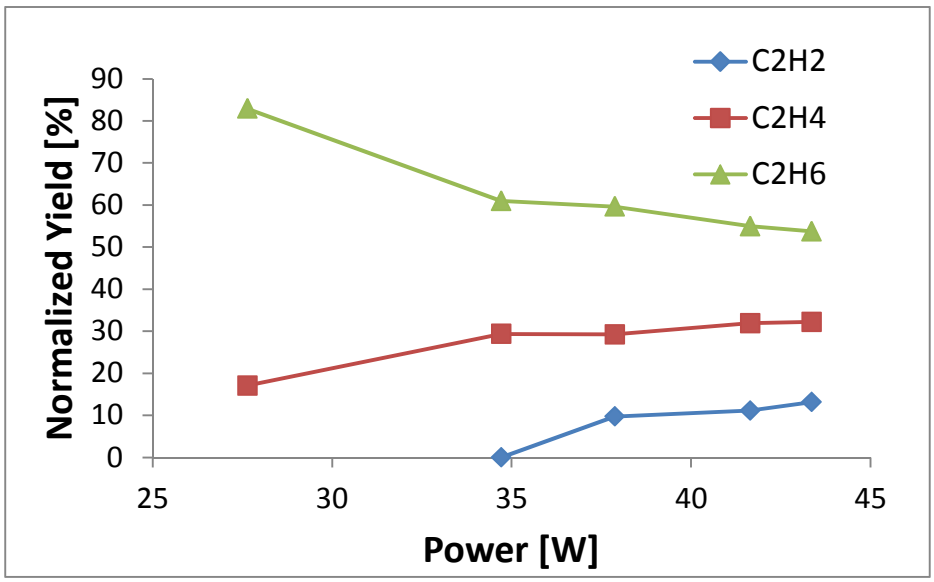

Figure 6.7 Variation of normalized yields with discharge power in counter flow micro plasma system

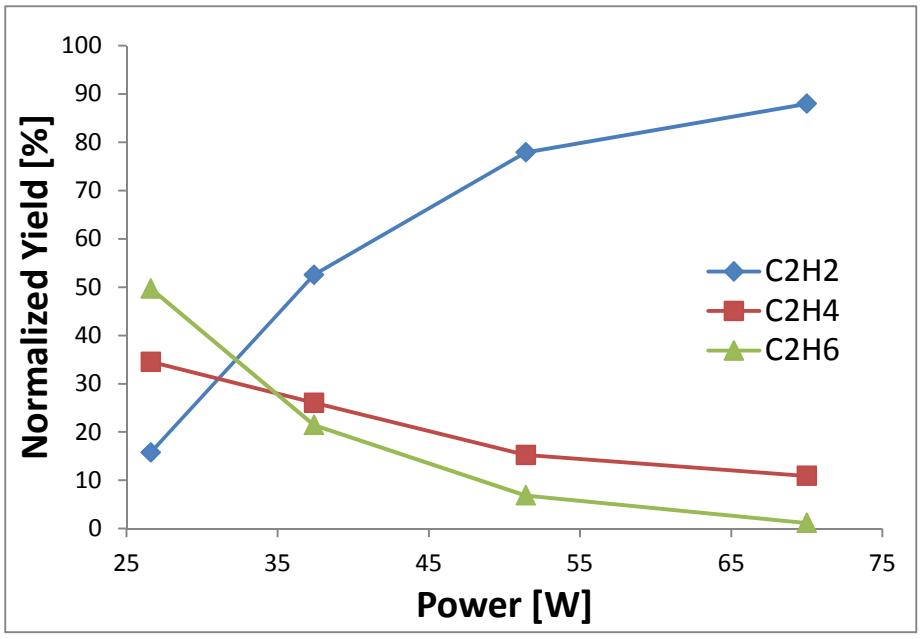

Figure 6.8 Variation of normalized yields with power in magnetic glow discharge system

the products is expected at higher powers. A upward directed curve of acetylene at 44W and an visible rapid increase in carbon deposition above 50W indicate the same.

ii. Magnetic glow discharge: Variation in product normalized yields with respect to changing power in magnetic glow discharge is shown in Figure 6.8. It appears that lower powers seem to give better selectivity towards ethylene and acetylene while lowering the selectivity of ethane. But considering the discharge gap is lower in magnetic glow system, trends of normalized yields are same as with micro plasma. Ethylene and acetylene show a normalized yield of 34% and 15% respectively at input power of 26W. As we move to higher powers, acetylene normalized yield shoots to more than 50%, whereas ethylene and ethane drop below 10%. This indicates that, for the residence time offered by the magnetic glow system (0.48 ms) we were already operating the discharge at higher power conditions favoring acetylene production. Whereas in micro plasma system with comparatively short residence time (0.05 ms) the input powers were not enough to bring the similar shift in selectivity's of products. Hence, the graphs with varying power would look the same, if the power tried for magnetic glow system were much lower. So essentially the trends with power are same in both micro plasma and magnetic glow discharge case, which is expected because both are glow discharges with similar electrode configurations. The advantage being that there is much less soot formation in the case of magnetic glow discharge as explained before. A maximum ethylene selectivity of 38% at 25 W and an acetylene selectivity of 89% at 70W are achieved in magnetic glow system.

6.3.2 Effect on Concentrations

6.3.2.1 Variation of flow rate: Flow rate power is varied in both reactors systems is conducted and its effect on concentration is discussed below.

i. Counter flow micro plasma - Figure 6.9 shows the variation in concentrations of product and conversion rate of methane with changing flow rate in micro plasma system. Conversion rate drops rapidly from 0.5 slpm to 2 slpm and for flow rates above 2 slpm the conversion rate drop is much less. All the product concentrations show a similar trend i.e decrease with increasing flow rate. The effect of flow rate on concentration can be better understood through the effect of residence time. Higher flow rates result in lower residence times and hence lower amount of gas is being treated by plasma resulting in lower conversion rate. Whereas higher residence times, which happens at lower flow rates, gave higher conversion rate. The maximum conversion rate achieved are 5.06% and the product yields achieved are in the range of 0.01% - 2 %, while the product concentrations are in the range of 0.01 - 0.3 % of output stream.

ii. Magnetic glow discharge - Trends in this system are shown in Figure 6.10. Conversion rate and product concentrations show a similar trend to the one observed in micro plasma discharge. All of them essentially decrease with higher flow rates i.e. lower residence times. Highest conversion rate in this case is 2% at 0.5slpm and a discharge power of 26W.

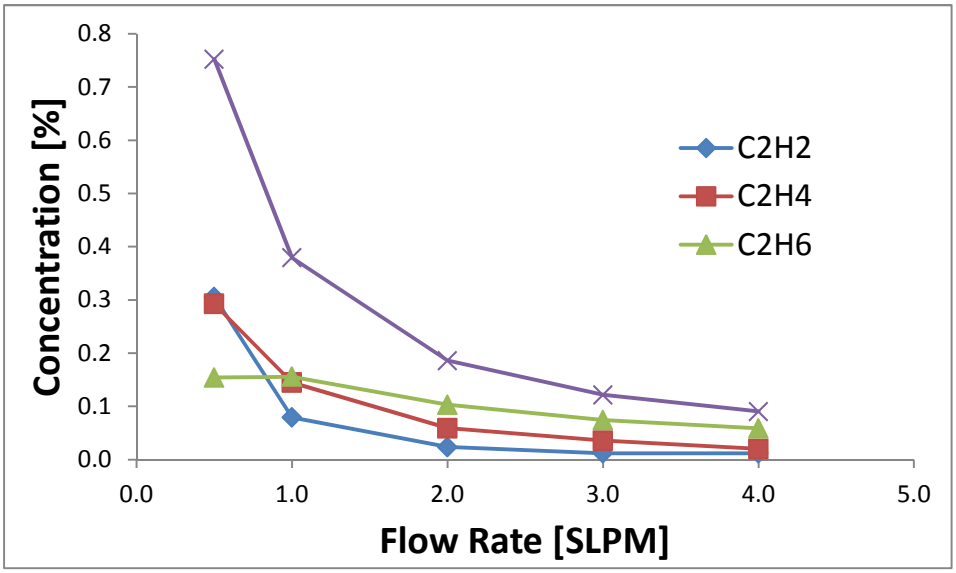

Figure 6.9 Variation of product concentrations with flow rate in counter flow micro plasma system

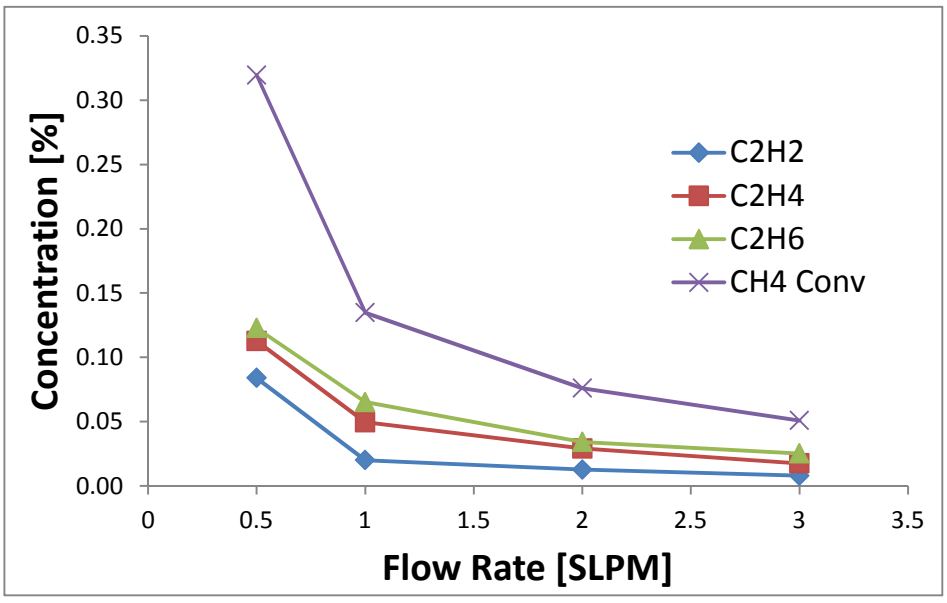

Figure 6.10 Variation of concentrations with flow rate in magnetic glow discharge system

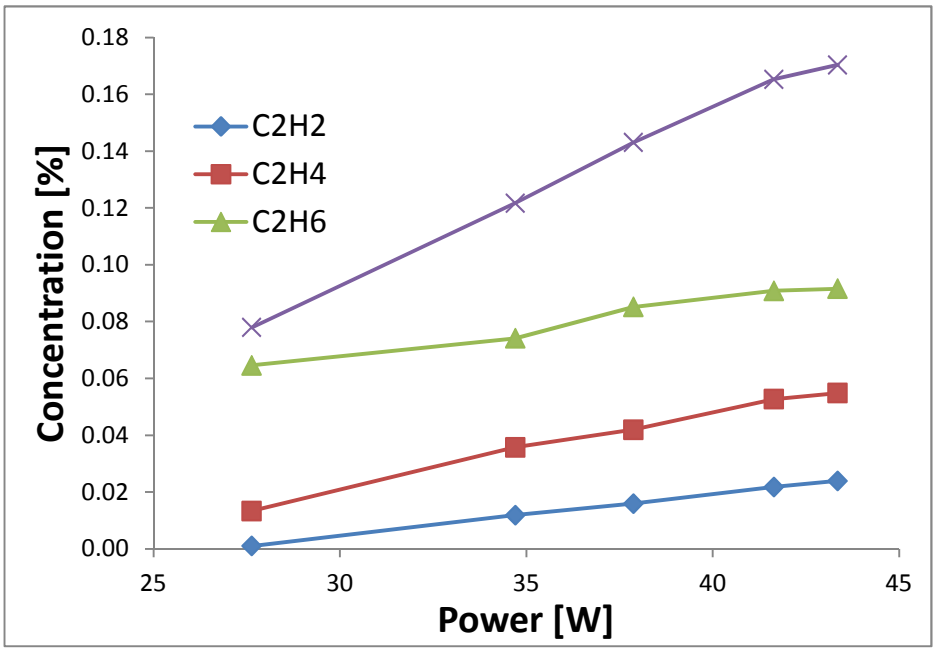

Figure 6.11 Variation of concentrations with power

in counter flow micro plasma system

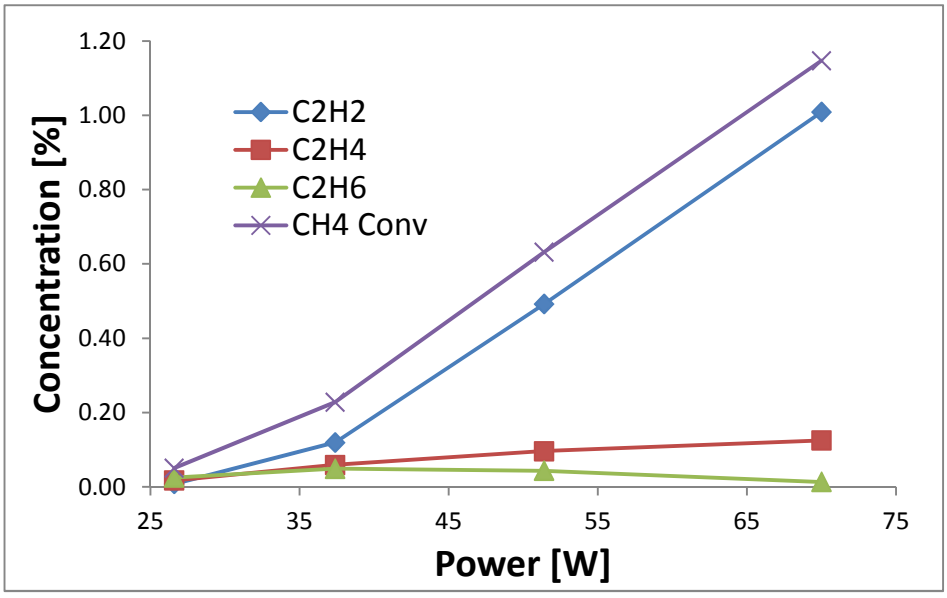

Figure 6.12 Variation of concentrations with power

in magnetic glow discharge system

6.3.2.2 Variation of discharge power: Discharge power is varied in both reactors systems is conducted and its effect on product concentrations is discussed below.

i. Counter flow micro plasma - Figure 6.11 shows the variation in concentrations of product and conversion rate of methane with changing power in micro plasma system. Conversion rate and there by product concentrations increase with increase in power input and variation is linear. Higher power implies larger current and therefore more number of energetic electrons interacting with same amount of methane and hence it leads to better conversion rates. The highest conversion rate of methane is 1.2% at 44W and 3 slpm.

ii. Magnetic glow discharge - Trends of product concentrations and conversion rate in this system are shown in Figure 6.12. Although both systems show increasing trends, in micro plasma the increase is linear for all the products whereas in magnetic glow, acetylene along with conversion rate increases linearly while ethane and ethylene show little increase. This is only due to the fact that these systems are operating in different power regimes in accordance with their residence times. But magnetic glow system clearly offers an advantage of operating the discharge with higher powers and long residence times with relatively less carbon deposition. The highest conversion rate of methane achieved in this system is 9.04 % at 70W and 3 slpm.

6.3.3 Effect on Product Specific Energy

Product specific energy is the crucial output parameter of this research. Trends of it in both reactor systems are plotted to identify the low product specific energy conditions.

6.3.3.1 Variation of flow rate: Flow rate is varied in both reactors systems is conducted and its effect on product specific energy is discussed below.

i. Counter flow micro plasma - Fig 6.13 shows variation in the product specific energy with respect to changing flow rate in micro plasma case. Product specific energy of all the products increase with flow rate, while energy spent to convert methane is same at all flow rates. Since power input is maintained constant, the increasing energy costs are due to lower conversion rates and corresponding lower yields. The lowest ethylene specific energy of 1162 MJ/Kg was measured at 0.5 slpm . For acetylene it is 1191 MJ/Kg at same conditions.

ii. Magnetic glow discharge - Figure 6.14 shows variation in the product specific energies with respect to changing flow rate in magnetic glow case. Product specific energies which are predominantly dependent on conversion rate in this case show little variation over the flow rate change. This is because the conversion rate is linear with increase in flow rate and selectivity is relatively not effected by residence time changes. The only random variation is increase in specific energy of acetylene from 0.5 slpm to 1 slpm. This is attributed to the sudden increase in acetylene selectivity at high flow rate. This is the point where the residence time is long enough (2.9 ms) that it starts to affect the reaction system.

6.3.3.2 Variation of discharge power: Discharge power is varied in both reactors systems is conducted and its effect on product specific energy is discussed in this section.

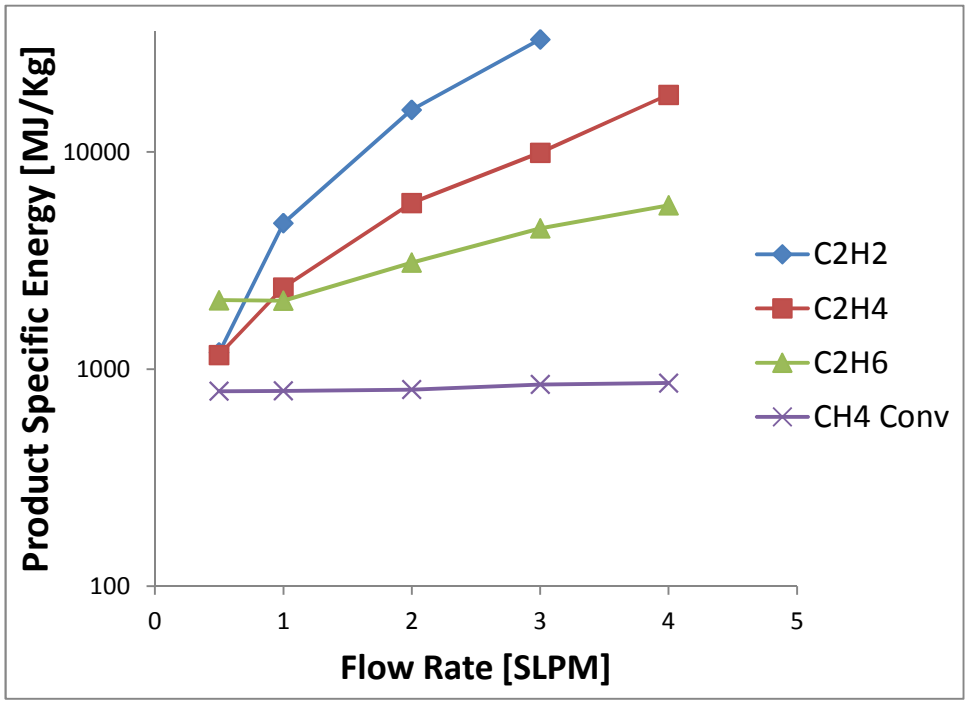

Figure 6.13 Variation of product specific energy with flow rate in counter flow micro plasma system

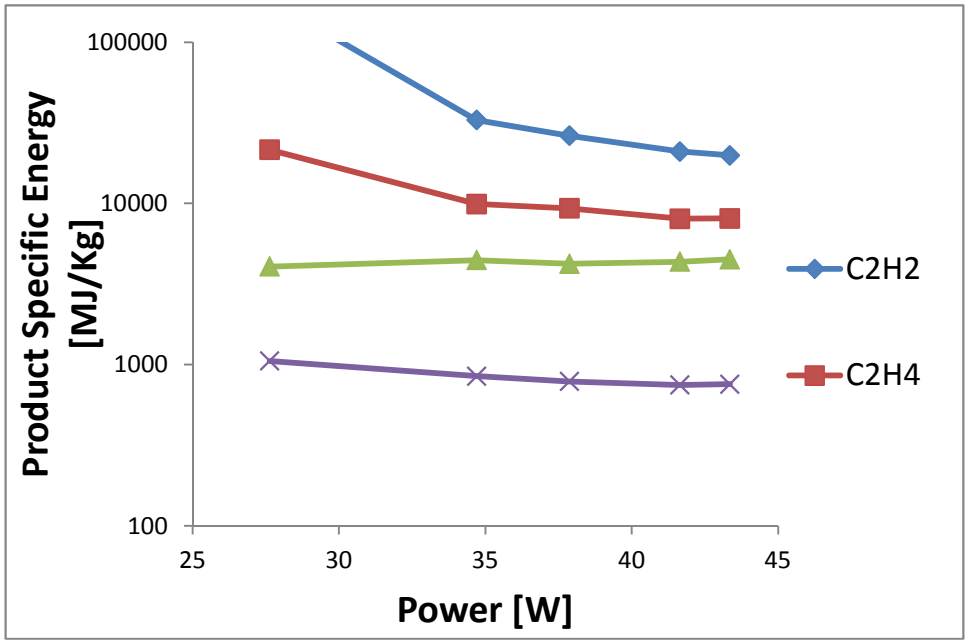

Fig 6.14 Variation of product specific energy with flow rate in magnetic glow discharge system

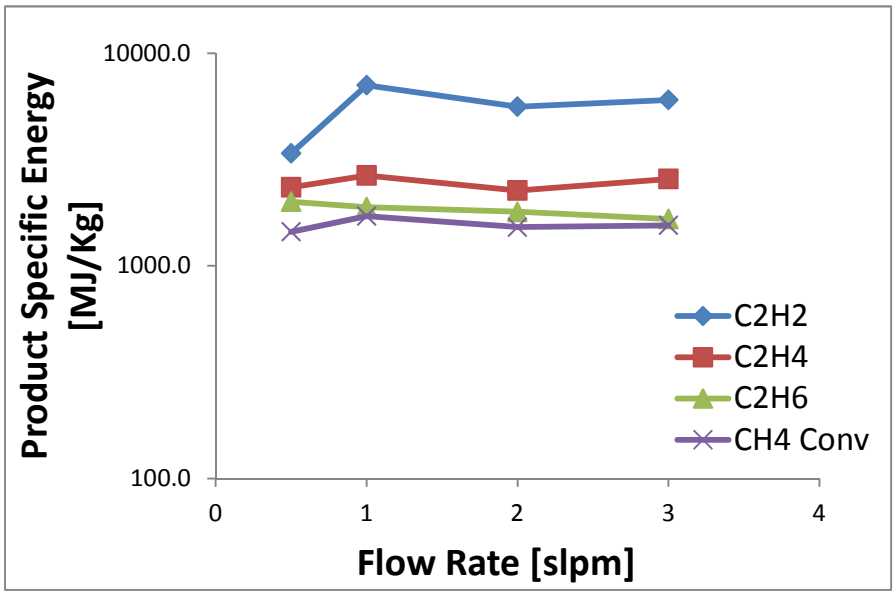

Figure 6.15 Variation of product specific energy with power in counter flow micro plasma system

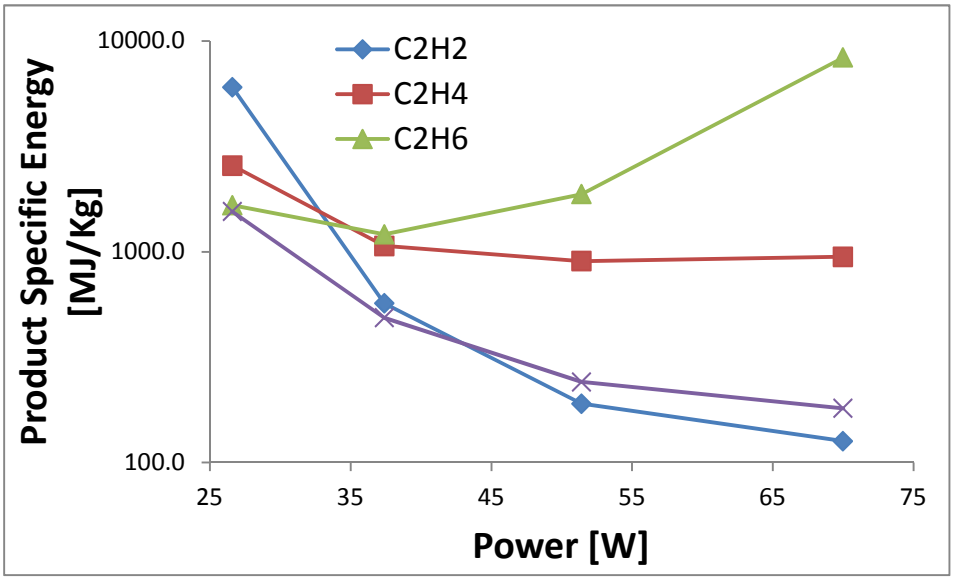

Figure 6.16 Variation of product specific energy with power in magnetic glow discharge system

i. Counter flow micro plasma - Figure 6.15 shows variation in the product specific energies with respect to changing input power in micro plasma system. In congruence with the results from concentration and selectivity's the specific energy cost of the products decrease with increasing power. As the product concentrations rise at higher powers along with better selectivity's for acetylene and ethylene..it leads to lower ratio of input power to product flow rate. Since the conversion rate of methane increases linearly with power there is no change in specific energy cost for converted methane.

ii. Magnetic glow discharge - Figure 6.16 shows variation in the product specific energies with respect to changing input power in magnetic glow case. Ethylene specific energy reaches a saturation point after 46W and acetylene specific energy decreases by huge margin due to high selectivity of 89% and a methane conversion rate of 9%. A lowest acetylene specific energy of 126 MJ/Kg is achieved at this point with 75W input power and 3 slpm flow rate.

6.3.4 Effect of Input Specific Energy on Output Parameters

In this section variation of concentration, product specific energy and normalized yields with changing input specific energy are discussed. A change made to each of the input variable (flow rate , discharge gap , methane in the mixture and power) changes the amount of energy spent on input methane feed. Although all the measured output parameters would still be dependent on the way input specific energy is varied, it is only the values that would change and the trends will still remain the same in the range of values of input variables.

6.3.4.1 Normalized yields: Figures 6.17 & 6.18 shows a change of normalized yields in micro plasma and magnetic glow respectively with respect to change in input specific energy of methane.

i. Counter flow micro plasma - Ethylene and acetylene that have higher reaction enthalpies turn out to be the major products at higher input specific energies with decreasing ethane normalized yields. The effect of acetylene dominating the other species is observed at higher input specific energies and ethylene curve is almost saturated.

ii. Magnetic glow discharge - Magnetic glow discharge has better selectivity's for acetylene and ethylene at lower input specific energies with acetylene being most selective as we move towards higher input specific energies. These results again have to be understood in conjunction with the effect of longer residence times in these discharges. The only difference in trends of results for discharges is that the shift towards better selectivity's for acetylene is happening at different input specific energies and the latter is more effective in minimizing soot production. A 40 % normalized yield for ethylene is achieved with an input specific energy of 35MJ/Kg of methane in micro plasma system, whereas the same normalized yield was achieved at only 5MJ/Kg of methane in magnetic glow discharge system.

6.3.4.2 Product concentrations: Figures 6.19 & 6.20 shows a change of product concentrations ,conversion rates in micro plasma and magnetic glow respectively with respect to change in input specific energy of methane.

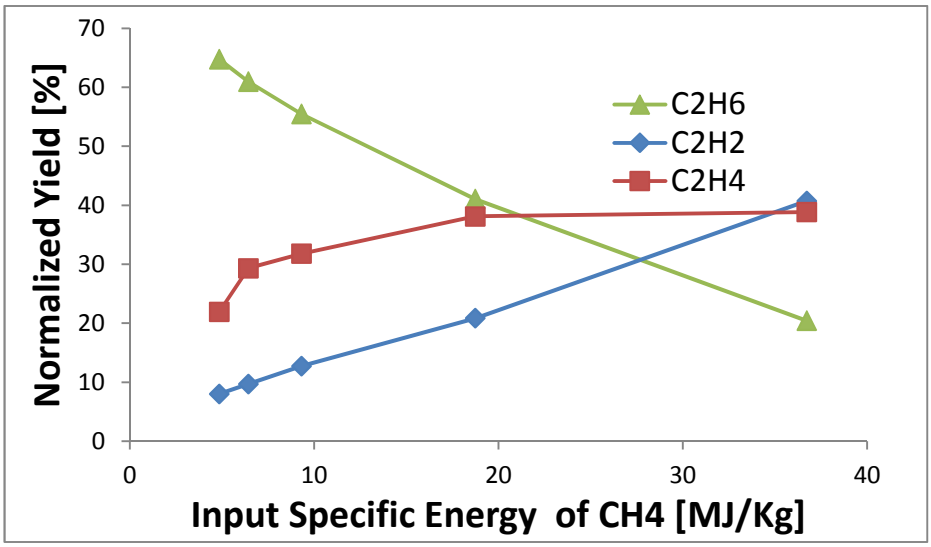

Figure 6.17 Variation of normalized yields with input specific energy in counter flow micro plasma system

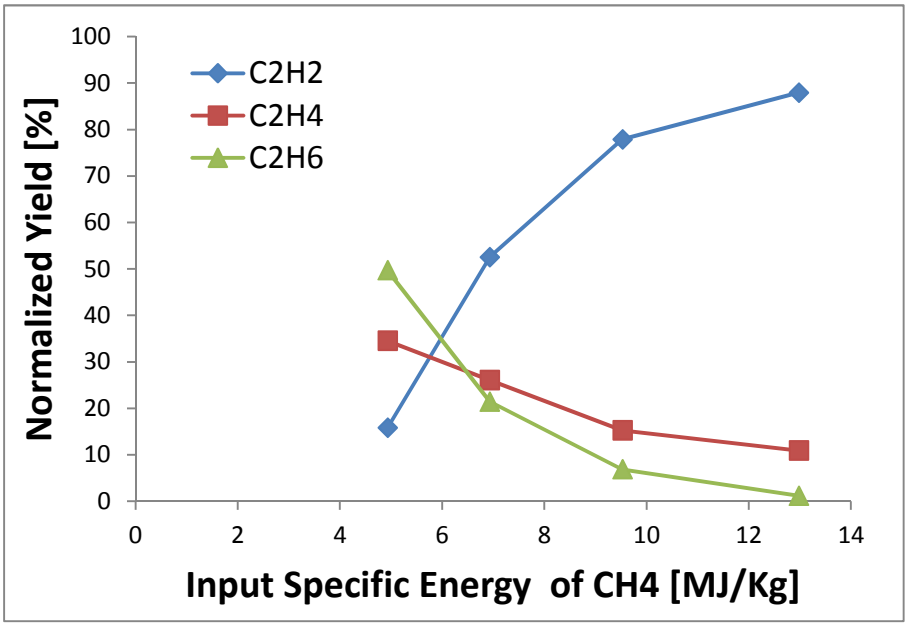

Figure 6.18 Variation of normalized yields with input specific energy in magnetic glow discharge system

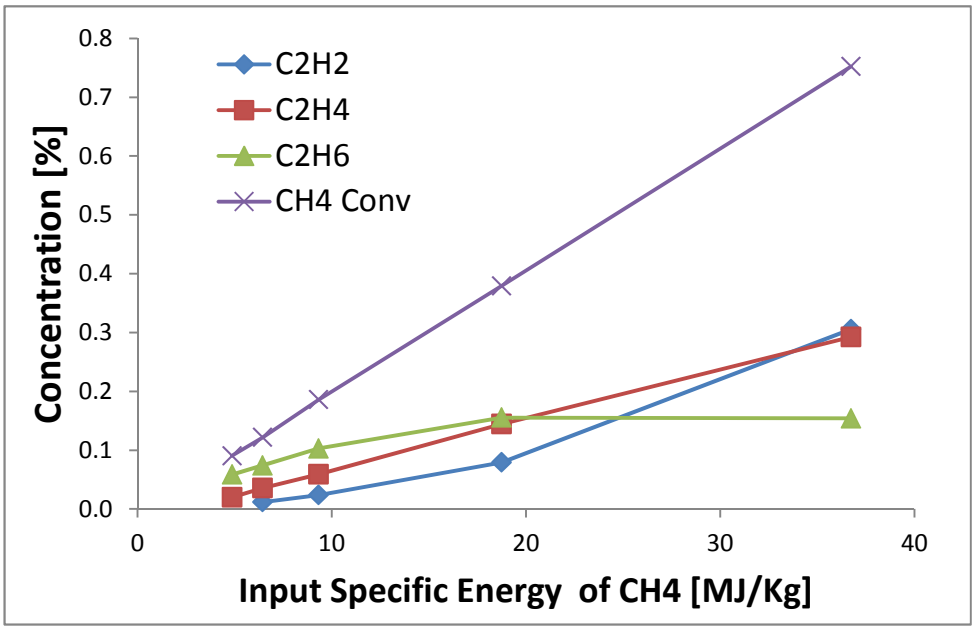

Figure 6.19 Variation of concentrations with input specific energy in counter flow micro plasma system

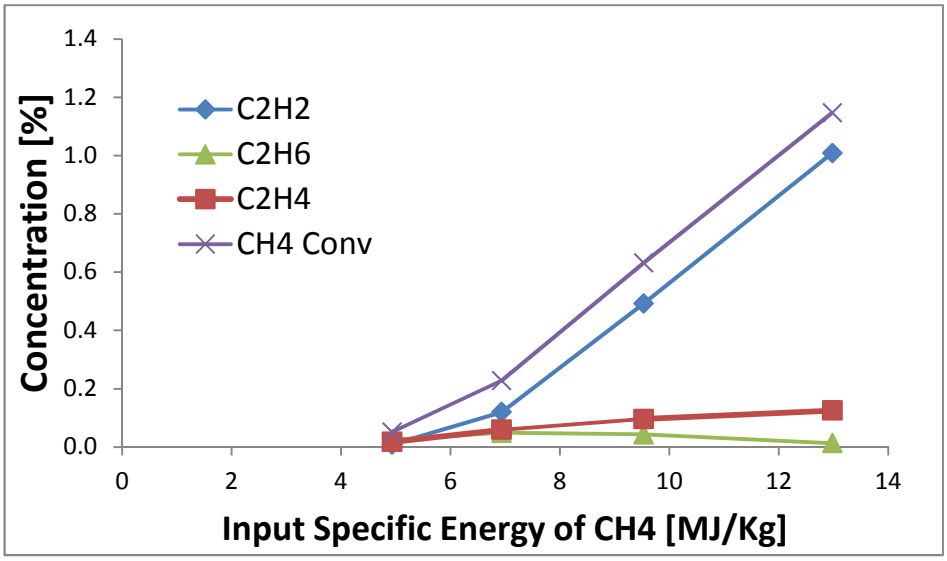

Figure 6.20 Variation of concentrations with input specific energy in magnetic glow discharge system

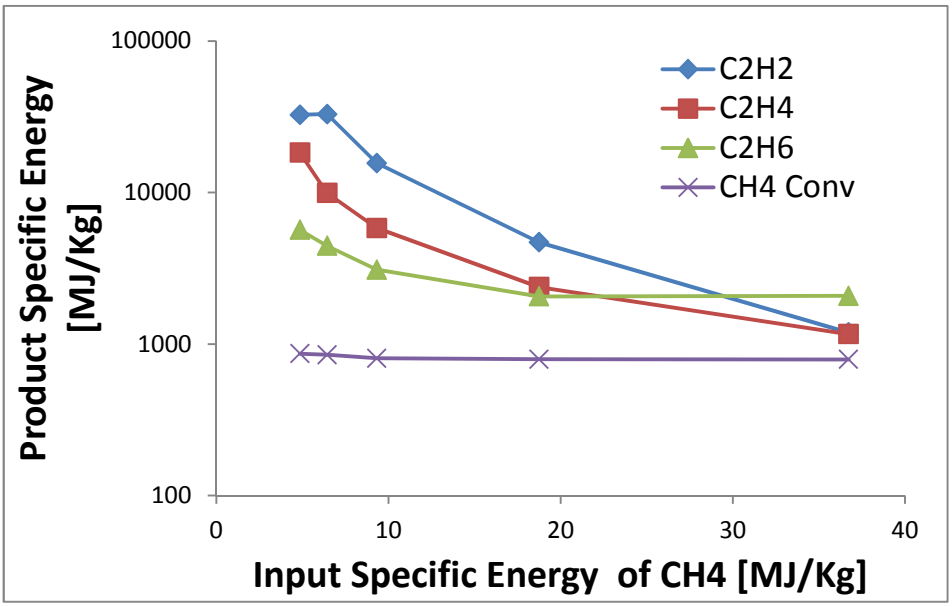

Figure 6.21 Variation of product specific energy with input specific energy in counter flow micro plasma system

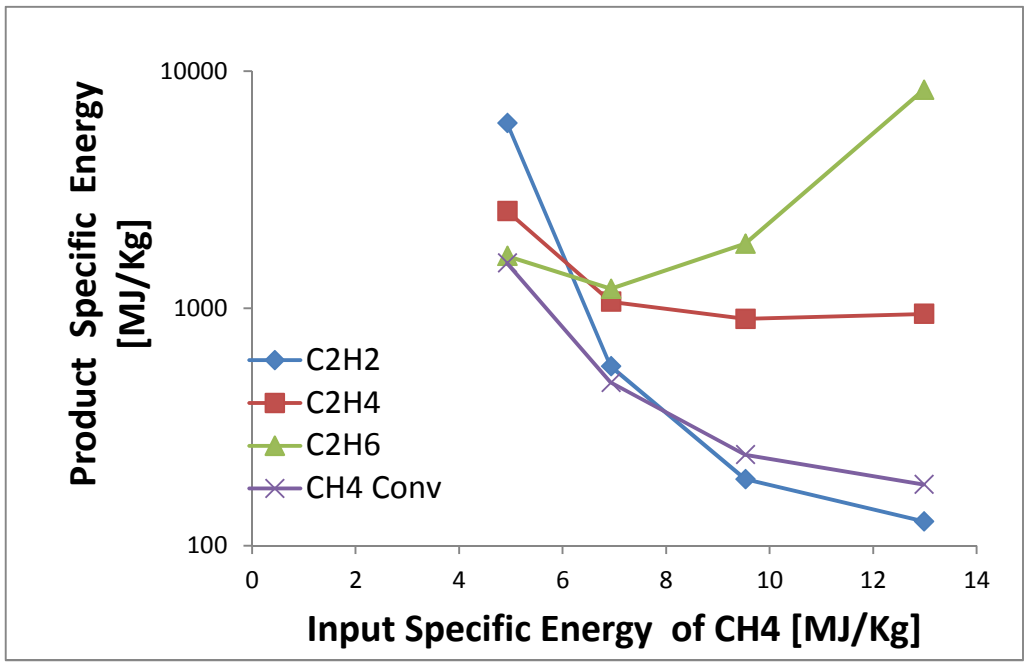

Figure 6.22 Variation of product specific energy with input specific energy in magnetic glow discharge system

i. Counter flow micro plasma - While conversion rate varies linearly with changing input specific energy, product concentrations show increasing trends with higher input specific energy. At 30MJ/Kg of methane input acetylene increases in concentration, indicating a shift towards higher temperature products.

ii. Magnetic glow discharge - Conversion rate and product concentrations follow the same trends in the case magnetic glow discharge, with the exception that yields are slightly better and with less carbon deposition.

Again, an ethylene concentration of 0.2% is measured in results of both the systems, but with an input energy of 36MJ/Kg of methane in the case of micro plasma and only 13 MJ/kg of methane in the case of magnetic glow discharge system. In addition, of the remaining products ethane content is minimized in magnetic glow discharge output.

6.3.4.3 Product specific energies: Plot 6.21 & 6.22 shows a change of product specific energies in micro plasma and magnetic glow respectively with respect to change in input specific energy of methane.

i. Counter flow micro plasma - The product specific energy is a function of conversion rate, selectivity and changing input power. Higher input specific energies with increased conversion rate and better selectivity's for ethylene and acetylene results in lower product specific energies of these products.

ii. Magnetic glow discharge - Same trends are repeated in magnetic discharge case, with the higher yields at lower input specific energies of methane. Ethylene product specific

energy curve saturates while acetylene specific energy shows a downward curve. These trends are analogous to their normalized yields.

6.4 Summary of observed trends

- Carbon produced is higher in the case of counter flow micro plasma when compared to magnetic glow discharge due to its low temperature longer residence time characteristic. Also the rotating discharge helps in avoiding the hotspots on either of the electrodes which is a common case in micro plasma system especially at higher powers.

- Magnetic glow has much higher residence times than micro plasma and hence it represents the case of thermal mechanism with longer residence times and lower temperatures. Whereas micro plasma has lower residence times but operates at slightly higher temperatures.

- Ethane, Ethylene and acetylene are the only hydrocarbon products detected.

- Carbon deposition rate was found to be very low with Cs < 0.006% of out mixture flow.

- Higher powers and lower flow rates favor better ethylene productivities in counter flow micro plasma discharge reactors.

- Magnetic glow discharges are productive for ethylene at higher powers with flow rates not having any significant effect.

- Product concentrations and conversion rates increase with higher power and decrease with higher flow rates in both systems.

- Higher input specific energies lead to lower product specific energies in both the systems and this is attributed to better conversion rates.

- The best conversion rates achieved in micro plasma and magnetic glow discharge are 6.4% and 9.04% respectively , both at lowest flow rate tested i.e. 0.5 slpm.

- Product specific energies of 458 MJ/Kg for ethylene is the best result achieved with magnetic glow discharge system under the conditions of 0.5 slpm, 26W input power.

- The lowest achieved with micro plasma system is 1162MJ/Kg for ethylene at conditions of 0.5slpm and 33W input power.

- Lowest specific energy achieved for acetylene was 126MJ/Kg in the case of magentic glow discharge at conditions of 3 slpm and 70W.

- In terms of lowering the product specific energies, magnetic glow discharge system is more efficient as compared to micro plasma discharges. A product specific energy of 1100 MJ/Kg for ethylene is achieved with an input specific energy of 36 MJ/Kg for micro plasma discharge and it is just 6.9 MJ/Kg of methane for a magnetic glow discharge.

6.5 Comparison to results from literature and thermal equilibrium results

A comparison of results from micro plasma and magnetic glow discharge experiments to the results from literature and thermal equilibrium is presented in this section. Figures 6.23 & 6.24 shows product specific energy of ethylene vs input specific energy for different methods in literature, out results against the thermal mechanism result. The blue line indicates variation of ethylene/acetylene specific energy under conditions of thermal equilibrium without sooting and ideal quenching. It is plotted using GRI 3 mechanism and cantera in matlab. Results from literature are indicated by green dots and red dots. Results from literature that based on catalyst enhancement are indicated by red dots. Blue dots show results from counter flow micro plasma and yellow dots refer to results from magnetic glow discharge.

Results are for ethylene are shown in Figure 6.23. The thermal equilibrium line shows that the product specific energy of ethylene decreases for input specific energy above 8MJ/kg , reaches a minimum at 13 MJ/Kg and increases thereafter. There are very few published results for production of ethylene with non thermal plasmas (as on aug 2010).

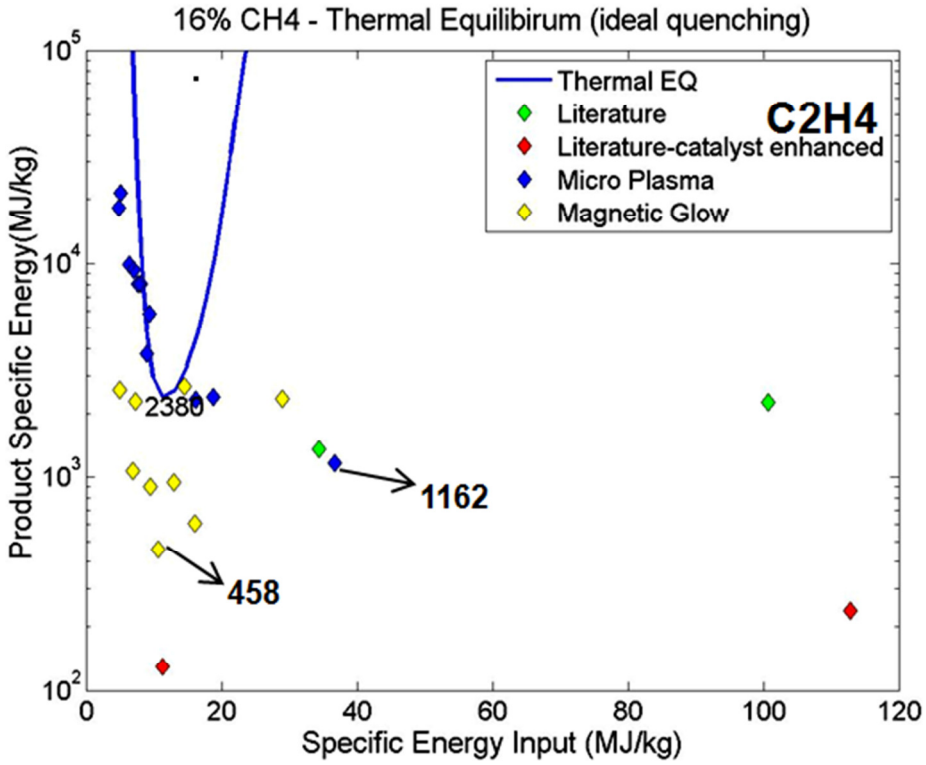

Figure 6.23 Plot of product specific energy vs specific energy input showing literature results, PEDL lab results and thermal equilibrium results for ethylene

Most of them are glow discharge systems coupled with catalyst activation for better ethylene normalized yields. Although catalysts are proved to be efficient in increasing selectivity towards ethylene, their working is frequently affected by coke deposition. Also, in calculating product specific energy the cost of catalyst and energy input to maintain catalyst at required temperatures is not considered thereby leaving a large uncertainty in the end values.

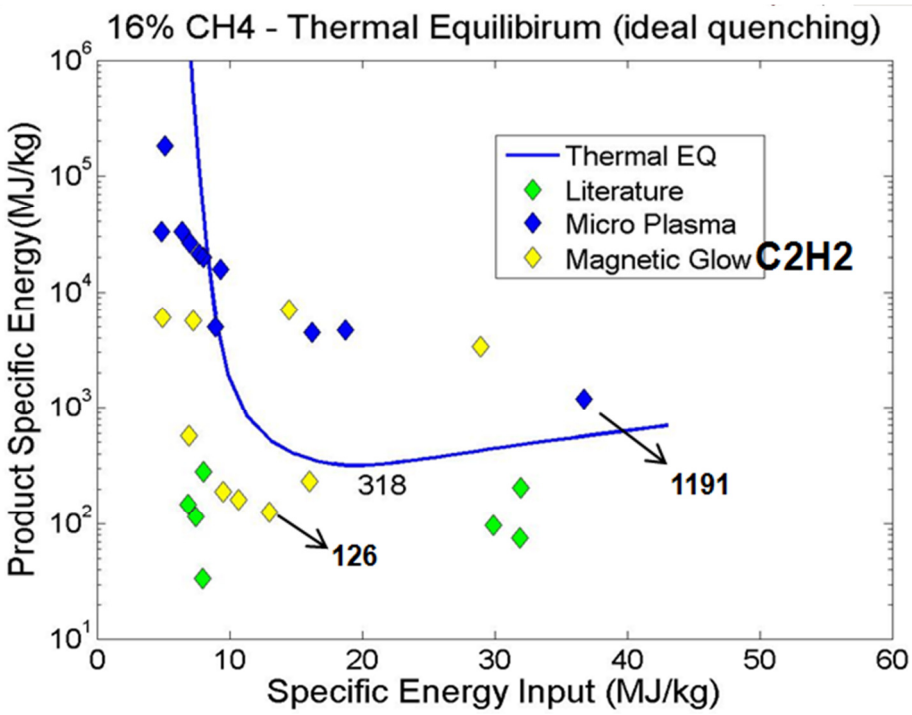

Figure 6.24 Plot of product specific energy vs specific energy input showing literature results, PEDL lab results and thermal equilibrium results for acetylene

Our results with micro plasma, shown in blue dots, are varying from 1162 to more than 10000 MJ/Kg. While the higher specific energy results belong to the higher flow rates, they drop with lower flow rate and lower powers. The lowest product specific energy of 1162 MJ/Kg is achieved in micro plasma is at 36MJ/Kg of input specific energy. While results from magnetic glow discharge are obtained at input specific energies in the range of 5- 30 MJ/Kg and most of them are better than thermal equilibrium results with the best result of 458MJ/Kg achieved at input specific energy of only10.7MJ/Kg of methane. The same comparative plot made for acetylene results is shown in Figure 6.24. A variety of non thermal discharges and reactor systems have been tried for producing

acetylene This includes gliding arc discharge, pulsed corona systems , high frequency pulsed plasmas and microwave plasmas. Product specific energies less than 50 MJ/Kg have been achieved high energy density plasma systems. The lowest acetylene specific energy reported is 33 MJ/Kg at an input energy cost of 7.9 MJ/kg in a high frequency pulsed plasma. In case of acetylene we are able to achieve a 126MJ/Kg product specific energy with magnetic glow discharge system at an input energy cost of 12.9 MJ/kg. While most of micro plasma results are above the thermal equilibrium case, a low power low flow rate magnetic glow discharge is able to produce acetylene at low acetylene energy costs better than thermal equilibrium results.

A generalization from these results can made that glow discharges with lower power and lower flow rates we can produce ethylene at lower specific energies if the reactor system provides a combination of optimum residence time and temperatures in addition to better quenching.

7. CONCLUSIONS AND FUTURE RECOMMENDATIONS

7.1 Research goals accomplished by this thesis

- Experimentally investigated the effects of residence time, input specific energy on the ethylene normalized yields in glow discharges and evaluated the conversion rate, product specific energy trends under different discharge conditions.
- Lowered the cost of ethylene production by while maximizing its normalized yield and minimized carbon content in the product through efficient plasma reactor systems.
- Reviewed results of methane reforming in various discharge systems from literature & performed a comparison of past and current work including this thesis to thermal equilibrium results in terms of achieved product specific energies.

7.2 Conclusions

Methane reforming in warm non-equilibrium discharges is investigated. Two different reactor systems, counter flow micro plasma and magnetic glow discharge, are constructed for the purpose. Methane hydrogen mixtures were varied in proportion and stable discharge conditions, with very low sooting, were possible for hydrogen dilution above 80%. It is observed that hydrogen dilution leads to low conversion rates, but better yields of C_2 hydrocarbons along with reduction in carbon generation.

In all the experiments ethane, ethylene, acetylene and carbon are the only detected hydrocarbon products. The maximum carbon particle flow (corresponding to lowest flow rate and highest power tested) was ~ 0.01% of the output carbon product stream. No other higher hydrocarbons were detected. With detection limits of Helium ionization detector as low as 50 ppm, any possible higher hydrocarbon products are considered to be negligible.

7.2.1 Summary of Results

7.2.1.1 Normalized yields: Normalized yields in case of micro plasma are affected by changing residence time and power. With increasing power, C_2 product yields increased (in the range of tested values) with ethylene approaching saturation and acetylene continuing to increase. A further increase in power is expected to show an increase in normalized yield of acetylene with decreasing trends for ethylene and ethane. Residence time has a similar effect with normalized yields of ethylene reaching a maximum of 40% at longest residence time of 0.3ms in counter flow micro plasma reactor. Unlike micro plasma the flow residence time shows relatively no effect on normalized yields in case of magnetic glow discharge. This is attributed to the non-changing residence time of this reactor due to discharge rotation. In magnetic glow a 38% normalized yield of ethylene was obtained at 3slpm. Input specific energies or input powers give the same trends of normalized yields in both reactors. At a flow rate of 3slpm and in both systems, ethylene normalized yields seems to increase with increase in input specific energy, reach a maximum and then decrease. It is important to consider the combined effect of

residence time and input energy. Both micro plasma and magnetic glow systems result in a maximum ethylene normalized yield of 40% at 3slpm, but with lower specific input power in the case of magnetic glow. The maximum ethylene normalized yield of 40% is achieved only at input specific energy of 5 MJ/Kg of methane in magnetic glow discharge system. Lower powers and lower flow rates give better normalized yields for ethylene in general.

7.2.1.2 Conversation rate and product concentrations: Conversion rates show same trends in micro plasma and magnetic glow discharge systems. They are essentially increasing with high powers and longer residence times, with the rate of increase comparable for both reactor systems.. Since the overall temperature in magnetic glow is less and the residence time has less effect on reaction system, the conversion rates show little increase over the range of flow rates tested. The highest conversion rates in these systems are 6 % and 9% at 0.5 slpm in the micro plasma and magnetic glow systems respectively. Ethylene yields reach a maximum as we move from lower to higher input specific energies and then drop. Product concentrations of ethylene up-to 0.2% and acetylene up to 0.9% have been achieved. Only soot production resulting in soot entrained in the gas flow was measured and it was found to be less than 0.006% of total hydrocarbon mass flow at 3 slpm flow rate.

7.2.1.3 Product specific energy: Product specific energy is the most important parameter in terms of efficiency. Low product specific energy are desirable and is the most important objective of this work. Ethylene has lower specific energies at higher powers

and lower flow rates (refer to Figure 6.13-16) in both reactors. In general for all the products, specific energy costs decrease with increasing power. As we defined earlier, product specific energy is a ratio of input power to product flow rate. Hence, as higher product concentrations were obtained at higher powers combined with better normalized yields, it resulted in a lower ratio of input power to product flow rate for ethylene and acetylene. With increasing flow rate product specific energies increase, primarily due to decrease in specific yields.

The difference between the two reactor systems is that the micro glow discharge systems offers a lower product specific energy by offering higher yields at lower input specific energies of methane. This is probably due to longer residence times and more energy transfer from plasma to chemical potential of the products and less heat losses, thereby creating favorable conditions for the reactions to generate C_2 hydrocarbons at lower input powers along with less carbon deposition. In micro plasma system the lowest specific energy of ethylene, 1162 MJ/Kg and of acetylene, 1191 MJ/Kg are obtained at 0.5slpm, power of 27W. For magnetic glow discharge system, a lowest ethylene specific energy of 458MJ/Kg and a lowest acetylene specific energy of 126MJ/Kg are achieved at 0.5 slpm, 33W and 3 slpm,70W respectively. When compared to thermal equilibrium result (2380 MJ/kg for ethylene at input specific energy of 15 MJ/kg of methane) our best ethylene specific energy is 5 times lower and also achieved at much lower input specific energy of 10 MJ/kg of methane.

7.3 Recommendations for future work

i. *Reactors in Series* - Although magnetic glow discharge system has better optimized conditions, still the conversion rates are found to be less than 9 % of methane. Hence, a similar system in series with existing MGD system can be investigated. Ideally, it should increase total amount converted. The second system will have the product stream of first system as its input feed. Hence, ethane may have increased conversion to ethylene, acetylene. Similarly a test with natural gas as input feed which has both C_1 and C_2 saturated hydrocarbons would be interesting. With any one of these input feeds, depending on the reactor conditions, increase in carbon deposition is a possible deleterious effect.

ii. *Supersonic flows* - We have seen the effect of residence time and input power conditions. Experiments and thermal equilibrium calculations show that higher powers and lower flow rates along with fast quenching favor ethylene yields. An optimized condition of these parameters is limited in our reactors. Supersonic flows offer the possibility of high power systems combined with a very fast quenching. It can be studied for better ethylene yields and lower carbon deposition.

iii. *Arrays* - Micro hollow cathode discharges are characterized by high electron densities. The non-equilibrium conditions and high input energy possibility offered by micro hollow cathode arrays makes them a good choice of investigation for methane reforming. This calls for a parallel rather than series processing for higher throughputs.

iv. *For diagnostics* - Argon can be mixed with input gases to perform a more accurate mass balance, so as to improve accuracy of output flow rate calculations. Optical emission spectroscopy temperature studies can also be performed to study the discharge conditions in more detail.

REFERENCES

1. NGSA-Washington DC, what is natural gas - http://www.naturalgas.org/overview/background.asp , NGSA.org, 09/20/2010.
2. NGSA-Washington DC, resources - http://www.naturalgas.org/overview/resources.asp ,NGSA.org, 09/20/2010.
3. Reed business information-New york, ethylene uses - http://www.icis.com/v2/chemicals/9075777/ethylene/uses.html, ICIS.com, 09/20/2010.
4. Jack H. Lunsford 2000 *Catal. Today* **63** 165–174.
5. Anders Holmen 2009 *Catal. Today* **142** 2–8.
6. Pyatnitskii.Yu.I., 2003 *Theo. and Exp. Chem.* **39**, No. 4, 201-218.
7. Anders Holmen 1995 *Fuel Process. Tech.* **42** 249-267.
8. Pak.S, Qiu.P, J.H. Lunsford, 1998 *J. Catal*. **179** 222.
9. Periana .R.A., D.J. Taube, S. Gamble, H. Taube, T. Satoh, H. Fujii, 1998 *Science* **280** 560.
10. Otsuka .K., Yamanaka .I, Wang .Y., 1998 *Stud. Surf. Sci. Catal*. **119** 15.
11. Grandy J D ; Peter C. Kong ; Brent A. Detering ; Larry D. Zuck 2007, Report: INL/CON-06-11945, *Plasma processing of hydrocarbon,* Idaho National Laboratory.
12. Gladisch H., 1962 *Hydrocarbon Processing and Petroleum Refiner*, **41**, 159–164.

13. Holmes J. M., 1969, *Evaluation of Dupont arc process for acetylene and vinyl chloride monomer production*, ORNL-TM-2725

14. Daniel Maniero, et. Al 1972 *U.S. Patent No*. 3,697,612.

15. Goldston R.J.,.Rutherford P.H, 1995 *Introduction to plasma physics* Taylor & Francis 147-148.

16. Alexander .F, Kennedy .L. A, 2004, *Plasma Phyics and Engineering*, CRC press 8-10.

17. Alexander Fridman, 2008, *Plasma Chemistry*, Cambridge University Press 4-6; 598.

18. Yuri P. Raizer, 1991, *Gas Discharge Phyiscs,* Springer, 172-174.

19. Olsvik, O., Rokstad O.A. and Holmen, A., 1994. *Chem. Eng. Technol.*

20. Happel, J. and Kramer, L., 1967. *Ind. Eng. Chem.,* **59**(l): 39-50.

21. Broutin, P., Busson, C., Weill, J. and Billaud, F., 1992. L.F. Albright,B.L. Crynes and Nowak .S (Eds.), Marcel Dekker, 239-258.

22. Timothy Eastman, plasma applications- http://www.plasmas.org/applications.htm, plasmas.org, 09/20/2010.

23. Plasmas International, plasma applications - http://www.cartage.org.lb/en/themes/sciences/physics/plasmaphysics/Applications/Applications.htm , plasmas.org, 09/20/2010.

24. Thomas nelis, http://www.glow-discharge.com/Index.php?Physical_background:Glow_Discharges:Discharge_Regimes, glowdischarge.com, 09/20/2010.

25. http://en.wikipedia.org/wiki/File:Electric_glow_discharge_schematic.png

26. Zhao.G.B et al, 2006, *Chem. Eng. J.,* 125, 2 , **15** , 67-79 .

27. Zhu, Aimin et al, 2000, *Sci. in China Ser. B Chem.,* **43**, 2, 208-214.

28. Yang et al.Y, 2003, *Plasma Chem. Plasma Process*, **23**, 2, 283–296.

29. Kado.S et al, 1999, *Chem. Commun.* **24** 2485–2486.

30. Xiao-Song Li et al, 2008 *J. Phys. D: Appl. Phys*. **41** 17, 5203.

31. Xiao-Song Li et al, 2004, *Catal. Today* , **98** ,4, 617-624.

32. Schmidt-Sza lowski.K et al, 2007 *Plasma Process. Polym.*, **4**, 7-8, 728 - 736.

33. Liu.C, Mallinson.R.G et al, 1998, *J. Catal.* , **179**, 1 , 326-334.

34. Liu.C et al, 1999, *Appl. Catal. A*, **178**, 1, 17-27.

35. Liu .C.A et al, 1997, *Appl. Catal. A*,**164,** 1-2, 21-33.

36. Yao .S et al, 2001 *AIChE J.* ,**47**, 2 ,419–426.

37. Yao .S et al, 2001 *Catal. Today*,**71**, 1-2, 15, 219-223.

38. Yao .S et al, 2002 *AIChE J.,* **47**, 2 , 413-418.

39. Yao .S.L et al 2001 *Energy & Fuels* **15** (5), 1300-1303.

40. Yao .S.L. et al, 2002, *Plasma Chem. Plasma Process*. **22**, 2 , 225–237.

41. Caldwell et al 1998 *216thACS National Meeting*; *Division of Fuel Chemistry*, **43**, 490.

42. Jeong HK, Kim SC et al, 2001 *Korean J of, Chem.Eng*. , **18**, 2 196-201.

43. Thanyachotpaiboon et al, 1998 *AlChE J*,44, **10** , 2252-2257.

44. Tarverdi.H et al, *Iran. J. Chem. Eng*. **24**, 4,63-71, 2005

45. Baowei Wang et al , , 2008 *Front. Chern. Eng. China* 2008, **2**, 4, 373-378.

46. Heintze.M and Magureanu.M, 2002 *J. Appl. Phys*. **92**, 2276.

47. Jun-qi Zhang et al, 2002 *Energy & Fuels*, **16**(3), 687-693.

48. Babaritsky et al, 1991 *Kurchatov Inst. Of Atomic Energy*, 5350/12 , Moscow.

49. Sergey Y. Savinov et al, 2004 *Korean J Chem Eng.,* **21**, 3, 601-610.

50. Pedro Patiño et al, *Fuel* , 2005 84, **16** , 2008-2014 .

51. Dai Wei ,Yu Hui, Chen Qi, Yin Yongxiang, Dai Xiaoyan , 2005 *Plas. Sci. and Tech*., **7**, 6.

52. Gladisch, H., 1962 *Hydrocarbon Process. Petrol. Refiner*, **41**, 159.

53. Yang Y, *Ind. Eng. Chem. Res.* 2002, **41**, 5918-5926.

54. Nongnuch R, 2009 *Chem. Eng. J* **155** 874–880.

55. Wang Kangjun 2008 *Plas. Sci. and Tech.,* **10**, 5.

56. Moltek.M 2009 *Appl. Catal. A: Gen.* **366** 232–241.

57. Vora .B 1997 *Stud. in Surf. Sci. and Catal.* **107** Pages 87-98.

58. Open source code, http://code.google.com/p/cantera/, 09/20/2010.

59. Micheal .F et. al, University of California berkeley, http://www.me.berkeley.edu/gri_mech/version30/files30/grimech30.dat, me.berkeley.edu, 09/20/2010.

60. Blekkan, E.A., Myrstad, R., Olsvik, 0. and Rokstad, O.A., 1992. *Carbon* **30**(4): 665-673.

61. Bokros, J.C., 1969. *Chemistry and Physics of Carbon*, Vol. 5. Marcel Dekker, New York, pp. 1-118.

62. Palmer, H.B., Lahaye, J. and Hou, K.C., 1968. *J. Phys. Chem.,* **72**(l): 348-353.

63. Albright, L.F. and Marek, J.C., 1988. *Ind. Eng. Chem. Res*., **27**: 755-759.

64. Frenklach, M. and Wang, H., 1991. *Proc. Int. Symp. on Combust*., **23**: 1559-1566.

65. Billaud, F.G., Baronnet, F. and Gueret, C.P., 1993. *Ind. Eng. Chem. Res.,* **32**: 1549-1554.

66. Ranzi, E., Dente, M., Costa, A. and Bruzzi, V., 1988. *Ing. Chem. Ital*. **24**(1-2): 2-8.

67. Kunugi, T., Tamura, T. and Naito, T., 1961. *Chem Eng. Prog*., **57**(11): 43-49.

68. Holmen, A., Rokstad, O.A. and Solbakken, A., 1979. *Ind. Eng. Chem., Process Des. Dev*., **18**: 653-657.

69. Yampolskii, Yu, P., Gordon, M.D. and Lavrovskii, K.P., 1968. *Neftekhimiya,* g(2): 198-208.

70. Holmen, A., Rokstad, O.A. and Solbakken, A., 1976. *Ind. Eng. Chem., Process Des. Dev*., **15**: 439-444.

APPENDIX A

Instruments used and their properties

1. Power supplies – The following two power supplies are used for generating glow discharge in magnetic glow discharge system and counter flow micro plasma reactor system respectively.
   i. Glassman Tech DC power supply (Used for magnetic glow discharge)

Glassman High voltage DC power supply

Resistor ballast box (37.5KΩ – 200KΩ)

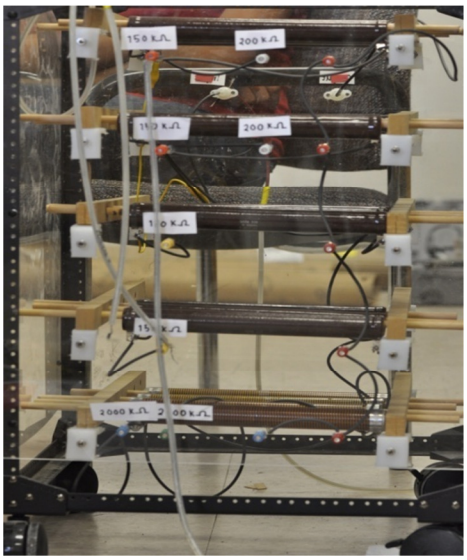

Power type : Direct Current

Voltage range : 1 – 9.9 KV

Current range : 0 – 250 mA (For magnetic discharge load)

Efficiency : 50% (with no ballast resistance)

ii. Plasma driver power supply 400X

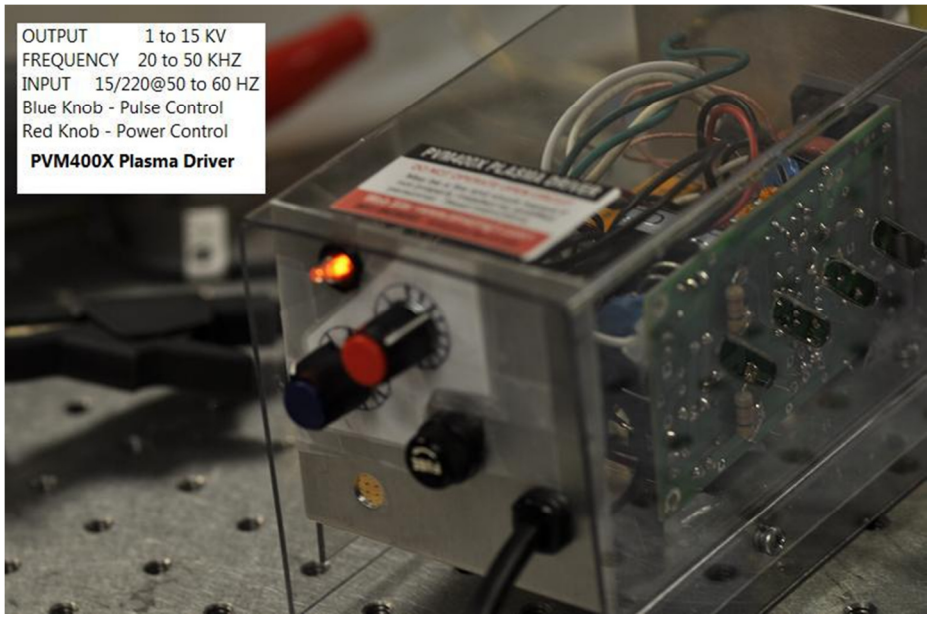

Power type : Pulsed

Voltage range : 1-15 KV

Current range : 0 – 80 mA (with micro plasma load)

Frequency : 27.1 MHz

Efficiency : 56%

2. Measurement instruments

i. Mass flow controllers - 2 Alicat Scientific mass controllers

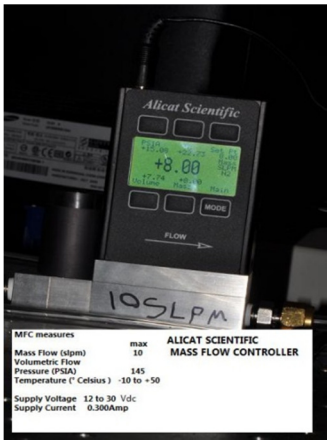

Mass flow : 0 – 10 slpm, 0 –1slpm

Pressure : 14.7 – 145 Psi

Temperature : -10 C to 50 C

Supply voltage : 12 to 30 Vdc

Supply current : 0.3 A

ii. Power meters – For measuring line power

a. Watts up Pro power meter

Specifications

Power in : 120 VAC, 60 Hz, 15 amps continuos

Type : True power, RMS voltage, RMS current measured and displayed

Accuracy : +/- 1.5% + 3 counts

b. PEDL lab power meter - Power from mains goes to load through Rs R01 R02 as shown in figures in next page. Voltage is across Rs and R02 is fed into isolation amplifiers. These amplifiers are powered by DC/DC converters (TEL 3- 1213) in series with a AC/DC converter. Output of isolation amplifiers is a AC measurement of voltage drop across the resistances and can be generated as waveforms on oscilloscope through BNC connections. The resistances and detailed circuit are shown in figure 1 and 2 in next page. A comparison and performance of these meters is provided in Figure 3.

Specifications

Power in : 120VAC , 60Hz , 7.7 amps continuous

Type : Mean Power, RMS Voltage , RMS Current Measured on Oscilloscope

Accuracy : +/- 1% to 5%

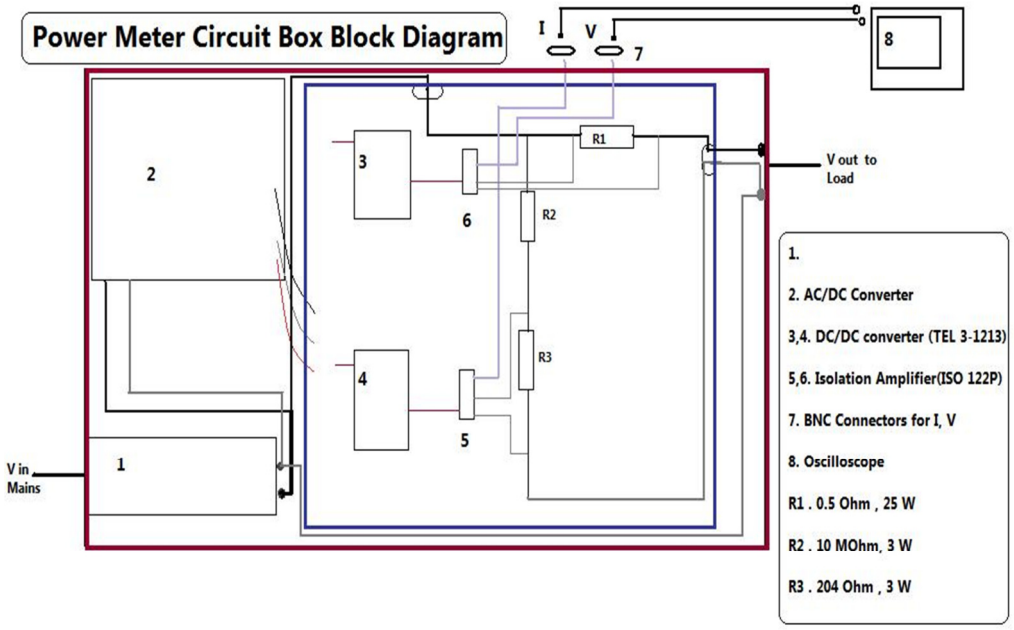

Figure A.1 Power meter circuit box block diagram showing different components

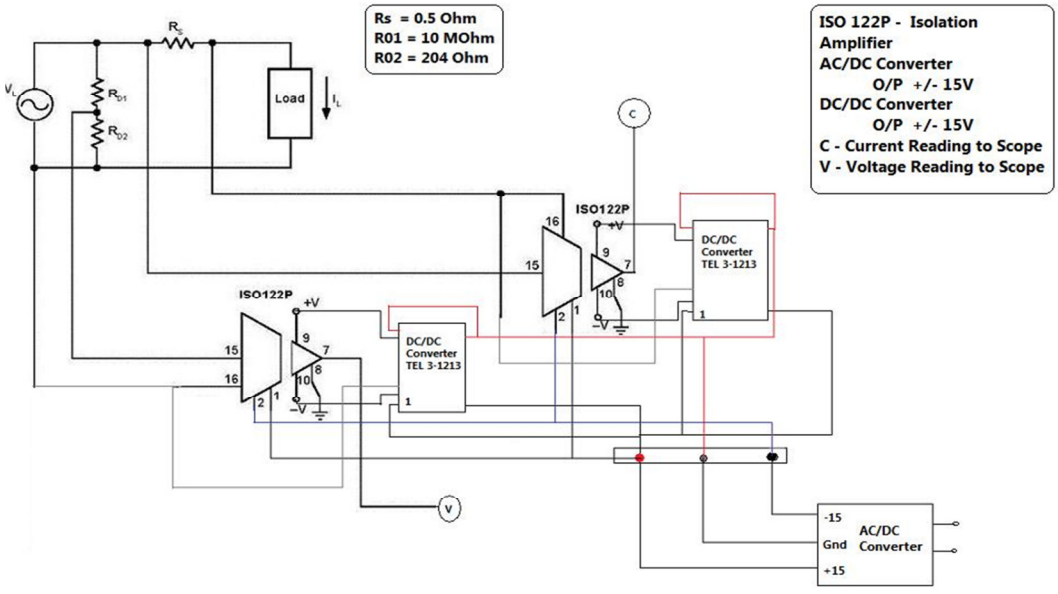

Figure A.2 Circuit design of power meter used for generating voltage and current waveforms

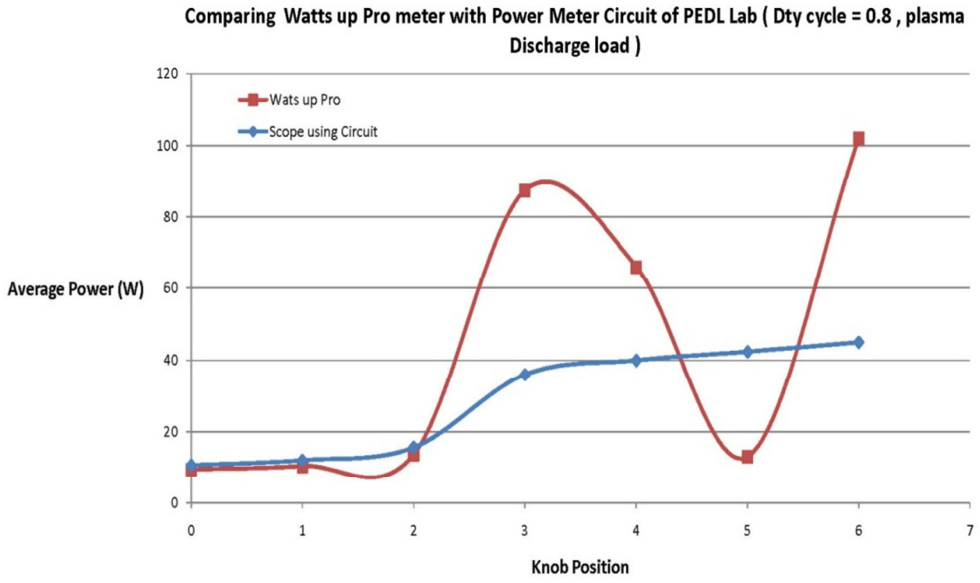

Figure A.3 Performance comparison I under different conditions for watt up pro and new circuit used

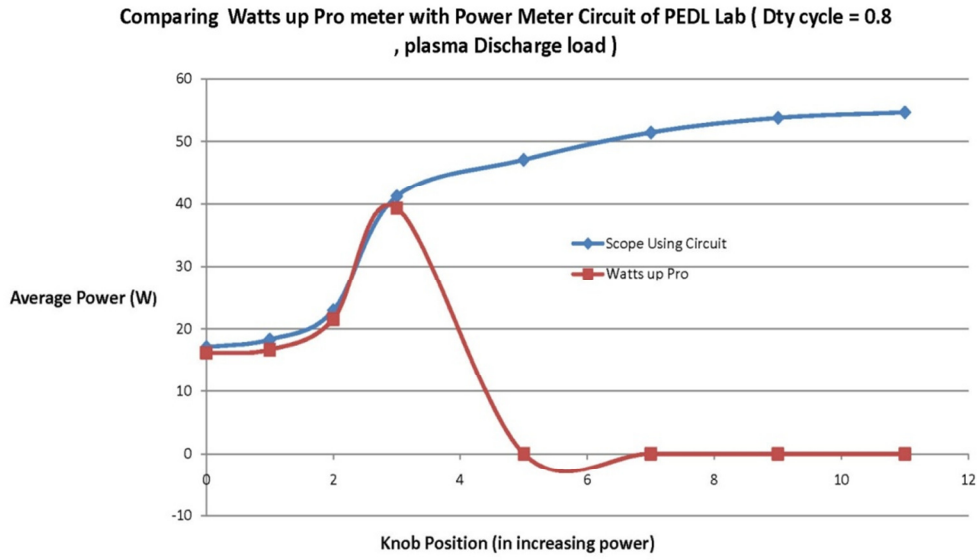

Figure A.4 Performance comparison II under different conditions for watt up pro and new circuit used

iii. Gas chromatograph – To determine output gas composition. O2, N2, Ar, H2, CO, CH4 are separated in molecular sieve while CO2 and higher hydrocarbons are separated in silica gel column. TCD and HID are in series to detect all compounds.

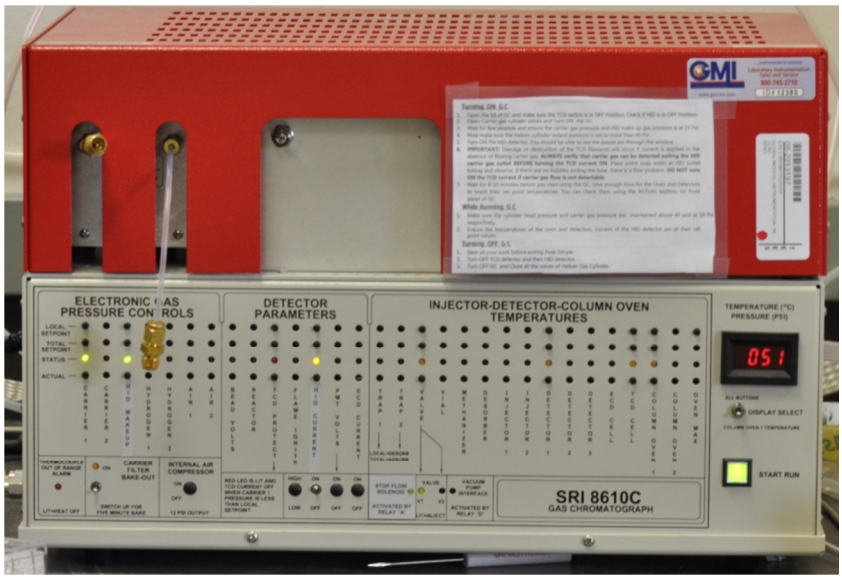

Specifications

Model :	Multiple gas analyzer # 3, SRI 8610C
Columns :	Molecular Sieve 13X in series with Silica Gel
Detectors:	6X
:	Thermal conductivity detector (for >1 %)
Carrier gas (Flow rate &	Helium ionization detector (50 – 50,000 ppm)
Pressure) :	Helium (19 sccm & 25 psi)

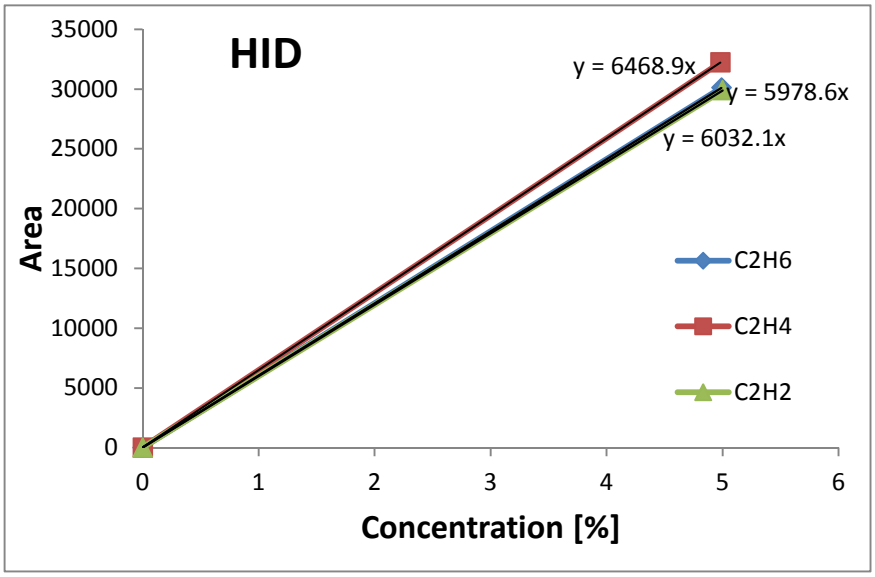

Figure A.5 Calibration constant plot for experiments done in micro plasma system

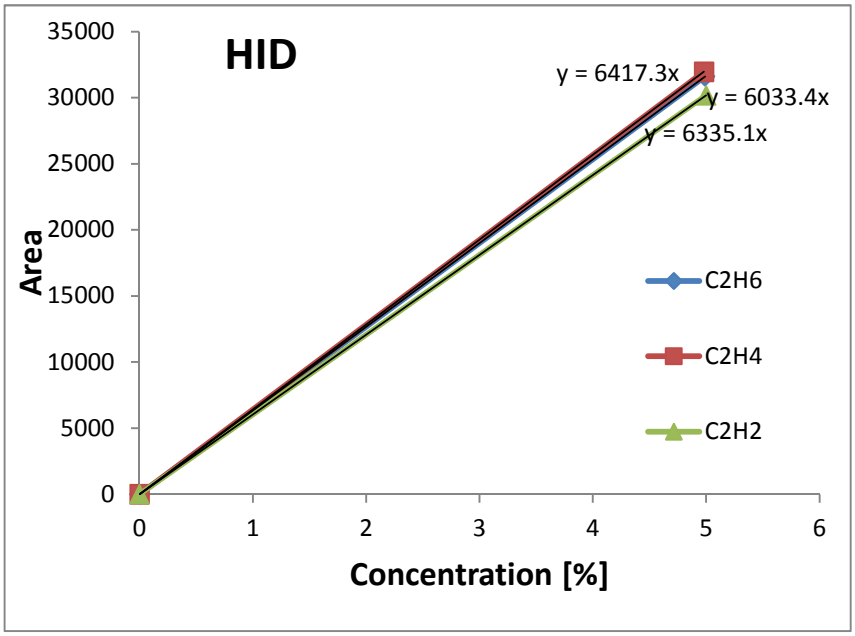

Figure A.6 Calibration constant plot for experiments done in magnetic glow system

Table A.1 Calibration constants from gas chromatograph, used in determining output composition

Discharge system	Calibration constants [K]			Areas			% = Area × K		
	C2H6	C2H4	C2H2	C2H6	C2H4	C2H2	C2H6 [%]	C2H4 [%]	C2H2 [%]
Counter flow micro plasma	1.62E-04	1.54E-04	1.67E-04	1057	2047	1873	0.171	0.315	0.312
Magnetic glow discharge	2.14E-04	2.11E-04	1.74E-04	303	345	1015	0.065	0.073	0.177

iv. Power measurement

a. Oscilloscope

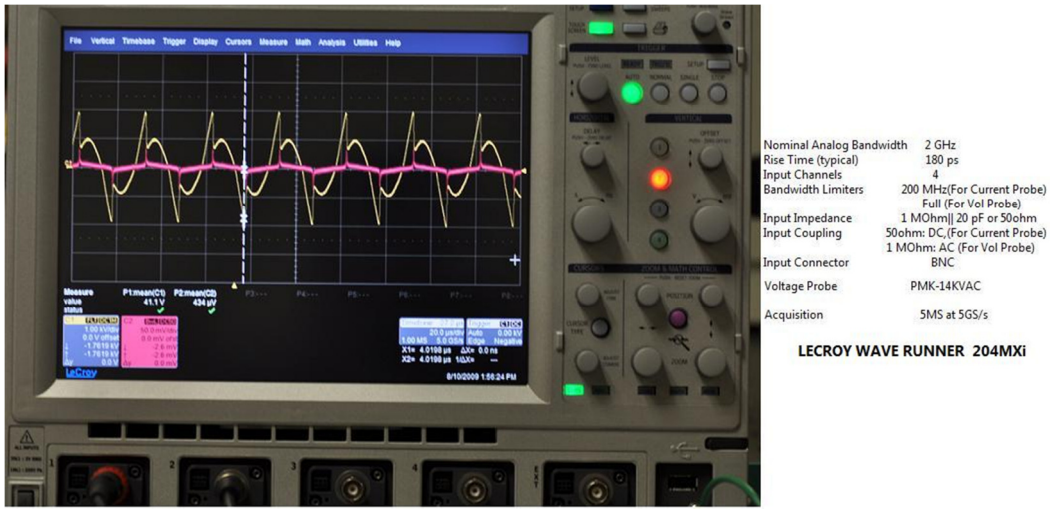

Specifications

Model : Lecroy wave runner 204 MXi

Bandwidth : 2 GHz

Input Channels : 4

Bandwidth Limiters : 200 MHz for current probe &

Full for current probe

Input connectors : BNC

Acquisition : 2MS at 5GS/s

b. Voltage probe

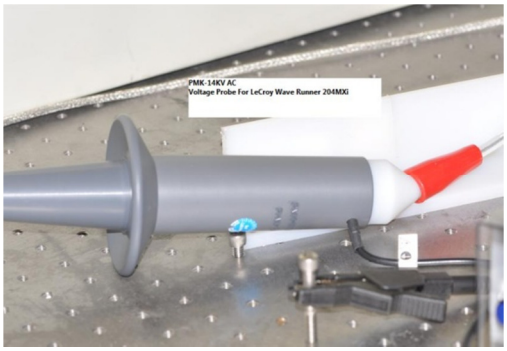

Model : PMK 14 KV AC

c. Current transformer

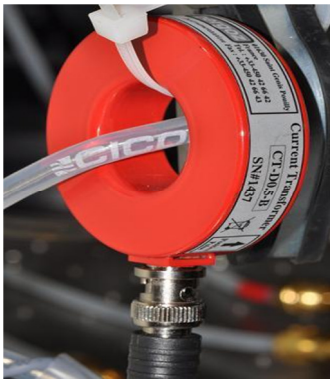

Model : Bergoz CT-B0.5

Max Rms current 11 A

Frequency range 48 Hz – 200 MHz

Output (V/A) in : 1 MHΩ 0.5

50Ω 0.25

APPENDIX B

Matlab codes

Voltage and current waveforms from oscilloscope are post-processed in matlab and a power waveform is generated. An example of power wave form is given in Figure 6. This data is integrated to get average power over 10- 12 cycles.

The code used to calculate RMS Voltage, RMS current, Average power:

Table B.1 Matlab code with comments

Code	Comments

load('F05R3v.dat');
T1_2 = F05R3v(:,1);
V_2 = F05R3v(:,2);
figure
plot(T1_2,V_2);
saveas(gca,'VoltageFull ','jpeg')
load('F05R3i.dat');
T11_2 = F05R3i(:,1);
C_2 = 2*F05R3i(:,2);
figure
	# loading the matlab data of voltage
	#assigning first column of time data to a variable
	# assigning second column of voltage data
	#plotting Voltage Vs Time
	# saving the plot
	#loading the matlab data of current

Table B.1 continued.

plot(T11_2,C_2);	# multiply the current data with 2 to
saveas(gca,'CurrentFull ','jpeg')	account for current transformer attenuation
IP_2 = C_2.*V_2;	
figure	
plot(T11_2,IP_2);	
saveas(gca,'PowerFull ','jpeg')	# power = product of votage and current
a = cumtrapz(T11_2,IP_2);	# plot of power Vs time
c = a(end);	# integration of power data
t = T11_2(end);	# finding the final value from this data
Power = c/t	# finding the time value of corresponding
figure	final power value and a ration of them
plot(T11_2,a)	gives avg. Power
I_rms_P1 = sqrt(mean(C_2.^2))	# RMS current
V_rms_P2 = sqrt(mean(V_2.^2))	# RMS Voltage

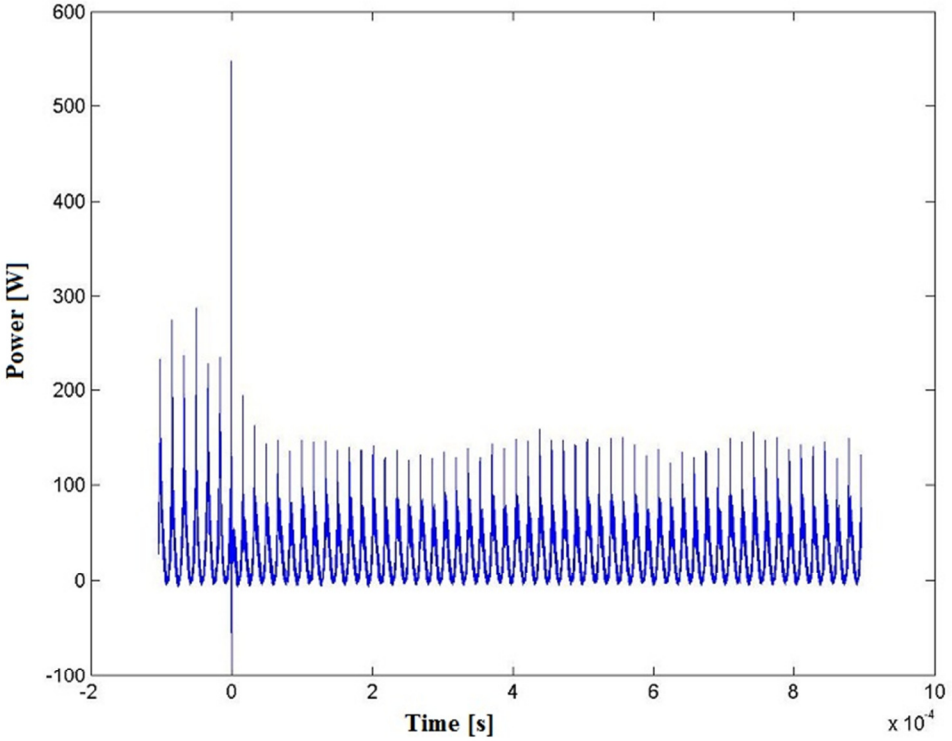

Figure B.1 Power waveform generated in matlab

APPENDIX C

Tables of experimental data

Table C.1 Experimental data for Magnetic glow discharge system for experimental set 1,2 (refer to pg: 84)

CH4 Concenration (%)	Ein (W)	Flow Rate (SLPM)	GC AREAS				CH4 out amt (%)	CH4 conv amt (%)	C2H6 amt (%)	C2H4 amt (%)	C2H2 amt (%)
			CH4 Area	C2H6 Area	C2H4Area	C2H2 Area					
10	18	1	18.2	526.7	1114.11	2715.09	9.36	0.64	0.07	0.15	0.42
15	18	1	28	695	1475	3947	9.10	0.90	0.10	0.20	0.61
16	26.6	3	33.1	183	130	52	15.95	0.05	0.03	0.02	0.01
16	37.4	3	32.7	353.9	440	776	15.77	0.23	0.05	0.06	0.12
16	51.4	3	31.2	313.7	713.5	3187.7	15.37	0.63	0.04	0.10	0.49
16	70	3	28.9	96	927	6536	14.85	1.15	0.01	0.13	1.01
16	26	0.5	32.2	890	835	544	15.68	0.32	0.12	0.11	0.08
16	26	1	32.8	472	367	130	15.87	0.13	0.07	0.05	0.02
16	26	2	32.9	248	216	82	15.92	0.08	0.03	0.03	0.01
16	26.6	3	33.1	183	130	52	15.95	0.05	0.03	0.02	0.01
16	22	3	32.2	223	206	208	15.87	0.13	0.05	0.04	0.04
16	26	3	32	275	315	430	15.80	0.20	0.06	0.07	0.07
16	30	3	31.8	377	295	514	15.77	0.23	0.08	0.06	0.09
16	33	3	31.5	327	319	745	15.73	0.27	0.07	0.07	0.13
16	37	3	31	303	345	1015	15.69	0.31	0.06	0.07	0.18

Table C.2 Experimental data for Micro glow discharge system for experimental set 1,2 (refer to pg: 84)

			GC AREAS								
CH4 Concenration(%)	Ein (W)	Flow Rate (SLPM)	CH4 Area	C2H6	C2H4	C2H2	CH4 out amt (%)	CH4 conv amt (%)	C2H6 amt (%)	C2H4 amt (%)	C2H2 amt (%)
16	33.0	0.5	27.4	952.0	1899.5	1835.5	15.134	0.747	0.153	0.290	0.303
16	33.7	1	28.4	960.7	939.0	475.7	15.562	0.378	0.155	0.144	0.079
16	33.5	2	29.0	636.3	384.3	142.3	15.785	0.186	0.103	0.059	0.024
16	34.7	3	29.2	458.0	232.0	71.3	15.859	0.122	0.074	0.036	0.012
16	34.9	4	28.9	361.3	129.3	71.7	15.895	0.090	0.058	0.020	0.012
16	27.6	3	28.9	399.0	86.7	10.0	15.908	0.080	0.065	0.013	0.002
16	34.7	3	29.2	458.0	232.0	71.3	15.859	0.122	0.074	0.036	0.012
16	37.9	3	29.9	526.3	272.3	95.7	15.834	0.143	0.085	0.042	0.016
16	41.6	3	30.0	561.3	342.3	130.7	15.809	0.165	0.091	0.053	0.022
16	43.4	3	29.5	566.0	356.0	143.7	15.803	0.170	0.091	0.055	0.024
16	16.1	1	28.3	601.5	280.0	214.0	15.796	0.176	0.097	0.043	0.036
16	29.2	1	29.7	905.7	830.3	433.7	15.599	0.345	0.146	0.127	0.072
16	33.7	1	28.4	960.7	939.0	475.7	15.562	0.378	0.155	0.144	0.079

VITA

Name: Sreekar Parimi

Address: c/o Dr. David Staack

Texas A&M University
College of Engineering
3123 TAMU
Engineering Physics Building, Room 328
College Station, TX 77843

Email Address: sreekar.parimi@neo.tamu.edu

Education: B.Tech, Mechanical Engineering, JB Institute of Engineering and Technology, 2008

M.S., Mechanical Engineering, Texas A&M University, 2010